Available online at www.sciencedirect.com
SCIENCE DIRECT®
Coordination Chemistry Reviews 249 (2005) 2094–2131
COORDINATION CHEMISTRY REVIEWS
www.elsevier.com/locate/ccr

Review

Group 13 imido metallanes and their heavier analogs $[RMYR']_n$ (M = Al, Ga, In; Y = N, P, As, Sb)

Alexey Y. Timoshkin

Inorganic Chemistry Group, Department of Chemistry, St. Petersburg State University, University Pr. 26, Old Peterhof 198504, Russia

Available online 23 May 2005

Contents

Abstract

The chemistry of group 13 imido metallanes and their heavier analogs has been reviewed. Methods for the synthesis of these compounds, structural and thermodynamic properties, as well as reactivity, donor–acceptor properties and their potential as single-source precursors to group 13–15 binary materials have been discussed.

Keywords: Group 13–15 compounds; Rings; Cages; Synthesis; Structures; Theoretical studies

E-mail address: alextim@AT11692.spb.edu.

0010-8545/$ – see front matter © 2005 Elsevier B.V. All rights reserved.
doi:10.1016/j.ccr.2005.03.016

1. Introduction

Chemistry of group 13–15 compounds has grown dramatically in the last 15 years, mostly due to their importance as precursors for 13–15 semiconductors. Group 13–15 binary compounds are prospective materials for micro- and nanoelectronics, serving as light-emitting diodes, UV photodetectors, high electron mobility transistors, important solar cell elements and advanced ceramic materials [1]. As an example, unique properties of GaN, its applications and significance for future technology were highlighted in a recent issue of *Chemistry World* [2]. Since earlier studies of Wiberg [3], one of the common pathways to the 13–15 materials starts with 13–15 donor–acceptor complexes:

$$[\underset{\text{mp } 56.7\,^\circ\text{C}}{Me_3Al(NH_3)}] \xrightarrow[-CH_4]{70\,^\circ\text{C}} [\underset{\text{mp } 134.2\,^\circ\text{C}}{Me_2AlNH_2}]$$

$$\xrightarrow[-CH_4]{200\,^\circ\text{C}} [MeAlNH]_x \xrightarrow[-CH_4]{} AlN \quad (1)$$

Subsequent methane elimination leads to formation of amido and imido compounds, and finally, to aluminum nitride. Thus, amido and imido compounds appear to be natural precursors to group 13 nitrides. The same reaction pathway operates for the heavier group 15 elements.

When Veith published an extensive review in 1990 [5] on the ring and cage compounds of main group elements, only several 13–15 oligomer compounds have been known, mostly amido and imido alanes. Since then, many new group 13–15 compounds have been obtained and structurally characterized. Amido alanes have been reviewed by Sauls and Interrante [6]. An excellent review of amido compounds of gallium and indium has appeared recently [7]. Hydrazine compounds of group 13 metals have been recently reviewed by Uhl [8]. Chemistry and structures of imido compounds have been briefly discussed in several books devoted to group 13 metal chemistry [9–13], but there is no systematic review devoted exclusively to the imido compounds and their heavier analogs. Due to recent substantial activity in the field and potential importance of $[RMYR']_n$ compounds as single-source precursors to 13–15 binary materials and composites, an up-to-date review of their structural and thermodynamic properties is essential. Boron-containing imido compounds and their heavier group 15 analogs have been reviewed before [14] and will not be discussed in the present review.

The present review is focused on structural and thermodynamic properties of $[RMYR']_n$ compounds, where M = Al, Ga, In; Y = N, P, As, Sb; n = 1–8, ∞; R, R′—organic or inorganic substituents. Results of both experimental and theoretical studies have been summarized. Major synthetic approaches, structural properties, reactivity and donor–acceptor properties will be discussed.

In the present review, the degree of oligomerization was chosen as a classification. General trends in structural and thermodynamic properties are also discussed. The following abbreviations will be used:

Me: methyl; Et: ethyl; Pr: propyl; Bu: butyl; Xyl: $-C_6H_3$-2,6-Me_2; py: pyridine; Mes: mesityl (2,4,6-trimethylphenyl or $-C_6H_2$-2,4,6-Me_3); Mes*: 2,4,6-tri-*tert*-butylphenyl or ($-C_6H_2$-2,4,6-$^tBu_3$); Dipp: 2,6-diisopropylphenyl ($-C_6H_3$-2,6-$^iPr_2$); Trip: triisopropylphenyl ($-C_6H_2$-2,4,6-$^iPr_3$); Cp: C_5H_5; Cp*: C_5Me_5; Ad: adamantyl; THF: tetrahydrofuran; Hx: hexyl; r.t.: room temperature.

2. Synthetic methods of production of imido compounds

There are several major synthetic methods for production of the imido compounds and their heavier analogs.

2.1. Elimination reactions

Thermolysis (thermal activation) of 13–15 donor–acceptor complexes is the first method employed for the synthesis of imido compounds [3], and it remains one of the major synthetic methods for their generation. It has been mostly used for the synthesis of imido compounds from primary amines. Reaction of RR''_2M with NH_2R' initially produces the donor–acceptor complex $[RR''_2M(NH_2R')]$, which upon thermolysis produces amido, and afterwards imido compounds:

$$RR''_2M + NH_2R' = \underset{\text{adduct}}{[RR''_2M(NH_2R')]} \overset{-HR''}{=} \underset{\text{“amido”}}{[RR''MNHR']_{2,3}}$$

$$\overset{-HR''}{=} \underset{\text{“imido”}}{[RMNR']_n} \quad (2)$$

As was shown by numerous experimental studies, the oligomerization degree n for the generated compounds strongly depends on the bulkiness of the substituents R, R′ [9,11]. The more bulky substituents result in lower degrees of oligomerization. The influence of the amine groups on degrees of oligomerization of imido compounds was discussed in [15]. Bulky substituents have been successfully used to obtain dimers via an elimination route [16,17], but monomeric imido compounds could not be produced by this route.

One of the major disadvantages of thermal activation is a spate of byproducts caused by the high temperatures. Most common are orthometallation reactions due to activation of C–H bonds [18]. Thus, synthesis of $[CpAlNDipp]_2$ was possible from reaction of $AlCp_3$ and NH_2Dipp [17], but the analogous reaction of $AlMe_3$ with NH_2Mes^* resulted in metallation of ^tBu group of the Mes* [18,19]. Analogous metallation of ^tBu group of Mes* was observed upon thermal decomposition of monomeric amide $Et_2GaNHMes^*$ [161]. Thermolysis reaction between $GaMe_3$ and $NH(CH_2Ph)_2$ also resulted in an orthometallated compound with 65% yield [165]. In order to reduce side reactions, thermolysis of solid amido compounds was carried out at mild conditions (130 °C, 10^{-2} Torr) for 12–36 days to afford the desirable cubanes [20]. Modification of the traditional thermolysis method is discussed in [21], where reactions between

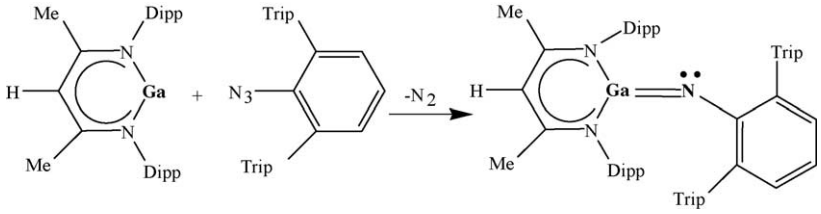

Scheme 1. Reaction of β-ketiminate monomers with sterically encumbered azide.

$MAlH_4$ (M = Li and Na) and NH_2R in hydrocarbon solvents were employed. Resulting products are either soluble polyimidoalanes $[HAlNR]_n$ or their insoluble complexes with LiH and NaH. NMR characterization of the products of such reactions has been reported in [22].

In most of the cases, the leaving groups in elimination reactions are an organic radical R on group 13 metal center and a H atom on the group 15 center. However, hydrogen is not the only substituent that can be used. Group 14-based substituents on the nitrogen center (such as $SiMe_3$ [23] and $SnMe_3$ [24]) were shown to be good leaving groups. Reaction of $GaCl_3$ with $As(SiMe_3)_3$ in the presence of the donor molecules P^tBu_2Me leads to the donor–acceptor stabilized dimeric compound $[ClGaAsSiMe_3]_2{\cdot}2P^tBu_2Me$ with liberation of $ClSiMe_3$ [23]. Thermolysis of $[(Me_2GaN(^iBu)SnMe_3)]_2$ at 160 °C resulted in $SnMe_4$ elimination with formation of $[MeGaN^iBu]_6$ [24].

As was shown by Beachley and Coates [25], an elimination pathway can be used for the production of not only imido compounds, but their heavier analogs as well. Formation of the colored involatile polymeric materials $[MeMYR]_n$ was reported by reactions of Me_3M with YH_2R (M = Al, Ga, In; Y = P, As; R = Me, Ph) [25]. Almost two equivalents of methane was evolved (1.86–2.02). In the case of Ga compounds, the elimination of methane was incomplete, it varied from 1.41 to 1.94 even at elevated (≈200 °C) temperatures. Consequently, P–H and As–H stretching vibrations were observed in all spectra of gallium-containing polymers, but no such absorptions were present in the spectra of Al and In polymers. No further characterization and isolation of the compounds was performed. Despite this example, the general use of thermal activation methods for P, As compounds is limited due to their low thermal stability and formation of byproducts.

2.2. Oxidative addition

Due to recent remarkable successes in the low valent chemistry of group 13 elements, synthesis of 13–15 rings and clusters via the oxidative addition route is now widely used. Reactions of Cp*Al and Cp*Ga with azides yield dimeric imido compounds [26,27]:

$$\tfrac{1}{2}(Cp^*Al)_4 + 2R_3SiN_3 = [Cp^*AlNSiR_3]_2 + 2N_2 \quad (3)$$

$$2Cp^*Ga + 2Xyl\text{–}N_3 = [Cp^*GaNXyl]_2 + 2N_2 \quad (4)$$

Needless to say, reactions of this type are not always successful due to possible C–H bond activation of the substituent and formation of amido compounds [26], for example,

$$\tfrac{1}{2}(Cp^*Al)_4 + 2MesN_3 = [Cp^*Al\{\mu\text{-}NH(C_6H_2\text{-}4, 6\text{-}Me_2\text{-}2\text{-}CH_2)\}]_2 + 2N_2 \quad (5)$$

Reaction of the metal(I) β-ketiminate monomers with sterically encumbered azide yielded the first stable monomeric imides (see Scheme 1) [28]:

$$\{HC(MeC\{2, 2\text{-}^iPr_2C_6H_3\}N)_2\}M + N_3\text{-}(2, 6\text{-}Trip_2C_6H_3) = [\{HC(MeC\{2, 2\text{-}^iPr_2C_6H_3\}N)_2\}MN\text{-}(2, 6\text{-}Trip_2C_6H_3)] + N_2 \quad (6)$$

Recently, reactions of Ar′MMAr′ dimers (Ar′ = C_6H_3-2,6-$Dipp_2$) with two equivalents of the azide N_3Ar'' (Ar″ = C_6H_3-2,6(Xyl-4-^tBu)$_2$ at 0 °C afforded monomeric imido compounds Ar′MNAr″ with coordination number 2 on both the metal and nitrogen centers [29].

2.3. Metathesis reactions

This synthetic method is mostly used for the synthesis of phosphorus and arsenic-containing compounds. Thus, reaction between doubly lithiated group 15 species Li_2YR' and organometallic group 13 halides X_2MR yields the desired oligomer species $[RMYR']_n$ (R′ = SiR''_3) [30,31]:

$$2X_2MR + 2Li_2YSiR''_3 = 4LiX + [RMYSiR''_3]_2 \quad (7)$$

2.4. Substitution reactions

Due to the presence of an active hydrogen atom on aluminum in $[HAlNR]_n$ imido compounds, substitution reactions are possible. Substitutions by Cl [32], Br [33,34], F [35], Me [36], Et [36], C≡CR [33,34] and $CpFeC_5H_4C{\equiv}C$ [37] have been accomplished. This route provides access to compounds with degrees of oligomerization that are not accessible by other methods. As an example, reactions of $[HAlN^iPr]_6$ with $AlMe_3$ and $AlEt_3$ produce methyl and ethyl substituted hexamer species. By the elimination route (thermolysis reaction of $AlMe_3$ and $AlEt_3$ with $NH_2{}^iPr$) only the corresponding tetramers were achieved [38]. HCl, $HgCl_2$ and $TiCl_4$ were used to obtain partially or fully chlorinated

poly(*N*-alkyliminoalanes), starting from the corresponding hydride derivatives [32]:

$$[HAlNR]_n + nHCl \xrightarrow{Et_2O} [ClAlNR]n + nH_2 \quad (8)$$

$$[HAlNR]_n + \tfrac{n}{2}HgCl_2 \longrightarrow^{Et_2O} [ClAlNR]_n + \tfrac{n}{2}Hg + \tfrac{n}{2}H_2 \quad (9)$$

$$[HAlNR]_n + nTiCl_4 \xrightarrow{n\text{-heptane}} [ClAlNR]_n + nTiCl_3 + \tfrac{n}{2}H_2 \quad (10)$$

A series of Cl, Br-substituted compounds was recently obtained by substitution from $[HAlNCH_2Ph]_6$ [33,34,37]. Six ferrocene units were recently introduced as substituents by Roesky and co-workers to form very unusual compound $[CpFeC_5H_4C{\equiv}CAlNCH_2Ph]_6$ [37]. Only partial substitution of H by F atoms was achieved for the heptameric compound $[HAlNCH_2(1\text{-adamantyl})]_7$ in the reaction with Me_3SnF [35], resulting in $[F_{0.32}H_{0.68}AlNCH_2(1\text{-Ad})]_7$.

Reaction of $[HAlNR]_4$ with $ZpCp_2Me_2$ leads to stepwise substitution of H into Me groups, forming $[Me_{0.22}H_{0.78}AlNR]_4$, $[Me_{0.5}H_{0.5}AlNR]_4$ and $[MeAlNR]_4$ [36]. Reaction was found to show first-order dependence on the concentration of both reagents. Given the lack of evidence for cage opening in imido alanes, the authors proposed the following transition state structure with 5-coordinated Al [36]:

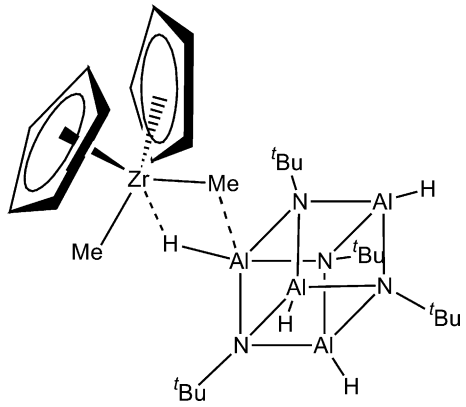

The enthalpy and entropy of activation were obtained in the temperature range of 323–348 K, $\Delta H^{\#} = 104 \pm 1$ kJ mol^{-1}, $\Delta S^{\#} = 18.8 \pm 0.4$ J (mol K)$^{-1}$ [36].

Series of substitution reactions have been performed for the $[HAlNR]_n$ compounds ($n = 4$, 6, 8) by Nöth and Wolfgardt, resulting in full or partially substituted compounds $X_mH_{n-m}[AlNR]_n$ (X = D, Cl, Br, I) [163,164]. The mechanism of a hydrogen/deuterium exchange via formation of intermediates with pentacoordinate aluminum was also discussed [164]. Despite numerous successful examples, the application of substitution reactions is limited due to undesired side processes (cage degradation to form amido compounds) [32]. A cage degradation reaction was also observed in [34] for PhSH with $[HAlNCH_2(C_4H_3S)]_6$, producing the amido compound $[(PhS)_2AlNHCH_2(C_4H_3S)]_2$ instead of the desired $[PhSAlNCH_2(C_4H_3S)]_6$. Theoretical studies [39] suggest that both H substitution reactions and cage degradation reactions with formation of amido compounds are thermodynamically favorable.

2.5. Special reactions

Direct synthesis of polyalkylimidoalanes has been reported [40]. Aluminum reacts with primary amines under hydrogen pressure to form oligomeric compounds:

$$Al + RNH_2 = \tfrac{1}{n}[HAlNR]_n + \tfrac{1}{2}H_2 \quad (11)$$

This reaction does not proceed without an activator, which may be Na, $NaAlH_4$ or $[HAlNR]_6$. Such reactions also require hydrogen pressure. Therefore, it has been assumed that in situ formation of AlH_3 is a necessary condition for the reaction. Reaction of $LiAlH_4$ with $RNH_2{\cdot}HCl$ has also been used to generate imido alanes [41]:

$$LiAlH_4 + RNH_2 \cdot HCl = \tfrac{1}{n}[HAlNR]_n + 3H_2 + LiCl \quad (12)$$

Cucinella et al. [41] report that reaction of $[AlH_3(NMe_3)]$ with nitriles RCN results in the formation of imidoalanes:

$$[AlH_3(NMe_3)] + RCN = \tfrac{1}{n}[HAlNCH_2R]_n + NMe_3 \quad (13)$$

Reactions between $[AlH_3(NMe_3)]$ and nitriles RCN have recently been employed by Roesky and co-workers for the synthesis of various hexamer compounds [33], which were used as a starting materials for different substitution reactions [33,34,37].

3. Structural features of imido compounds

In the following section, experimental and theoretical studies of structural features are described. The major structural parameters are summarized in Tables 1–8, 11–13.

3.1. Monomers

The classical formulae for the monomeric imido compounds and their heavier analogs is RMYR′, in which both the metal and pnictogen centers adopt a coordination number of 2. Consequently, such molecules are expected to exhibit high reactivity, including head-to-tail dimerization. Therefore, in order to protect this low coordination number, a bulky ligand is required on both the groups 13 and 15 centers. Experimental attempts to synthesize such compounds have only recently been successful. Only nitrogen-containing monomer compounds are known at present, and all of them have been obtained using “oxidative addition” reactions:

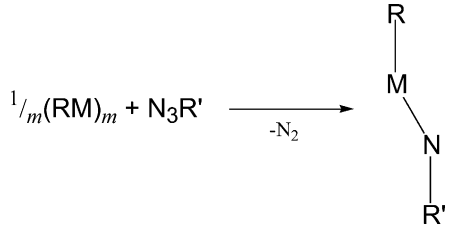

1: M=Ga, R=C_6H_3-2,6-$Dipp_2$, R'=C_6H_3-2,6-(Xyl-4-^{t}Bu)$_2$, m=2 [29]

2: M=In, R=C_6H_3-2,6-$Dipp_2$, R'=C_6H_3-2,6-(Xyl-4-^{t}Bu)$_2$, m=2 [29]

3: M=Al, R=HC(CMe-DippN)$_2$, R'=C_6H_3-2,6-$Trip_2$, m=1 [28]

4: M=Ga, R=HC(CMe-DippN)$_2$, R'=C_6H_3-2,6-$Trip_2$, m=1 [28]

Stable, monomeric imides of Al and Ga with β-diketiminato ligands were reported in 2001. These compounds have the general formulae [{HC(CMeDippN)$_2$}MN-(2,6-$Trip_2C_6H_3$)] [28]. The imido compounds with the β-diketiminato ligand have the following structure:

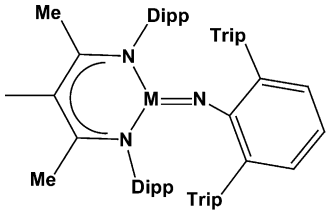

M= Al, Ga

Although these compounds do have a coordination number of 2 on nitrogen, the coordination number 3 is observed for the metal center, so that this compound is not a RMYR′ type. Gallium compound **4** was structurally characterized, and it has a relatively short Ga–N bond length of 1.742 Å [28]. Latent reactivity of such ketimidine stabilized imido compounds has recently been explored (see Scheme 2) [42].

Intramolecular reactions were observed, which include either intramolecular C–H activated addition involving the methyl group of the ^{i}Pr substituent on the β-diketiminato ligand (route a), or cycloaddition of the phenyl ring of the aromatic substituent on imido nitrogen (route b). In both cases, formation of formally monomeric "amido" species A and B, which are thermally stable, was evidenced. Rearrangements of B to A proceed at 50 °C in [D_8]toluene without changing the monomeric nature of the products.

Imido compounds with low coordination number 2 on both metal and nitrogen substituents were reported in 2003 by Power and co-workers [29]. Reaction between recently obtained group 13–13 metal–metal bonded species and azide (0 °C, in hexane) has been used:

$$Ar'MMAr' + 2N_3Ar'' = 2Ar'MNAr'' + 2N_2 \quad (14)$$

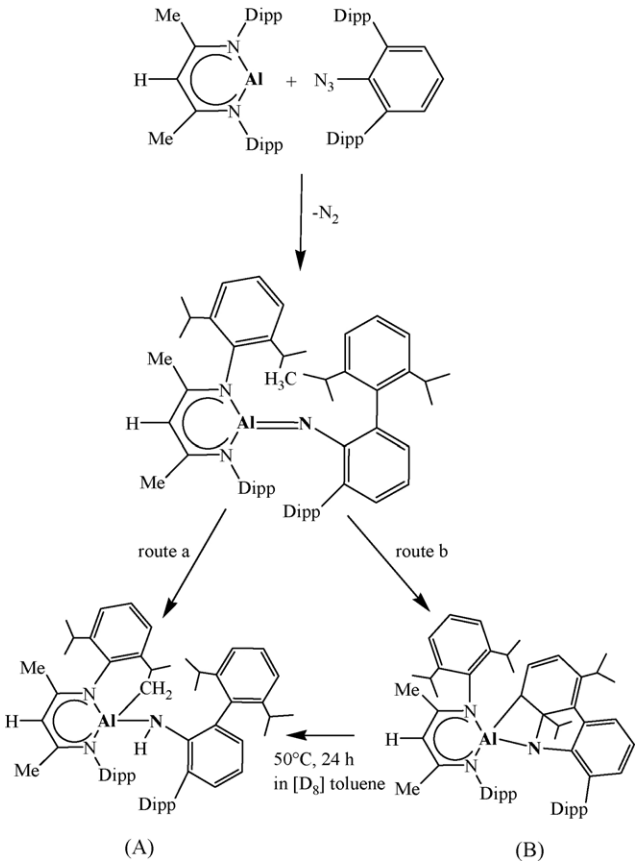

Scheme 2. Latent reactivity of ketimidine stabilized imido compounds.

where M = Ga, In; Ar = C_6H_3-2,6-$Dipp_2$; Ar″ = C_6H_3-2,6(Xyl-4-^{t}Bu$_2$).

Major structural parameters of the compounds are given in Table 1. Molecules Ar′MNAr″ possess distorted geometry, angles at nitrogen are 141.7° and 134.9°; at metal 148.2° and 142.2° for **1** and **2**, respectively. This finding is in contrast to the linearity of boron imides RBNH [43]. The Ga–N bond length in **1** is 1.701 Å, which is considerably shorter than the Ga–N bond length in **4** (1.742 Å).

Summary of theoretical studies of different RMYR′ compounds is given in Table 2. Theoretically predicted Ga–N bond lengths in HGaNH compounds (1.678–1.705, see Table 2) are close to 1.701 Å observed experimentally for **1**. Substitution of the hydrogen atom for a methyl group on the gallium center results in *increase* of the Ga–N bond length of about 0.007 Å (for halogen 0.012 Å), while substitution of the

Table 1
Experimentally structurally characterized monomeric compounds

No.	Compound	M–Y	R–M–Y	M–Y–R″	Comments	Reference
1	(C_6H_3-2,6-$Dipp_2$)GaN{C_6H_3-2,6(Xyl-4-^{t}Bu$_2$)}	1.701	148.2	141.7	Reaction RMMR with N_3Ar''	[29]
2	(C_6H_3-2,6-$Dipp_2$)InN{C_6H_3-2,6(Xyl-4-^{t}Bu$_2$)}	1.928	142.2	134.9	Reaction RMMR with N_3Ar''	[29]
4	{HC(MeCDippN)$_2$}GaN-(2,6-$Trip_2C_6H_3$)	1.742	140.2	134.6	Reaction RM with N_3Ar''	[28]

Bond lengths in angstroms and angles in degrees.

hydrogen atom on the nitrogen center results in *decrease* of the Ga–N distance by about 0.020 Å [44]. Theoretical computations predict that angles at gallium are greater than those at nitrogen, but absolute values differ significantly for different theoretical methods. Note that at lower levels of theory HAlNH is predicted to be linear, while use of the more sophisticated methods results in a bent structure (Fig. 1c). Theoretical methods predict a very low energy difference between linear and bent HMYH isomers (0.1 and 20 kJ mol^{-1} for HAlNH and HGaNH, respectively). As mentioned in [45], "the potential well is extremely shallow with respect to the bending coordinates". This may explain large differences between predicted bond angles at different levels of theory.

An alternative approach to stabilizing monomeric RMYR′ compounds would be matrix isolation experiments at low temperatures. In a series of recent experimental works on reactions of group 13 metals with ammonia [46] and phosphine [47], Himmel et al. investigated products trapped in matrixes. MYH_2 species were observed among the other products, rather than HMYH imido compounds. There are many theoretical works devoted to small compounds of MYH_2 composition. High level ab initio calculations of H–Al–N and H–Al–P systems by Davy and co-workers [48,49] show that MYH_2 isomers are much lower in energy than HMYH. Although the MYH_2 isomer is a global minimum with C_{2v} symmetry (Y = N) (Fig. 1a) or C_s symmetry (Y = P, As) (Fig. 1b), the following trend in the M–Y bond length was observed:

$$M{-}YH_3 > H_3M{-}YH_3 > M{-}YH_2 > HM{-}YH_2 \geq H_2M{-}YH_2 > HM{-}YH$$

with the shortest bond corresponding to HMYH isomers (Fig. 1c and d) [45].

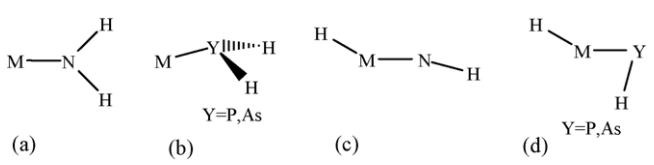

Fig. 1. Structures of HMYH compounds.

All currently synthesized monomeric RMYR′ compounds are imido metallanes, probably due to quite different orientation (distortion) of P, As centers in monomeric compounds (Fig. 1d). Theoretically predicted angles at P and As centers are on average about 90°,[1] which is small compared to imido monomers. Thus, the bulky protective groups, which are sufficient to stabilize monomeric imido compounds, may not be sufficient to stabilize P, As-containing monomers.

3.2. Dimers

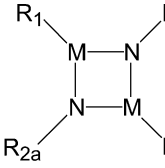

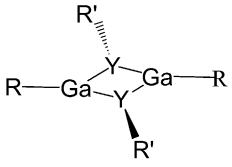

5: M=Al, R_1=η^1-Cp*, R_{1a}=N(SiMe$_3$)$_2$, R_2=Al(η^1-Cp*)$_2$, R_{2a}=Al(η^1-Cp*){N(SiMe$_3$)$_2$} [26]

6a: M=Al, R_1=R_{1a}=Mes*, R_2=R_{2a}=Ph [16a]

6b: M=Al, R_1=R_{1a}=Mes*, R_2=R_{2a}=SiPh$_3$ [16b]

6c: M=Al, R_1=R_{1a}=Mes*, R_2=R_{2a}=SiMe$_3$ [16c]

7: M=Al, R_1=R_{1a}=η^5-Cp, R_2=R_{2a}=Dipp [17]

8: M=Al, R_1=R_{1a}=η^5-Cp*, R_2=R_{2a}=NSi^{i}Pr$_3$ [62]

9: M=Al, R_1=R_{1a}=η^1-Cp*, R_2=R_{2a}=NSiPh$_3$ [62]

10: M=Al, R_1=R_{1a}=η^1-Cp*, R_2=R_{2a}=NSi^{t}Bu$_3$ [62]

11: M=Ga, R_1=R_{1a}=η^1-Cp*, R_2=R_{2a}=Xyl [27]

12: Y=P, R=^{t}Bu, R'=Mes* [58]

13: Y=As, R={Li(THF)$_3$}As(Si^{i}Pr$_3$), R'=Si^{i}Pr$_3$ [63]

25: Y=P, R=PH(Si^{t}Bu$_3$), R'=Si^{t}Bu$_3$ [67]

Dimeric imido compounds have a coordination number 3 on donor and acceptor centers. Structural properties of experimentally known compounds are summarized in Table 3. These compounds can be produced both by metathesis and elimination routes. In [27], compound **11** was obtained by reaction of η^5-Cp*Ga with XylN$_3$. Different reaction products are formed in comparable reactions with (Cp*Al)$_4$, which range from dimeric imido alanes [62] to unsymmetrical imido alane **5** after complicated rearrangements [26]. Reaction with *o*-methylated phenyl azide does not yield imido alane, but the product of subsequent C–H activation [26]. All donor-free compounds have an essentially planar M_2Y_2 core, both nitrogen and metal centers retain planarity, while P, As atoms in **12** and **13** have a pyramidal environment.

Table 4 summarizes results of the theoretical studies of dimer molecules. All nitrogen-containing rings are planar with D_{2h} symmetry (Fig. 2a), while for P, As compounds two isomers are possible (Fig. 2b and c). Interestingly,

[1] Note that predicted MYH angles significantly depend on the basis set used: for example, for HGaAsH GaAsH angle varies from 119.7° at B3LYP/LANL2DZ(d,p) [39] to 81.6° at B3LYP/TZP [50].

Table 2
Summary of theoretical studies of monomeric RMYR′ compounds

RMYR′		r_{MY}	RMY	MYR′	μ	S°_{298}	Method	Reference
HAlNH	C_s	1.627	167.2	157.4			B3LYP/6-311G(d)	[45]
HAlNH	C_s	1.654	–	–			B3LYP/6-31G*	[51]
HAlNH	$C_{\infty v}$	1.597	180.0	180.0			RHF/6-31G*	[52]
HAlNH	C_s	1.615	179.8	179.8	2.18	211.3	B3LYP/LANL2DZ(d,p)	[39]
HAlNH	C_s	1.633	165.2	154.5			CCSD/TZ2P	[49]
HAlNH	C_s	1.629	179.9	179.8			CCSD(T)/cc-pVTZ	[39]
HAlNH	C_s	1.637	166.8	157.9	2.51	243.0	B3LYP/TZVP	[50]
(CH_3)AlNH	$C_{\infty v}$	1.621	180.0	180.0	2.81	296.2	B3LYP/pVDZ	[53]
HAlN(CH_3)	$C_{\infty v}$	1.626	180.0	180.0	1.69	285.6	B3LYP/pVDZ	[53]
FAlNH	C_s	1.659	158.7	132.2	2.02	266.3	B3LYP/LANL2DZ(d,p)	[39]
ClAlNH	C_s	1.687	158.2	127.1	3.20	278.3	MP2/DZP	[54]
ClAlNH	C_s	1.675	158.9	128.0	2.20	279.2	B3LYP/DZP	[54]
ClAlNH	C_s	1.651	159.0	136.8	2.03	278.8	B3LYP/LANL2DZ(d,p)	[39]
ClAlNH	C_s	1.677					B3LYP/6-31G*	[55]
BrAlNH	C_s	1.652	159.4	137.2	2.21	290.3	B3LYP/LANL2DZ(d,p)	[39]
IAlNH	C_s	1.652	159.8	138.7	2.46	298.7	B3LYP/LANL2DZ(d,p)	[39]
HGaNH	C_s	1.699	141.9	140.7			B3LYP/6-311G(d)	[45]
HGaNH	C_s	1.678	159.4	131.3	2.81	251.2	B3LYP/LANL2DZ(d,p)	[39]
HGaNH	C_s	1.694	161.5	126.0	2.45	251.1	B3LYP/pVDZ	[44]
HGaNH	C_s	1.705	161.2	123.6	2.99	251.2	B3LYP/TZVP	[50]
(CH_3)GaNH	C_s	1.701	161.7	123.9	3.36	309.8	B3LYP/pVDZ	[44]
HGaN(CH_3)	C_s	1.676	158.1	151.7	1.61	297.0	B3LYP/pVDZ	[44]
(CH_3)GaN(CH_3)	C_s	1.682	158.3	149.6	2.69	360.0	B3LYP/pVDZ	[44]
FGaNH	C_s	1.706	160.3	114.8	1.97	277.1	B3LYP/LANL2DZ(d,p)	[39]
ClGaNH	C_s	1.706	160.3	116.2	2.13	290.1	B3LYP/LANL2DZ(d,p)	[39]
ClGaNH	C_s	1.713	162.6	112.3			B3P86/6-311G(d,p)	[56]
ClGaNH	C_s	1.722	162.3	112.4	1.91	289.3	B3LYP/pVDZ	[57]
BrGaNH	C_s	1.706	160.5	116.7	2.33	301.8	B3LYP/LANL2DZ(d,p)	[39]
IGaNH	C_s	1.707	161.0	117.4	2.60	310.0	B3LYP/LANL2DZ(d,p)	[39]
HInNH	C_s	1.835	135.9	136.9			B3LYP/LANL2DZ(d)	[45]
HInNH	C_s	1.847	158.7	123.9	3.15	260.6	B3LYP/LANL2DZ(d,p)	[39]
HInN(CH_3)	C_s	1.919	149.9	142.7	2.01	305.1	B3LYP/pVDZ	[53]
FInNH	C_s	1.876	167.0	106.9	1.82	286.9	B3LYP/LANL2DZ(d,p)	[39]
ClInNH	C_s	1.877	158.4	113.0	2.09	301.5	B3LYP/LANL2DZ(d,p)	[39]
BrInNH	C_s	1.878	159.0	113.2	2.20	312.9	B3LYP/LANL2DZ(d,p)	[39]
IInNH	C_s	1.879	159.7	113.5	2.40	321.1	B3LYP/LANL2DZ(d,p)	[39]
HAlPH	C_s	2.149	177.0	76.4			CCSD/TZ2P	[48]
HAlPH	C_s	2.154	177.1	75.6			CCSD(T)/cc-pVTZ	[39]
HAlPH	C_s	2.152	179.3	80.2	3.01	263.5	B3LYP/TZVP	[50]
HAlPH	C_s	2.154	177.1	84.3			B3LYP/6-311G(d)	[45]
HAlPH	C_s	2.157	178.9	82.0	2.89	264.4	B3LYP/LANL2DZ(d,p)	[39]
FAlPH	C_s	2.181	139.0	112.7	2.47	289.6	B3LYP/LANL2DZ(d,p)	[39]
ClAlPH	C_s	2.157	178.1	82.0	1.65	301.8	B3LYP/LANL2DZ(d,p)	[39]
BrAlPH	C_s	2.164	174.2	85.1	2.04	312.7	B3LYP/LANL2DZ(d,p)	[39]
IAlPH	C_s	2.162	178.2	82.2	2.36	320.7	B3LYP/LANL2DZ(d,p)	[39]
HGaPH	C_s	2.149	177.8	85.0	2.70	271.0	B3LYP/TZVP	[50]
HGaPH	C_s	2.145	177.3	85.9			B3LYP/6-311G(d)	[45]
HGaPH	C_s	2.167	142.5	117.0	2.54	272.4	B3LYP/LANL2DZ(d,p)	[39]
FGaPH	C_s	2.194	153.8	101.7	1.64	298.9	B3LYP/LANL2DZ(d,p)	[39]
ClGaPH	C_s	2.175	177.2	84.3	1.10	308.6	B3LYP/LANL2DZ(d,p)	[39]
BrGaPH	C_s	2.176	178.0	83.7	1.42	320.8	B3LYP/LANL2DZ(d,p)	[39]
IGaPH	C_s	2.185	165.6	91.9	1.85	330.7	B3LYP/LANL2DZ(d,p)	[39]
HInPH	C_s	2.335	114.7	98.4			B3LYP/LANL2DZ(d)	[45]
HInPH	C_s	2.346	146.4	111.9	3.02	282.4	B3LYP/LANL2DZ(d,p)	[39]
FInPH	C_s	2.375	142.3	107.6	2.39	314.2	B3LYP/LANL2DZ(d,p)	[39]
ClInPH	C_s	2.356	169.8	89.4	1.10	320.8	B3LYP/LANL2DZ(d,p)	[39]
BrInPH	C_s	2.359	168.0	90.1	1.41	333.9	B3LYP/LANL2DZ(d,p)	[39]
IInPH	C_s	2.355	177.1	85.3	1.60	340.3	B3LYP/LANL2DZ(d,p)	[39]
HAlAsH	C_s	2.242	174.6	73.4	2.50	277.1	B3LYP/TZVP	[50]
HAlAsH	C_s	2.258	177.2	77.5	2.57	277.6	B3LYP/LANL2DZ(d,p)	[39]
FAlAsH	C_s	2.291	129.6	116.6	2.36	305.2	B3LYP/LANL2DZ(d,p)	[39]

Table 2 (*Continued*)

RMYR′		r_{MY}	RMY	MYR′	μ	S°_{298}	Method	Reference
ClAlAsH	C_s	2.280	146.3	103.4	1.87	315.6	B3LYP/LANL2DZ(d,p)	[39]
BrAlAsH	C_s	2.281	150.0	100.6	1.89	327.6	B3LYP/LANL2DZ(d,p)	[39]
IAlAsH	C_s	2.279	163.9	91.5	2.01	333.9	B3LYP/LANL2DZ(d,p)	[39]
HGaAsH	C_s	2.245	179.8	81.6	2.27	284.0	B3LYP/TZVP	[50]
HGaAsH	C_s	2.272	137.2	119.7	2.23	286.4	B3LYP/LANL2DZ(d,p)	[39]
HGaAsMe	C_s	2.251	174.6	100.5	–	–	RHF/HUZSP*	[160]
FGaAsH	C_s	2.283	178.9	81.7	0.34	310.6	B3LYP/LANL2DZ(d,p)	[39]
ClGaAsH	C_s	2.282	179.1	81.8	0.69	322.4	B3LYP/LANL2DZ(d,p)	[39]
BrGaAsH	C_s	2.284	179.1	81.7	1.02	334.4	B3LYP/LANL2DZ(d,p)	[39]
IGaAsH	C_s	2.285	179.3	81.8	1.39	342.4	B3LYP/LANL2DZ(d,p)	[39]
HInAsH	C_s	2.447	139.8	115.5	2.01	296.8	B3LYP/LANL2DZ(d,p)	[39]
FInAsH	C_s	2.486	136.3	110.6	2.28	330.4	B3LYP/LANL2DZ(d,p)	[39]
ClInAsH	C_s	2.470	152.1	98.6	1.58	340.2	B3LYP/LANL2DZ(d,p)	[39]
BrInAsH	C_s	2.468	158.5	94.6	1.32	350.7	B3LYP/LANL2DZ(d,p)	[39]
IInAsH	C_s	2.473	172.9	91.6	1.21	348.8	B3LYP/LANL2DZ(d,p)	[39]

Structural parameters (bond lengths in angstroms and angles in degrees), dipole moments, μ, in Debye and standard entropies S°_{298} in J (mol K)$^{-1}$.

Table 3
Experimentally structurally characterized dimeric [RMYR′]$_2$ compounds

No.	Compound	M—Y	Y—M—Y	M—Y—M	Comments	Reference
5	η^1-Cp*{(Me$_3$Si)$_2$N}AlN(μ-Alη^1-Cp*)(μ-Al{N(SiMe$_3$)$_2$}NAl(η^1-Cp*)$_2$	1.803–1.819; 1.811 mean	95.5–95.6	84.2–84.3	Oxidative addition at 70 °C; (Cp*Al)$_4$ + Me$_3$SiN$_3$	[26]
6a	[Mes*AlNPh]$_2$	1.824	88.75	91.25	Thermolysis of (H$_2$AlMes*)$_2$ and NH$_2$Ph at 125 °C	[16a]
6b	[Mes*AlNSiPh$_3$]$_2$	1.841–1.842	93.3	86.7	Thermolysis of (H$_2$AlMes*)$_2$ and NH$_2$SiPh$_3$ at 125 °C	[16b]
7	[(η^5-Cp)AlNDipp]$_2$	1.796–1.811; 1.804 mean	89.2	90.8	Thermolysis of AlCp$_3$ + amine; [(η^5-C$_5$H$_5$)$_2$AlNH (2,6-^{i}Pr$_3$C$_6$H$_3$)]$_{2,3}$ as intermediates	[17]
10	[Cp*AlNSi^{t}Bu$_3$]$_2$	1.835–1.842	92.9–93.2	85.2	Oxidative addition at 50–75 °C; (Cp*Al)$_4$ + ^{t}Bu$_3$SiN$_3$	[62]
11	[η^1-Cp*GaNXyl]$_2$	1.850–1.870	89.2	90.8	Cp*Ga with azides	[27]
12	[^{t}BuGaPMes*]$_2$	2.274	93.1	86.9	Thermolysis at 110 °C; (^{t}BuGa(PH(2,4,6-^{t}Bu)C$_6$H$_2$)$_2$	[58]
13	[{Li(THF)$_3$AsSi^{i}Pr$_3$}GaAsSi^{i}Pr$_3$]$_2$	2.473–2.436	98.4	81.6	GaCl$_3$ + Li$_2$AsSi^{i}Pr$_3$ THF/heptane	[63]
14	[ClAlPSi^{i}Pr$_3$]$_2$·2Py	2.320–2.336	101.1	78.9	From ladder **L1** by acting Py	[64]
15	[(2,6-CH$_2$NMe$_2$)C$_6$H$_3$GaPSiPh$_3$]$_2$; intramolecular DA stabilized	2.388	94.25	85.75	Li$_2$PSiPh$_3$ + Cl$_2$Ga(2,6-CH$_2$NMe$_2$)C$_6$H$_3$	[31]
16	[ClGaPSiMe$_3$]$_2$·2(P^{t}Bu$_2$Me); DA stabilized	2.351–2.361; mean 2.356	98.1	79.7	GaCl$_3$P^{t}Bu$_2$Me + Li$_2$PSiMe$_3$	[23]
17	[HAlAsSi^{i}Pr$_3$]$_2$·2NMe$_3$; DA stabilized	2.447	100.4	76.2	H$_3$AlNMe$_3$ + H$_2$AsSi^{i}Pr$_3$, 35 °C	[65]
18	[ClAlAsSi(CMe$_2$^{i}Pr)Me$_2$]$_2$·2NEt$_3$	2.432–2.454; mean 2.444	101.8–102.3	76.7–77.1	From ladder **L3** by acting NEt$_3$	[64]
19	[ClGaAsSiMe$_3$]$_2$·2P^{t}Bu$_2$Me; DA stabilized	2.443–2.453; mean 2.448	99.1	78.3	GaCl$_3$P^{t}Bu$_2$Me + As(SiMe$_3$)$_3$	[23]
20	[^{t}BuGaAsC$_6$H$_3$(CH$_2$NMe$_2$)$_2$]$_2$; intramolecular stabilized dimer	2.457	98.8	81.3	[^{t}BuGaCl$_2$]$_2$ + Li$_2$AsC$_6$H$_3$ (CH$_2$NMe$_2$)$_2$; in Et$_2$O	[61]
21	[ClGaSbSi^{i}Pr$_3$]$_2$·2PPh^{n}Pr$_2$	2.635–2.651; mean 2.641	98.4–99.0	75.1–75.3	GaCl$_3$PPh^{n}Pr$_2$ + Sb(SiMe$_3$)$_2$Si^{i}Pr$_3$	[66]
25	[^{t}Bu$_3$SiP(H)-GaPSi^{t}Bu$_3$]$_2$; P inequivalent, heteroallyl structure	2.252–2.338; mean 2.297	97.7	84.1	Metathesis GaCl$_3$ + 3K^{t}Bu$_3$SiPH	[67]
	Cp*Al(P^{t}Bu)$_3$	2.359–2.360	90.9		(Cp*Al)$_4$ + ^{t}Bu$_3$P	[68]

Bond lengths in angstroms and angles in degrees.

Table 4
Summary of theoretical studies of dimeric $[RMYR']_2$ compounds

$[RMYR']_2$	Point group	r_{MY}	YMY	MYM	μ	S°_{298}	Method	Reference
$[HAlNH]_2$	D_{2h}	1.803	90.8	89.2	0	–	CCSD/DZP	[70]
$[HAlNH]_2$	D_{2h}	1.812	90.9	89.1	0	–	CCSD(T)/cc-pVTZ	[39]
$[HAlNH]_2$	D_{2h}	1.800	90.7	89.3	0	–	RHF/6-31G*	[52]
$[HAlNH]_2$	D_{2h}	1.813	90.9	89.1	0	–	B3LYP/6-31G*	[51]
$[HAlNH]_2$	D_{2h}	1.806	91.0	89.0	0	290.9	B3LYP/LANL2DZ(d,p)	[39]
$[HAlN(CH_3)]_2$	C_{2h}	1.815; 1.821	92.1	87.9	0	395.2	B3LYP/pVDZ	[53]
$[(CH_3)AlNH]_2$	C_{2h}	1.814	90.9	89.1	0	409.7	B3LYP/pVDZ	[53]
$[FAlNH]_2$	D_{2h}	1.795	91.8	88.2	0	336.2	B3LYP/LANL2DZ(d,p)	[39]
$[ClAlNH]_2$	D_{2h}	1.809	91.3	88.7	0	–	MP2/DZP	[54]
$[ClAlNH]_2$	D_{2h}	1.804	91.5	88.5	0	–	B3LYP/DZP	[54]
$[ClAlNH]_2$	D_{2h}	1.804				–	B3LYP/6-31G*	[55]
$[ClAlNH]_2$	D_{2h}	1.796	91.6	88.4	0	361.2	B3LYP/LANL2DZ(d,p)	[39]
$[BrAlNH]_2$	D_{2h}	1.797	91.5	88.5	0	385.3	B3LYP/LANL2DZ(d,p)	[39]
$[IAlNH]_2$	D_{2h}	1.798	91.4	88.6	0	402.6	B3LYP/LANL2DZ(d,p)	[39]
$[HGaNH]_2$	D_{2h}	1.864	88.1	91.9	0	320.2	B3LYP/pVDZ	[71]
$[HGaNH]_2$	D_{2h}	1.846	88.8	91.2	0	316.6	B3LYP/LANL2DZ(d,p)	[39]
$[HGaN(CH_3)]_2$	C_{2h}	1.867	89.2	90.8	0	423.0	B3LYP/pVDZ	[71]
$[(CH_3)GaNH]_2$	C_{2h}	1.868	87.9	92.1	0	440.6	B3LYP/pVDZ	[71]
$[FGaNH]_2$	D_{2h}	1.834	90.2	89.8	0	362.6	B3LYP/LANL2DZ(d,p)	[39]
$[ClGaNH]_2$	D_{2h}	1.836	90.0	90.0	0	388.0	B3LYP/LANL2DZ(d,p)	[39]
$[ClGaNH]_2$	D_{2h}	1.856	89.6	90.4	0	391.8	B3LYP/pVDZ	[57]
$[ClGaNH]_2$	D_{2h}	1.844	89.7	90.4	0		B3P86/6-311G(d,p)	[56]
$[BrGaNH]_2$	D_{2h}	1.837	89.9	90.1	0	412.6	B3LYP/LANL2DZ(d,p)	[39]
$[IGaNH]_2$	D_{2h}	1.839	89.8	90.2	0	429.8	B3LYP/LANL2DZ(d,p)	[39]
$[HInNH]_2$	D_{2h}	2.011	85.5	94.5	0	337.4	B3LYP/LANL2DZ(d,p)	[39]
$[HInN(CH_3)]_2$	C_{2h}	2.088	85.9	94.1	0	440.3	B3LYP/pVDZ	[53]
$[(CH_3)InNH]_2$	C_{2h}	2.082	84.2	95.8	0	476.0	B3LYP/pVDZ	[53]
$[FInNH]_2$	D_{2h}	2.002	86.9	93.1	0	387.4	B3LYP/LANL2DZ(d,p)	[39]
$[ClInNH]_2$	D_{2h}	2.001	86.9	93.1	0	413.3	B3LYP/LANL2DZ(d,p)	[39]
$[BrInNH]_2$	D_{2h}	2.003	86.7	93.3	0	437.2	B3LYP/LANL2DZ(d,p)	[39]
$[IInNH]_2$	D_{2h}	2.005	86.6	93.4	0	454.1	B3LYP/LANL2DZ(d,p)	[39]
cis$[HAlPH]_2$	C_{2v}	2.298	95.6	76.3	–	–	CCSD/DZP	[72]
trans$[HAlPH]_2$	C_{2h}	2.317	97.7	82.3	–	–	CCSD/DZP	[72]
cis$[HAlPH]_2$	C_{2v}	2.273	90.7	76.1	–	–	CCSD(T)/cc-pVTZ	[39]
cis$[HAlPH]_2$	C_{2v}	2.339	95.2	75.0	1.80	341.3	B3LYP/LANL2DZ(d,p)	[39]
cis$[FAlPH]_2$	C_{2v}	2.342	99.5	73.4	0.78	390.8	B3LYP/LANL2DZ(d,p)	[39]
cis$[ClAlPH]_2$	C_{2v}	2.341	98.7	73.7	0.74	414.6	B3LYP/LANL2DZ(d,p)	[39]
cis$[BrAlPH]_2$	C_{2v}	2.343	98.3	73.9	0.88	438.7	B3LYP/LANL2DZ(d,p)	[39]
cis$[IAlPH]_2$	C_{2v}	2.344	98.0	73.9	0.98	456.1	B3LYP/LANL2DZ(d,p)	[39]
cis$[HGaPH]_2$	C_{2v}	2.365	94.5	75.2	1.50	363.7	B3LYP/LANL2DZ(d,p)	[39]
cis$[FGaPH]_2$	C_{2v}	2.381	101.7	73.3	0.13	416.7	B3LYP/LANL2DZ(d,p)	[39]
cis$[ClGaPH]_2$	C_{2v}	2.377	100.5	73.8	0.25	440.6	B3LYP/LANL2DZ(d,p)	[39]
cis$[BrGaPH]_2$	C_{2v}	2.378	100.0	73.9	0.35	464.0	B3LYP/LANL2DZ(d,p)	[39]
cis$[IGaPH]_2$	C_{2v}	2.378	99.4	74.1	0.49	480.4	B3LYP/LANL2DZ(d,p)	[39]
cis$[\{H_2P\}GaPH]_2$	–	2.390	96.7	75.0	–	–	B3LYP/6-31G(d,p) (ECP on gallium)	[67]
cis$[\{SiH_3(H)P\}GaP\{SiH_3\}]_2$	–	2.380	97.5	77.1	–	–	B3LYP/6-31G(d,p) (ECP on gallium)	[67]
cis$[\{SiMe_3(H)P\}GaP\{SiMe_3\}]_2$	–	2.368; 2.378	97.8	77.8	–	–	B3LYP/6-31G(d,p) (ECP on gallium)	[67]
cis$[HInPH]_2$	C_{2v}	2.553	93.6	77.7	1.68	388.9	B3LYP/LANL2DZ(d,p)	[39]
cis$[FInPH]_2$	C_{2v}	2.577	102.1	76.0	0.30	443.5	B3LYP/LANL2DZ(d,p)	[39]
cis$[ClInPH]_2$	C_{2v}	2.573	101.2	76.0	0.15	467.3	B3LYP/LANL2DZ(d,p)	[39]
cis$[BrInPH]_2$	C_{2v}	2.574	100.6	76.1	0.24	490.4	B3LYP/LANL2DZ(d,p)	[39]
cis$[IInPH]_2$	C_{2v}	2.574	100.0	76.3	0.36	506.6	B3LYP/LANL2DZ(d,p)	[39]
cis$[HAlAsH]_2$	C_{2v}	2.459	97.9	72.2	1.11	368.7	B3LYP/LANL2DZ(d,p)	[39]
cis$[FAlAsH]_2$	C_{2v}	2.467	103.5	71.2	0.06	420.0	B3LYP/LANL2DZ(d,p)	[39]
cis$[ClAlAsH]_2$	C_{2v}	2.464	102.2	71.4	0.07	443.0	B3LYP/LANL2DZ(d,p)	[39]
cis$[BrAlAsH]_2$	C_{2v}	2.466	101.9	71.6	0.08	467.3	B3LYP/LANL2DZ(d,p)	[39]
cis$[IAlAsH]_2$	C_{2v}	2.467	101.5	71.7	0.19	484.7	B3LYP/LANL2DZ(d,p)	[39]

Table 4 (*Continued*)

$[RMYR']_2$	Point group	r_{MY}	YMY	MYM	μ	S°_{298}	Method	Reference
cis$[HGaAsH]_2$	C_{2v}	2.480	96.9	72.8	0.96	391.3	B3LYP/LANL2DZ(d,p)	[39]
cis$[FGaAsH]_2$	C_{2v}	2.501	105.5	72.0	0.39	447.7	B3LYP/LANL2DZ(d,p)	[39]
cis$[ClGaAsH]_2$	C_{2v}	2.497	104.3	72.3	0.33	469.7	B3LYP/LANL2DZ(d,p)	[39]
cis$[BrGaAsH]_2$	C_{2v}	2.498	103.6	72.3	0.26	493.1	B3LYP/LANL2DZ(d,p)	[39]
cis$[IGaAsH]_2$	C_{2v}	2.498	103.0	72.4	0.15	509.4	B3LYP/LANL2DZ(d,p)	[39]
cis$[HInAsH]_2$	C_{2v}	2.664	97.0	75.4	0.95	415.7	B3LYP/LANL2DZ(d,p)	[39]
cis$[FInAsH]_2$	C_{2v}	2.687	105.2	74.7	0.03	470.7	B3LYP/LANL2DZ(d,p)	[39]
cis$[ClInAsH]_2$	C_{2v}	2.684	104.9	74.7	0.17	496.1	B3LYP/LANL2DZ(d,p)	[39]
cis$[BrInAsH]_2$	C_{2v}	2.686	104.5	74.9	0.14	520.7	B3LYP/LANL2DZ(d,p)	[39]
cis$[IInAsH]_2$	C_{2v}	2.687	104.1	75.0	0.15	537.6	B3LYP/LANL2DZ(d,p)	[39]

Structural parameters (bond lengths in angstroms and angles in degrees), dipole moments, μ, in Debye and standard entropies S°_{298} in J (mol K)$^{-1}$.

planar C_{2h} isomers are always higher in energy, but the energy difference is very small (5–20 kJ mol^{-1} in favor of the C_{2v} symmetric structures) [59]. Thus, on the basis of the theoretical predictions, *cis*-structures with a non-planar M_2Y_2 core (Fig. 2b) are more stable for Y = P, As. Nevertheless, structurally characterized dimers **12** and **13** are effectively C_{2h} symmetric structures, probably due to the bulky substituents, which favor *trans*-orientation of the bulky ligands in the crystal structure. Compound **13** is believed to be stabilized by Ga=As double bonds to terminal As atoms, in contrast to intramolecular stabilization found for the donor–acceptor stabilized dimers [63]. A phosphorus "heteroallyl" structure **25** was recently reported [67]. Two phosphorus atoms in Ga_2P_2 ring of **25** are inequivalent: one adopts a planar coordination, while the other is pyramidal. Theoretical study of all possible isomers of model compounds $[R(H)PGaPR]_2$ (R = H, SiH_3, $SiMe_3$) reveals that they are very close in energy (the maximal energy difference is less than 18 kJ mol^{-1}) and the *cis* isomer (Fig. 2b) is the most stable in all cases [67].

On the basis of the experimental findings (bond lengths and sum of valence angles on P atom), the structure of the chemical bonding in $[RGaPR']_2$ dimers is believed to be close to A rather than B type [58], see Scheme 3. A more complicated picture occurs with phosphorus-containing substituent on the gallium center. To explain the experimentally observed inequality of two P atoms in the Ga_2P_2 ring in **25**, five resonance structures have been suggested on the basis of NBO analysis [67].

To prevent dimerization processes, bulky substituents have been employed on both 13 and 15 centers. Alternatively, a donor–acceptor stabilization of the product is necessary. Donor–acceptor stabilization may be achieved by using both external donor ligands or by intramolecular interactions. Since there are two possible isomers for $[RMYR']_2$ compounds (Fig. 2b and c), their interaction with donor molecules results in two isomers. Upon coordination of the donor molecules, metal atoms adopt a tetrahedral environment. As a result, for the *cis*-orientation of the donor molecules, the M_2Y_2 ring is distorted upon coordination, while for the *trans*-orientation of donor molecules, the M_2Y_2 ring remains essentially planar.

Examples of donor–acceptor stabilized dimeric rings are summarized in the following chart:

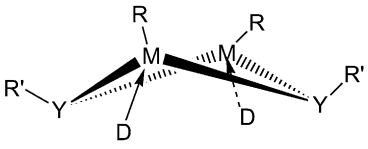

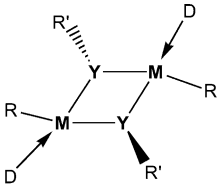

16: M=Ga, Y=P, R=Cl, R'=$SiMe_3$, D=P^{t}Bu$_2$Me [23]
17: M=Al, Y=As, R=H, R'=Si^{i}Pr$_3$, D=NMe_3 [65]
18: M=Al, Y=As, R=Cl, R'=Si(CMe$_2$^{i}Pr)Me$_2$, D=NEt_3 [64]
19: M=Ga, Y=As, R=Cl, R'=$SiMe_3$, D=P^{t}Bu$_2$Me [23]
21: M=Ga, Y=Sb, R=Cl, R'=Si^{i}Pr$_3$, D=P^{n}Pr$_2$Ph [66]
22: M=Al, Y=As, R=H, R'=Si(CMe$_2$^{i}Pr)Me$_2$, D=NMe_3 [65]

14: M=Al, Y=P, R=Cl, R'=Si^{i}Pr$_3$, D=Py [64]
15: M=Ga, Y=P, R=2,6-$(CH_2NMe_2)_2C_6H_3$, R'=$SiPh_3$, D=R (intramolecular stabilization) [31]
20: M=Ga, Y=As, R=^{t}Bu, R'=2,6-$(CH_2NMe_2)_2C_6H_3$, D=R' (intramolecular stabilization) [61]
23: M=Al, Y=N, R=H, R'=Dipp, D=NMe_3 [60]
24: M=Al, Y=N, R=H, R'=Dipp, D=$NEtMe_2$ [60]

Intramolecular interactions lead to higher stability of the compounds. Thus, compound **20** is reported to be air and moisture stable [61]. Note that its intramolecular stabilization comes from a substituent on the 15 center (As), while in **15** the same substituent is located on Ga center [31]. Donor–acceptor bond lengths in **20** (2.18 Å) are similar to those in 13–15 adducts such as $GaMe_3$–NH_2^{t}Bu (2.12 Å) and ^{t}Bu$_3$Ga–NH_2Ph (2.246 Å) [61]. In both **15** and **20**, *trans*-

orientation of the substituents leads to essentially planar Ga_2P_2 and Ga_2As_2 cores, respectively.

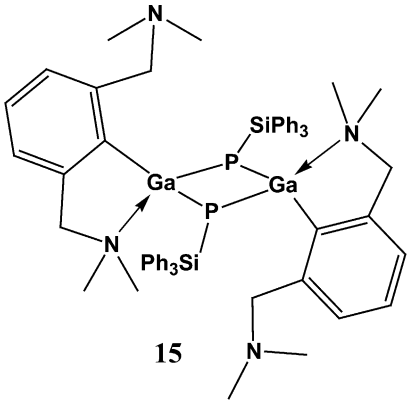

15

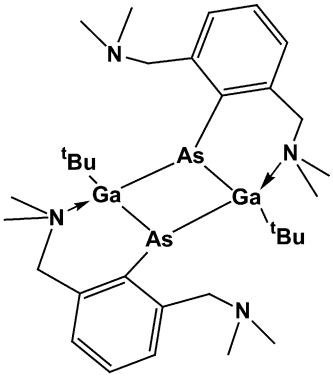

20

The strong tendency towards oligomerization of dimeric imido compounds can be illustrated by mass spectrometry study of $[HAlNDipp]_2{\cdot}2NMe_3$ and $[HAlNDipp]_2{\cdot}2NMe_2Et$. For these compounds, a molecular ion peak is not present in electron ionization mass spectra, but a fragment peak of *m*/*z* 812 was observed, indicating formation of the heterocubane $[HAlNDipp]_4$, presumably by dimerization after the loss of the NMe_3 donor molecules [60]. Formation of high mass aggregates (with Ga_3As_6 core) was indicated by negative-ion electrospray mass spectrometry of **13** [63]. High tendency to dimerization is also evident in the structure of the dimer **5**, which is in essence a rearranged form of cubic $[Cp^*AlNSiMe_3]_4$ [26]. While MS data cannot distinguish between an Al–N heterocubane and a dimeric imido metallane, crystal structure determination of **5** verified the presence of a dimeric compound [26].

Several other ring compounds can be mentioned which contain an MR group bonded to two group 15 elements. Compound $[Cp^*Al(P^tBu)_3]$ has an AlP_3 core with only one substituent on each center [68]. Reaction of cubane $[MeAlNMes]_4$ with $Li[PH(C_6H_{11})]$ leads to an imido anion which features two Al_2P_2 units bridged by PR ligands [129].

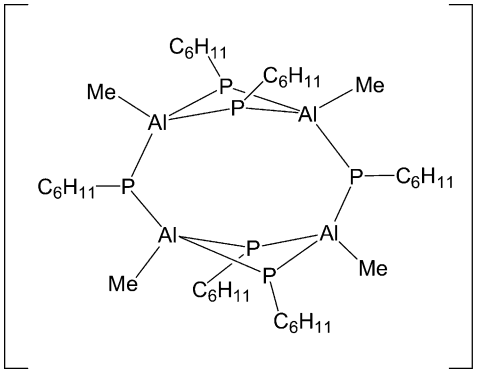

4-

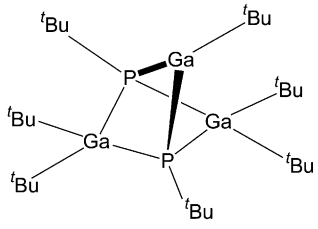

In [69], an unusual structure was reported with a Ga_3P_2 core featuring one GaR and two PR groups, as well as two GaR_2 groups. Formally, it can be considered as a product of the interaction between a $[^tBuGaP^tBu]_2$ dimer and one Ga^tBu_3 molecule.

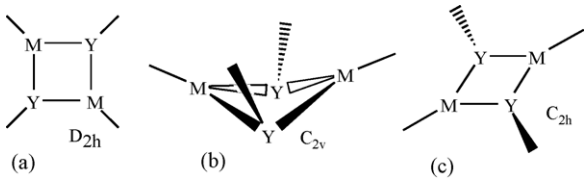

Fig. 2. Structures of $[RMYR']_2$ isomers.

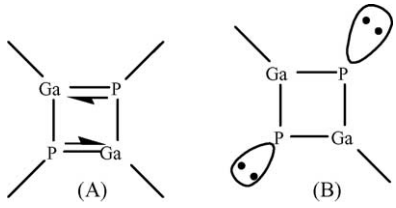

Scheme 3. Representation of chemical bonding in $[RGaPR']_2$ dimers.

Table 5
Experimentally structurally characterized trimeric $[RMYR']_3$ compounds

No.	Compound	M—Y	Y—M—Y	M—Y—M	Comments	Reference
26	$[MeAlN(2,6\text{-}^{i}Pr_2C_6H_3)]_3$	1.782	115.3	124.7	Thermolysis $AlMe_3 + H_2N2,6\text{-}^{i}Pr_2C_6H_3$ (thermolysis at 170 °C of dimeric aminoalane)	[73,18]
27	$[Mes^*AlPPh]_3$	2.323–2.336	103.1, 114.6, 118.9	108.1, 111.6, 113.4	Thermolysis of $(H_2AlMes^*)_2$ and PH_2Ph at 160 °C	[16]
28	$[Mes^*AlAsPh]_3$	2.418–2.435	101.3, 104.5, 121.0	108.4, 109.4, 116.1	Thermolysis of $(H_2AlMes^*)_2$ and AsH_2Ph at 140–160 °C	[16]
29	$[2,4,6\text{-}Ph_3C_6H_2GaP(cyclo\text{-}C_6H_{11})]_3$	2.279–2.338	118.6, 120.6, 114.7	108.5, 108.3, 103.9	$(2,4,6\text{-}Ph_3C_6H_2)GaCl_2 + Li_2P(cyclo\text{-}C_6H_{11})$ in Et_2O/toluene	[30]

Bond lengths in angstroms and angles in degrees.

3.3. Trimers

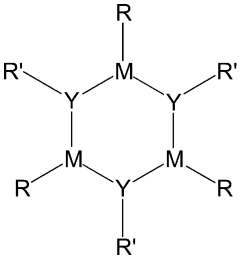

26: M=Al, Y=N, R=Me, R'=Dipp [18], [73]
27: M=Al, Y=P, R=Mes*, R'=Ph [16]
28: M=Al, Y=As, R=Mes*, R'=Ph [16]
29: M=Ga, Y=P, R=-C_6H_2-2,4,6-Ph_3, R'=*cyclo*-C_6H_{11} [30]

Structural parameters of known trimeric compounds are given in Table 5. In contrast to dimer $[RMYR']_2$ and tetramer $[RMYR']_4$ species, experimentally known trimeric imido metallanes (inorganic benzenes) and their analogs are still rare. They are known for N, P, As but numerous attempts to prepare their analogs have failed. It is believed that Power's compound $[MeAlN(2,6\text{-}^{i}Pr_2C_6H_3)]_3$ (**26**) possesses the optimal combination of the steric parameters of the ligands. More bulky ligands will favor dimer formation, while less bulky ligands will result in tetrameric or hexameric species. Note that in contrast to scarce examples of group 13 metals, boron-containing trimers (borazine and its substituted analogs) are numerous [14].

Table 6 summarizes data on theoretical studies of inorganic benzenes. Theoretical studies predict phosphorus and arsenic centers to be pyramidal, while nitrogen-containing compounds are perfectly planar, in accord with findings for the dimeric $[RMYR']_2$ species. Matsunaga and Gordon in their detailed work found that planar structures for P, As are not minima at SCF/ECP level of theory [75]. They considered several non-planar isomers and showed that the boat conformation (C_{3v} point group, Fig. 3b) is lower in energy, compared to the C_s symmetric chair conformation [75]. These SCF/ECP data are in agreement with subsequent density functional theory studies [50,76,78]. Thus, theoretical studies by Jemmis and Kiran [76] at B3LYP/6-31G* level of theory showed that planar $[HMYH]_3$ structures are higher in energy by 39.2, 63.1, 70.7 and 103.9 kJ mol^{-1} than non-planar (asymmetric or low symmetry structures) minima, for AlP, AlAs, GaP and GaAs, respectively. These can be compared to "planarization" energies of 49.0, 96.3, 81.4 and 119.3 kJ mol^{-1} reported with respect to C_{3v} symmetric structures by Timoshkin and Schaefer at B3LYP/LANL2DZ(d,p) level of theory [39].

The aromaticity issue of "inorganic benzenes" was discussed by Schleyer et al. (NICS values) [77], Jemmis and Kiran (electrophilic substitution reactions) [76] and Timoshkin and Frenking (dimerization enthalpies) [50]. Although borazine $[HBNH]_3$ is considered to be slightly aromatic, the alumazene and its heavier analogs are non-aromatic.

Quantum-chemical modeling of "true inorganic heterocycles" $[BAlGaNPAs]H_6$ have been performed [50]. The most stable structure was found to have a BNAlPGaAs core, closely followed by one with a BNAlAsGaP core. As expected, a strong tendency for dimerization of such species has been predicted. Interestingly, dimerization with forma-

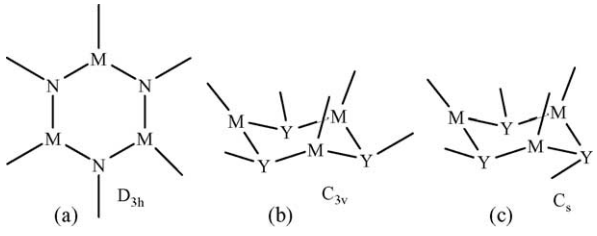

Fig. 3. Structures of $[HMYH]_3$ isomers: (a) planar, Y = N (D_{3h}); (b) C_{3v} symmetric Y = P, As; (c) one of the low-symmetry structures (C_s point group).

Table 6
Summary of theoretical studies of trimeric $[RMYR']_3$ compounds

$[RMYR']_3$		r_{MY}	YMY	MYM	μ	S°_{298}	Method	Reference
$[HAlNH]_3$	D_{3h}	1.791	114.7	125.3	0		RHF/6-31G*	[74]
$[HAlNH]_3$	D_{3h}	1.787	114.2	125.8	0		RHF/ECP	[75]
$[HAlNH]_3$	D_{3h}	1.791	114.8	125.2	0		RHF/6-31G*	[52]
$[HAlNH]_3$	D_{3h}	1.803			0		B3LYP/6-311 + G**	[77]
$[HAlNH]_3$	D_{3h}	1.801			0		B3LYP/6-31G*	[76]
$[HAlNH]_3$	D_{3h}	1.795	114.5	125.5	0	352.2	B3LYP/LANL2DZ(d,p)	[39]
$[HAlNH]_3$	D_{3h}	1.802	114.5	125.5	0	363.4	B3LYP/TZVP	[50]
$[HAlNH]_3$	D_{3h}	1.799	114.2	125.8	0		CCSD(T)/cc-pVTZ	[39]
$[FAlNH]_3$	D_{3h}	1.783	116.2	123.8	0	420.4	B3LYP/LANL2DZ(d,p)	[39]
$[ClAlNH]_3$	D_{3h}	1.784	115.9	124.1	0	457.0	B3LYP/LANL2DZ(d,p)	[39]
$[ClAlNH]_3$	D_{3h}	1.795	115.7	124.3	0		MP2/DZP	[54]
$[ClAlNH]_3$	D_{3h}	1.790	115.9	124.1	0		B3LYP/DZP	[54]
$[BrAlNH]_3$	D_{3h}	1.785	115.8	124.2	0	493.6	B3LYP/LANL2DZ(d,p)	[39]
$[IAlNH]_3$	D_{3h}	1.787	115.7	124.3	0	519.4	B3LYP/LANL2DZ(d,p)	[39]
$[HGaNH]_3$	D_{3h}	1.814	114.0	126.0	0		RHF/ECP	[75]
$[HGaNH]_3$	D_{3h}	1.827	113.8	126.2	0	384.4	B3LYP/LANL2DZ(d,p)	[39]
$[HGaNH]_3$	D_{3h}	1.848			0		B3LYP/6-31G*	[76]
$[HGaNH]_3$	D_{3h}	1.844	113.5	126.5	0	389.1	B3LYP/pVDZ	[71]
$[HGaNH]_3$	D_{3h}	1.849	113.2	126.8	0	396.6	B3LYP/TZVP	[50]
$[HGaN(CH_3)]_3$	C_{3h}	1.849	117.5	122.5	0	533.6	B3LYP/pVDZ	[71]
$[(CH_3)GaNH]_3$	C_{3v}	1.849	112.9	127.1	0	574.4	B3LYP/pVDZ	[71]
$[FGaNH]_3$	D_{3h}	1.812	117.0	123.0	0	454.0	B3LYP/LANL2DZ(d,p)	[39]
$[ClGaNH]_3$	D_{3h}	1.833	116.8	123.2	0	503.4	B3LYP/pVDZ	[57]
$[ClGaNH]_3$	D_{3h}	1.821	117.0	123.0	0		B3P86/6-311G(d,p)	[56]
$[ClGaNH]_3$	D_{3h}	1.813	116.7	123.3	0	490.9	B3LYP/LANL2DZ(d,p)	[39]
$[BrGaNH]_3$	D_{3h}	1.815	116.5	123.5	0	527.5	B3LYP/LANL2DZ(d,p)	[39]
$[IGaNH]_3$	D_{3h}	1.817	116.2	123.8	0	553.4	B3LYP/LANL2DZ(d,p)	[39]
$[HInNH]_3$	D_{3h}	1.993	111.9	128.1	0	421.9	B3LYP/LANL2DZ(d,p)	[39]
$[FInNH]_3$	D_{3h}	1.979	115.3	124.7	0	496.3	B3LYP/LANL2DZ(d,p)	[39]
$[ClInNH]_3$	D_{3h}	1.978	115.1	124.9	0	534.1	B3LYP/LANL2DZ(d,p)	[39]
$[BrInNH]_3$	D_{3h}	1.980	114.8	125.2	0	570.1	B3LYP/LANL2DZ(d,p)	[39]
$[IInNH]_3$	D_{3h}	1.982	114.5	125.5	0	595.4	B3LYP/LANL2DZ(d,p)	[39]
$[HAlPH]_3$	C_{3v}	2.321	116.4	103.6	2.15	429.3	B3LYP/LANL2DZ(d,p)	[39]
$[HAlPH]_3$	C_{3v}	2.315	117.1	106.8			RHF/ECP	[75]
$[HAlPH]_3$	C_{3v}	2.317	117.0	100.7	1.74	429.4	B3LYP/TZVP	[50]
$[FAlPH]_3$	C_{3v}	2.321	120.5	98.0	0.25	501.2	B3LYP/LANL2DZ(d,p)	[39]
$[ClAlPH]_3$	C_{3v}	2.321	119.2	98.7	0.20	536.1	B3LYP/LANL2DZ(d,p)	[39]
$[BrAlPH]_3$	C_{3v}	2.322	118.9	99.3	0.17	572.6	B3LYP/LANL2DZ(d,p)	[39]
$[IAlPH]_3$	C_{3v}	2.323	118.5	99.7	0.45	598.1	B3LYP/LANL2DZ(d,p)	[39]
$[HGaPH]_3$	C_{3v}	2.337	117.0	100.5	1.68	467.6	B3LYP/LANL2DZ(d,p)	[39]
$[HGaPH]_3$	C_{3v}	2.312	118.6	102.9			RHF/ECP	[75]
$[HGaPH]_3$	C_{3v}	2.323	117.1	100.3	1.72	457.0	B3LYP/TZVP	[50]
$[FGaPH]_3$	C_{3v}	2.341	124.0	95.8	1.51	534.1	B3LYP/LANL2DZ(d,p)	[39]
$[ClGaPH]_3$	C_{3v}	2.339	122.5	96.8	1.25	569.7	B3LYP/LANL2DZ(d,p)	[39]
$[BrGaPH]_3$	C_{3v}	2.341	121.8	97.2	0.89	605.6	B3LYP/LANL2DZ(d,p)	[39]
$[IGaPH]_3$	C_{3v}	2.341	121.0	97.7	0.52	630.4	B3LYP/LANL2DZ(d,p)	[39]
$[HInPH]_3$	C_{3v}	2.516	116.3	100.3	1.91	494.0	B3LYP/LANL2DZ(d,p)	[39]
$[FInPH]_3$	C_{3v}	2.524	124.2	95.9	2.03	582.0	B3LYP/LANL2DZ(d,p)	[39]
$[ClInPH]_3$	C_{3v}	2.521	123.1	96.4	2.28	609.7	B3LYP/LANL2DZ(d,p)	[39]
$[BrInPH]_3$	C_{3v}	2.523	122.3	96.8	1.77	645.1	B3LYP/LANL2DZ(d,p)	[39]
$[IInPH]_3$	C_{3v}	2.524	121.5	97.2	1.30	670.2	B3LYP/LANL2DZ(d,p)	[39]
$[HAlAsH]_3$	C_{3v}	2.436	117.7	97.5	1.20	468.6	B3LYP/LANL2DZ(d,p)	[39]
$[HAlAsH]_3$	C_{3v}	2.422	119.3	98.8			RHF/ECP	[75]
$[HAlAsH]_3$	C_{3v}	2.423	117.5	96.1	1.00	478.4	B3LYP/TZVP	[50]
$[FAlAsH]_3$	C_{3v}	2.437	122.0	93.7	1.45	542.1	B3LYP/LANL2DZ(d,p)	[39]
$[ClAlAsH]_3$	C_{3v}	2.437	120.5	94.4	1.40	576.2	B3LYP/LANL2DZ(d,p)	[39]
$[BrAlAsH]_3$	C_{3v}	2.439	120.3	94.9	1.01	613.7	B3LYP/LANL2DZ(d,p)	[39]
$[IAlAsH]_3$	C_{3v}	2.441	119.9	95.1	0.74	638.5	B3LYP/LANL2DZ(d,p)	[39]
$[HGaAsH]_3$	C_{3v}	2.451	118.2	96.2	0.98	499.4	B3LYP/LANL2DZ(d,p)	[39]
$[HGaAsH]_3$	C_{3v}	2.414	119.6	97.8			RHF/ECP	[75]
$[HGaAsH]_3$	C_{3v}	2.428	117.7	96.3	0.99	507.3	B3LYP/TZVP	[50]
$[FGaAsH]_3$	C_{3v}	2.458	125.7	92.6	2.56	586.2	B3LYP/LANL2DZ(d,p)	[39]
$[ClGaAsH]_3$	C_{3v}	2.455	123.9	93.6	2.29	612.0	B3LYP/LANL2DZ(d,p)	[39]

Table 6 (*Continued*)

$[RMYR']_3$		r_{MY}	YMY	MYM	μ	S°_{298}	Method	Reference
$[BrGaAsH]_3$	C_{3v}	2.457	123.3	94.0	1.91	648.6	B3LYP/LANL2DZ(d,p)	[39]
$[IGaAsH]_3$	C_{3v}	2.458	122.3	94.3	1.54	672.9	B3LYP/LANL2DZ(d,p)	[39]
$[HInAsH]_3$	C_{3v}	2.624	117.5	96.1	1.04	534.1	B3LYP/LANL2DZ(d,p)	[39]
$[FInAsH]_3$	C_{3v}	2.632	126.1	92.7	3.27	613.8	B3LYP/LANL2DZ(d,p)	[39]
$[ClInAsH]_3$	C_{3v}	2.630	125.0	93.4	3.55	651.6	B3LYP/LANL2DZ(d,p)	[39]
$[BrInAsH]_3$	C_{3v}	2.632	124.2	93.7	3.00	687.3	B3LYP/LANL2DZ(d,p)	[39]
$[IInAsH]_3$	C_{3v}	2.633	123.3	94.1	2.55	711.6	B3LYP/LANL2DZ(d,p)	[39]

Structural parameters (bond lengths in angstroms and angles in degrees), dipole moments, μ, in Debye and standard entropies S°_{298} in J (mol K)$^{-1}$.

tion of B–N bonds was found to be most exothermic, in stark contrast to endothermic dimerization of borazine. Bond distances in mixed heterocycles are similar to those in regular trimers $[HMYH]_3$.

In contrast to amido compounds, where the dimer–trimer equilibria have been numerously observed in the solution and in the gas phase, for imido compounds, such equilibria are not known, possibly due to stronger MY bonding in these compounds [57]. Theoretical studies predict high favorability of dimer–trimer reorganization, probably due to strong electrostatic repulsions in four-membered rings [54].

Trimeric compounds have active metal and pnictogen centers with low coordination number 3, which in principle allows both centers to participate in donor–acceptor interactions. The self interaction of trimers with less bulky substituents leads to dimerization (formation of hexamers), while more bulky substituents prevent such self-interaction, but allow to interact with smaller donor or acceptor molecules, which are able to "penetrate" the terminal group shield. In recent works, Pinkas et al. explored acceptor properties of **26** towards donor molecules $O{=}P(OR)_3$ and RCN [78]. Structures of the several bis and tris adducts have been obtained (see Scheme 4). The adamantine-type structure of $(MeAl)[2,6\text{-}^iPr_2C_6H_3N]_3\{Al[OP(OSiMe_3)_3]\}_2\text{-}(O_3POSiMe_3)$ (Scheme 4C) results from tris adduct after elimination of two moles of $SiMe_4$. Planarity of the Al_3N_3 ring disappears, as Al atoms become 4-coordinated due to complexation with the PO_4 unit. Reactions of **26** with nitriles RCN were also studied [78c], and the tris adduct was observed by mass spectrometry for $R{=}^i$PrCN only. Bis adducts in *cis* and *trans* forms were structurally characterized in the condensed phase for other nitriles.

Formation of adamantine-type cages similar to one shown in Scheme 4C is quite common for 13–15 chemistry. Reactions of **26** with titanocene fluorides resulted in several adamantine-type cages [155]. Treatment of $GaCl_3$ with Li_2As^tBu in the molar ratio 6:4 resulted in arsanido metalate $[Li(THF)_4]_2[(GaCl_2)_6(As^tBu)_4]THF$ with the adamantine-like dianion $[(GaCl_2)_6(As^tBu)_4]^{2-}$ [156]. An unusual dianion featuring trimeric $[HAlAsR]_3$ unit with Al_3As_3

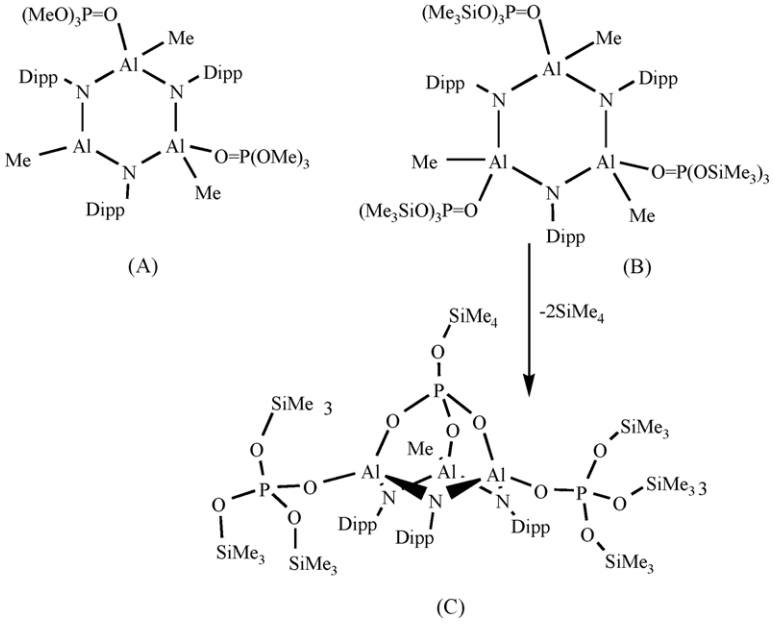

Scheme 4. Structures of bis (A) and tris (B) adducts of **26** and the product of dealkylsilylation reactions (C).

core with three additional H bounded to Li was reported in [79].

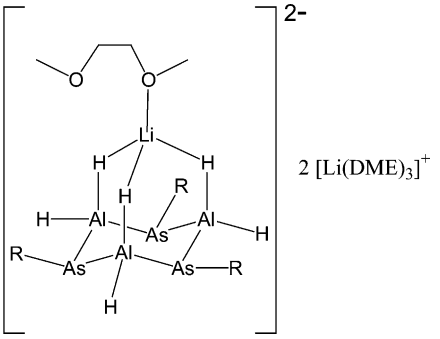

3.4. Tetramers

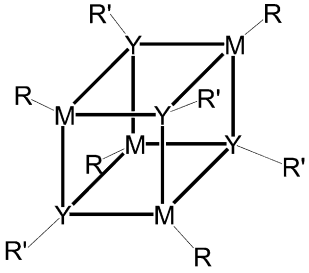

30: M=Al, Y=N, R=H, R'=^{i}Pr [80], [81]
31a: M=Al, Y=N, R=H, R'=^{t}Bu [36,164]
31b: M=Al, Y=N, R=D, R'=^{t}Bu [164]
32: M=Al, Y=N, R=$Me_{0.22}H_{0.78}$, R'=^{t}Bu [36]
33: M=Al, Y=N, R=Me, R'=^{i}Pr [80]
34: M=Al, Y=N, R=Me, R'=^{t}Bu [36]
35: M=Al, Y=N, R=Me, R'=Mes [18]
36: M=Al, Y=N, R=Me, R'=$SiMe_3$ [20]
37: M=Al, Y=N, R=Me, R'=$SiEt_3$ [20]
38: M=Al, Y=N, R=Me, R'=$SiPh_3$ [20]
39: M=Al, Y=N, R=Me, R'=C_6F_5 [84]
40: M=Al, Y=N, R=Me, R'=4-C_6H_4F [83]
41: M=Al, Y=N, R=Me, R'=o-Me-C_6H_4 [99]
42: M=Al, Y=N, R=Me, R'=p-Me-C_6H_4 [99]
43: M=Al, Y=N, R=Ph, R'=Ph [43]
44: M=Al, Y=N, R=^{i}Bu, R'=$SiPh_3$ [20]
45: M=Al, Y=N, R=^{i}Bu, R'=Si^{t}Bu$_2$H [20]
46a: M=Al, Y=N, R=Cl, R'=$SiPh_3$ [20]
46b: M=Al, Y=N, R=Cl, R'=^{t}Bu [164]
47: M=Al, Y=N, R=$Me_{0.5}H_{0.5}$, R'=^{t}Bu [36]
48: M=Ga, Y=N, R=Me, R'=^{t}Bu [85]
49: M=Ga, Y=N, R=Me, R'=$SiMe_3$ [86]
50: M=Ga, Y=N, R=Me, R'=C_6F_5 [87]
51: M=Ga, Y=N, R=Ph, R'=Ph [88]
52: M=Ga, Y=N, R=$Mes_{0.75}(C_6F_5NH)_{0.25}$, R'=$C_6F_5$ [84]
53: M=Ga, Y=N, R=Me, R'=^{i}Pr [85]
54: M=In, Y=N, R=Me, R'=^{t}Bu [90]
55: M=In, Y=N, R=Cl, R'=^{t}Bu [89]
56: M=In, Y=N, R=Br, R'=^{t}Bu [89]
57: M=In, Y=N, R=I, R'=^{t}Bu [89]
58: M=In, Y=N, R=Me, R'=C_6F_5 [87]
59: M=In, Y=N, R=Me+THF, R'=4-C_6H_4F [83]
60: M=In, Y=N, R=Me, R'=$SiMe_3$ [86]
61: M=Al, Y=P, R=^{i}Bu, R'=$SiPh_3$ [91]
62a: M=Ga, Y=P, R=Et, R'=$SiMe_2(CMe_2{}^{i}Pr)$ [144]
62b: M=Ga, Y=P, R=$Mes_{0.75}(PHMes)_{0.25}$, R'=Mes [92]
63: M=Ga, Y=P, R=^{i}Bu, R'=^{t}Bu [93]
64: M=Ga, Y=P, R=Mes, R'=^{t}Bu [93]
65: M=Ga, Y=P, R=$Mes_{0.75}(PH{}^{t}Bu)_{0.25}$, R'=^{t}Bu [93]
66: M=Ga, Y=P, R={$CpFe(CO)_2$}, R'=$SiMe_3$ [94]
67: M=In, Y=P, R=Mes, R'=Mes [95]
68: M=In, Y=P, R=^{i}Pr, R'=$SiPh_3$ [96]
69: M=In, Y=P, R={$CpMo(CO)_3$}, R'=$SiMe_3$ [97]
70: M=In, Y=P, R=Et, R'=Si^{i}Pr$_3$ [98]
71: M=In, Y=As, R=Et, R'=Si^{i}Pr$_3$ [98]

These are the smallest compounds to have coordination number 4 on both the metal and the pnictogen centers, and they are quite common. They adopt a cubane-type structure (Fig. 4a). Structural properties of the experimentally known cubanes are summarized in Table 7.

Theoretical studies of tetrameric compounds are summarized in Table 8. An alternative cyclic structure for the tetramer with coordination number 3 on metal and nitrogen centers (Fig. 3b) was found to be much higher in energy, despite the considerably shorter metal–nitrogen distances (Table 9).

It should be noted that formal $[RMYR']_4$ composition does not always correspond to a cubane structure. For example, a very unusual compound was recently reported by Roesky and co-workers [101]. It has Al_4 tetrahedral core (with angles of almost 60°) with N($SiMe_3$)2,6-$^{i}Pr_2C_6H_3$ substituents (see Fig. 4c). A molecular ion for this compound was

Table 7
Experimentally structurally characterized tetramer $[RMYR']_4$ compounds

No.	Compound	M—Y	Y—M—Y	M—Y—M	Comments	Reference
30	$[HAlN^iPr]_4$	1.897–1.926; mean 1.913	90.1	89.9	Thermolysis $LiAlH_4 + NH_2{}^iPr$	[80]
30	$[HAlN^iPr]_4$ (different crystal system and space group)	1.916–1.931; mean 1.922	Mean 90.6	Mean 89.4	Thermolysis of $[(AlH_2)_2(AlH)_2(N_2{}^iPr_2)_3]$	[81]
33	$[MeAlN^iPr]_4$	1.918–1.932; mean 1.923	90.4	89.6	Thermolysis $AlMe_3 + NH_2{}^iPr$	[80]
43	$[PhAlNPh]_4$	1.90–1.93; 1.914 mean	90.0–90.4; 90.2 mean	89.6–90.0; 89.8 mean	Thermolysis $AlPh_3 + NH_2Ph$	[82]
44	$[^i BuAlNSiPh_3]_4 \cdot 0.5$hexane	1.941–1.970; 1.954 mean	90.7–92.0; 91.2 mean	88.8	Thermolysis of $[^iBu_2AlN(H)SiPh_3]_2$ at 130 °C, 10^{-2} Torr, 12 days	[20]
31a	$[HAlN^tBu]_4$	1.907–1.929	90.3–91.1	89.0–89.6	Not reported	[36]
32	$[Me_{0.22}H_{0.78}AlN^tBu]_4$	1.89–1.918	89.3–90.6	89.0–90.4	Exchange $ZrCp_2Me_2 + [HAlN^tBu]_4$ r.t.	[36]
34	$[MeAlN^tBu]_4$	1.917–1.937	89.8–91.3	89.0–90.1	Exchange $ZrCp_2Me_2 + [HAlN^tBu]_4$ r.t.	[36]
35	$[MeAlNMes]_4 \cdot 3C_7H_8$	1.948	90.1	89.9	Thermolysis of $AlMe_3 + H_2NMes$ 170 °C	[18]
40	$[MeAlN(4\text{-}C_6H_4F)]_4$	1.918–1.951	89.3–90.0	90.0–90.72	Thermolysis $AlMe_3 + H_2N(4\text{-}C_6H_4F)$, crystallization at −20 °C from *n*-hexane	[83]
39	$[MeAlN(C_6F_5)]_4$	1.910–1.968	87.2–89.8	90.4–92.8	Thermolysis $AlMe_3 + H_2N(C_6F_5)$, crystallization at −25 °C from *n*-hexane	[84]
48	$[MeGaN^tBu]_4$	1.984–1.999	88.6–89.2	90.6–91.4	Thermolysis at 250–260 °C of $[Me_2GaNH(^tBu)]_2$	[85]
49	$[MeGaNSiMe_3]_4$	1.981–1.994	89.6–90.4	89.6–90.3	$[Br_2GaN(H)SiMe_3]_2$ with LiMe, purification by sublimation at 90 °C	[86]
50	$[MeGaN(C_6F_5)]_4$	1.972–2.039; mean 2.008	85.9–88.8	91.5–94.0	Thermolysis at 200 °C of $[Me_2GaNH(C_6F_5)]_2$	[87]
51	$[PhGaNPh]_4$	1.952–2.041; mean 2.003	85.9–90.6; mean 88.64	89.5–92.4; mean 91.33	Thermolysis $[Ph_2GaNHPh]_2$ at 180 °C (2 h) in vacuum	[88]
52	$(C_6F_5)HNGa(MesGa)_3(\mu_3\text{-}NC_6F_5)_4$	2.001–2.023	85–89; mean 87.9	>90	Thermolysis $[Mes_2GaNHC_6F_5]_2$	[84]
54	$[(MeInN^tBu]_4$	2.191–2.196; mean 2.193	86.5–86.6; mean 86.5	93.3–93.4; mean 93.4	$MeInCl_2 + LiNH^tBu$ in Et_2O, r.t.	[90]
55	$[ClInN^tBu]_4$	2.176–2.189; mean 2.181	87.3–88.0; mean 87.7	92.1–92.7; mean 92.3	$InCl_3 + LiNH^tBu$ in THF	[89]
56	$[BrInN^tBu]_4$	2.177–2.191; mean 2.185	86.5–88.4; mean 87.5	91.7–93.7; mean 92.5	$InBr_3 + LiNH^tBu$ in THF	[89]
57	$[IInN^tBu]_4$	2.190–2.202; mean 2.194	87.0–88.0; mean 87.6	92.1–92.8; mean 92.4	$InI_3 + LiNH^tBu$ in THF	[89]
58	$[MeInN(C_6F_5)]_4$	2.167–2.227; mean 2.200	84.3	95.5	Thermolysis at 220 °C of $[Me_2InNH(C_6F_5)]_2$	[87]
59	$[MeIn(THF)N(4\text{-}C_6H_4F)]_4$	2.136–2.279	83.7–85.8; mean 84.9	93.7–96.3; mean 94.9	Thermolysis at 220 °C of $[Me_2InNH(4\text{-}C_6H_4F)]_2$	[83]
61	$[^i BuAlPSiPh_3]_4$	2.409–2.417	90.9–92.3	87.7–89.0	Thermolysis at 80 °C of $[^iBu_2AlPH(SiPh_3)]_2$	[91]
62a	$[EtGaPSiMe_2(CMe_2{}^iPr)]_4$	2.411–2.421	90.2–91.9	88.1–89.8	Thermolysis at 180 °C $[Et_2GaPHSiMe_2(CMe_2{}^iPr)]_2$	[144]
62b	$(MesGa)_3[GaP(H)Mes](PMes)_4$toluene	2.410–2.440	86.5–92.4	87.5–92.8	$MesGaCl_2/GaCl_3 + MesPLi_2$, in THF	[92]
63	$[^iPrGaP^tBu]_4$	2.414–2.425	89.8–90.2	89.9–90.3	$^iPrGaCl_2$ + t-$BuPLi_2$, in THF	[93]
65	$[(MesGa)_3\{GaP(H)^tBu\}(P^tBu)_4]$	2.380–2.497	86.5–89.7	88.9–93.1	$MesGaCl_2/GaCl_3 + {}^tBuPLi_2$, in THF	[93]
66	$[\{CpFe(CO)_2\}GaP(SiMe_3)]_4$	2.418–2.438; mean 2.430	90.35, 90.31; 89.30		$\{CpFe(CO)_2\}_2GaCl + KP(SiMe_3)_2$ toluene, r.t.	[94]
67	$[MesInPMes]_4 4.5THF$	2.582–2.623	87.0–88.8	91.0–92.9	$MesInCl_2 + MesPLi_2$, r.t., Et_2O	[95]
68	$[^iPrInPSiPh_3]_4$	2.582–2.603; mean 2.591	87.3–89.7; mean 88.8	90.4–92.7; mean 91.2	$^iPrInI_2 + Li_2P(SiPh_3)$, r.t., Et_2O	[96]
69	$[\{CpMo(CO)_3\}InPSiMe_3]_4$	2.569–2.623	89.9–91.1	88.6–90.0	$\{CpMo(CO)_3\}InCl_2 + P(SiMe_3)_3$ in THF	[97]
70	$[EtInPSi^iPr_3]_4$	2.566–2.584	89.4–90.31	89.75–90.66	Thermolysis at 60 °C (5 h) $[Et_2InP(H)Si^iPr_3]_2$ in heptane	[98]
L1	$[(ClAl)_4(PSi^iPr_3)_4(OEt_2)_2]$	2.422–2.427	95.7	84.3	$AlCl_3$ with $Li_2PSi^iPr_3$, in Et_2O/heptane	[110]
L2	$[(ClAl)_4(PSiMe^iPr_2)_4(OEt_2)_2]$	2.398–2.415	96.7	83.3	$AlCl_3$ with $Li_2PSiMe^iPr_2$, in Et_2O/heptane	[110]
L3	$[(ClAl)_4(AsSi\{CMe_2{}^iPr\}Me_2)_4(OEt_2)_2]$	2.477–2.505	95.5	84.1	$AlCl_3$ with Li_2 $AsSi\{CMe_2{}^iPr\}Me_2$, in Et_2O/heptane	[64]
L4	$[(ClGa)_4(SbSi^iPr_3)_4(P^nPr_2Ph)_2]$	2.691–2.717	93.7	86.3	From solution of **21** in benzene	[66]

Table 7 (*Continued*)

No.	Compound	M—Y	Y—M—Y	M—Y—M	Comments	Reference
L5	$[(MeAl)_2(SnMe_2)_2(N^tBu)_4]$	1.965–1.982	87.9	92.1	$AlMe_3$ with $[Me_2Sn{=}N^tBu]_2$	[86]
L6	$[(MeGa)_2(SnMe_2)_2(N^tBu)_4]$	2.037–2.052	86.1	93.9	$GaMe_3$ with $[Me_2Sn{=}N^tBu]_2$ in toluene, 40–50 °C	[148]
L7	$[(MeIn)_2(SiMe_2)_2(N^tBu)_4]$	2.256–2.277	87.8	92.2		[149]
L8	$[(GaH)(GaH_2)(N^iPr)(N^iPr\text{-}N{=}CMe_2)]_2$	1.971–1.990	89.8	90.2	GaH_3NMe_2Et with 1,1,4,4-tetramethyl-2,3-diazabutadiene, r.t.	[102]
L9	$[(ClGa)_2(BPh)_2(N^tBu)_4]$	1.966–2.042	89.9	90.1	$GaCl_3$ with $\{Li_2[PhB(N^tBu)_2\}_2$	[147]

Bond lengths in angstroms and angles in degrees.

observed in EI mass spectrum, while under similar conditions the analogous $Al_4Cp_4^*$ exhibits only monomeric species in the gas phase.

There are also several hydrazine-based structures which formally correspond to the $[RMYR']_4$ composition, but possess M_4N_8 cores with five-membered rings. These compounds have been recently reviewed by Uhl [8].

Recent X-ray diffraction characterization of Cl, Br, I, Me-substituted In-containing cubanes allows comparison of trends in structural properties with change of the halide ligands (Table 10). While experimental In—N distances increase by 0.013 Å from Cl to I, theoretically predicted changes are less pronounced (0.003 Å). Both experimental and predicted In—N—In and N—In—N angles change only marginally.

Metal and pnictogen mixed cubes of the types $[(M_xM'_yM''_z)Y_4]H_8$ and $[M_4(Y_xY'_yY''_z)]H_8$ ($x+y+z=4$; M, M′, M″ = Al, Ga, In; Y, Y′, Y″ = N, P, As) were theoretically studied in [100]. Their structural parameters resemble those of non-mixed cubes. The process of the mixed cube generation is predicted to be thermodynamically favorable at higher temperatures.

Coordination number 4 on both the metal and pnictogen centers makes cubanes relatively stable species. Many of them are volatile and can be purified by vacuum sublimation. $[^iPrInPSiPh_3]_4$ is relatively stable towards alcoholysis, but unstable with respect to photolysis and electrochemical oxidation [96].

Despite a coordination number of 4 on the metal center, metal atoms in cubanes are able to participate in donor–acceptor interactions. Thus, each In atom in [MeIn(THF)N(4-C_6H_4F)]$_4$ is coordinated to THF [83]. This observation may be rationalized in terms of higher coordination number due to the larger radius of indium. The remarkable adduct between $[HAlN^iPr]_4$ and azopropane (1,2-diisopropyldiazene) molecule $^iPrN{=}N^iPr$, reflecting the acceptor properties of Al atoms of heterocubane, was observed by Uhl et al. [81]. Upon sublimation, this adduct decomposes to give pure $[HAlN^iPr]_4$ cubane, which indicates rather weak bonding. Donor–acceptor interaction with $^iPrN{=}N^iPr$ noticeably affects bonding in the cubane, resulting in an Al–N bond increase from 1.922 to 1.939 (by 0.017 Å) (face of coordination) and from 1.922 to 1.996 (by 0.074 Å) (faces adjacent to the coordination). At the same time, the Al–N bond not connected to the donor–acceptor interacting aluminum atoms, shortens significantly from 1.922 to 1.898 (by 0.024 Å) [81].

It is probable that interaction of weakly M–Y bonded cubanes with donor molecules will result in opening of the M_4Y_4 cage. Existence of the series of ladder compounds **L1**–**L4** of group 13–15 compounds supports this conclusion. Review of ladder approach has recently appeared in [157], and cubic tetramers and hexamers are considered as "closed ladder" structures. Known ladder compounds **L1**–**L4** have $[ClMYR]_4D_2$ composition, which formally corresponds to a cubane interacting with two donor molecules. Such donor–acceptor interactions prevent formation of $[ClMYR]_n$ cages due to much lower bond energies of P, As, Sb-containing cubanes [50]. Upon the removal of donor molecules, closure to tetramer or hexamer "closed ladders" is expected. Indeed, when synthesis of **L1** was carried out in

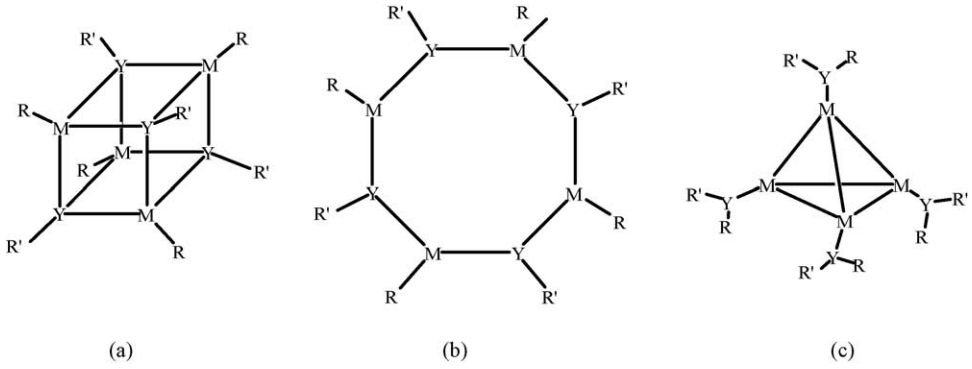

Fig. 4. Structures of $M_4Y_4R_4R'_4$ isomers: (a) cubane; (b) planar eight-membered ring; (c) tetrahedral cluster with M_4 core and YRR′ substituents.

Table 8
Summary of theoretical studies of tetrameric $[RMYR']_4$ compounds

$[RMYR']_4$	r_{MY}	YMY	MYM	S°_{298}	Level of theory	Reference
Planar $[HAlNH]_4$ D_{4h}	1.787	126.1	143.9		RHF/6-31G*	[52]
Planar $[HAlNH]_4$ D_{4h}[a]	1.797				B3LYP/6-31G*	[51]
$[HAlNH]_4$	1.936	89.2	90.8	354.5	B3LYP/LANL2DZ(d,p)	[39]
$[HAlNH]_4$	1.923	89.1	90.9		RHF/DZP	[70]
$[HAlNH]_4$	1.940	89.2	90.8	355.4	B3LYP/TZVP	[50]
$[HAlNH]_4$	1.943				B3LYP/6-31G*	[51]
$[HAlNH]_4$					B3LYP/pVDZ	[53]
$[HAlN(CH_3)]_4$	1.947	90.3	89.6	499.7	B3LYP/pVDZ	[53]
$[(CH_3)AlNH]_4$	1.943	89.1	90.9	531.1	B3LYP/pVDZ	[53]
$[FAlNH]_4$	1.925	89.8	90.2	442.4	B3LYP/LANL2DZ(d,p)	[39]
Planar $[ClAlNH]_4$ D_{4h}[a]	1.770				B3LYP/6-31G*	[55]
$[ClAlNH]_4$	1.933				B3LYP/6-31G*	[55]
$[ClAlNH]_4$	1.925	89.6	90.4	490.8	B3LYP/LANL2DZ(d,p)	[39]
$[ClAlNH]_4$	1.932	89.4	90.6	492.8	B3LYP/DZP	[54]
$[BrAlNH]_4$	1.929	89.5	90.5	539.9	B3LYP/LANL2DZ(d,p)	[39]
$[IAlNH]_4$	1.928	89.4	90.6	573.7	B3LYP/LANL2DZ(d,p)	[39]
$[HGaNH]_4$	1.984	88.0	92.0	399.1	B3LYP/LANL2DZ(d,p)	[39]
$[HGaNH]_4$	2.004	87.6	92.4	401.8	B3LYP/TZVP	[50]
$[HGaNH]_4$	2.001	87.7	92.3	397.9	B3LYP/pVDZ	[71]
$[HGaN(CH_3)]_4$	2.007	88.9	91.1	534.1	B3LYP/pVDZ	[71]
$[(CH_3)GaNH]_4$	2.005	87.6	92.4	580.2	B3LYP/pVDZ	[71]
$[FGaNH]_4$	1.973	88.9	91.1	490.7	B3LYP/LANL2DZ(d,p)	[39]
Planar $[ClGaNH]_4$ D_{4h}	1.814	131.0	139.0		B3P86/6-311G(d,p)	[56]
$[ClGaNH]_4$	1.978	90.0	90.0		B3P86/6-311G(d,p)	[56]
$[ClGaNH]_4$	1.974	88.6	91.4	539.9	B3LYP/LANL2DZ(d,p)	[39]
$[ClGaNH]_4$	1.992	88.4	91.5	540.7	B3LYP/pVDZ	[57]
$[BrGaNH]_4$	1.975	88.5	91.5	588.4	B3LYP/LANL2DZ(d,p)	[39]
$[IGaNH]_4$	1.977	88.4	91.6	621.6	B3LYP/LANL2DZ(d,p)	[39]
$[HInNH]_4$	2.155	85.8	94.1	442.8	B3LYP/LANL2DZ(d,p)	[39]
$[HInN(CH_3)]_4$	2.222	87.7	93.2	573.6	B3LYP/pVDZ	[53]
$[(CH_3)InNH]_4$	2.216	85.0	94.8	642.0	B3LYP/pVDZ	[53]
$[FInNH]_4$	2.146	86.6	93.3	539.3	B3LYP/LANL2DZ(d,p)	[39]
$[ClInNH]_4$	2.146	86.4	93.5	589.5	B3LYP/LANL2DZ(d,p)	[39]
$[BrInNH]_4$	2.147	86.2	93.7	637.9	B3LYP/LANL2DZ(d,p)	[39]
$[IInNH]_4$	2.149	86.1	93.8	670.3	B3LYP/LANL2DZ(d,p)	[39]
$[HAlPH]_4$	2.445	88.5	91.5	454.1	B3LYP/LANL2DZ(d,p)	[39]
$[HAlPH]_4$	2.438	88.8	91.2	456.1	B3LYP/TZVP	[50]
$[HAlPH]_4$	2.434	88.6	91.4		RHF/DZP	[70]
$[FAlPH]_4$	2.433	89.8	90.2	546.0	B3LYP/LANL2DZ(d,p)	[39]
$[ClAlPH]_4$	2.433	89.5	90.5	593.4	B3LYP/LANL2DZ(d,p)	[39]
$[BrAlPH]_4$	2.435	89.3	90.7	642.5	B3LYP/LANL2DZ(d,p)	[39]
$[IAlPH]_4$	2.435	89.1	90.9	676.4	B3LYP/LANL2DZ(d,p)	[39]
$[HGaPH]_4$	2.467	87.7	92.3	500.8	B3LYP/LANL2DZ(d,p)	[39]
$[HGaPH]_4$	2.449	87.6	92.3	496.8	B3LYP/TZVP	[50]
$[FGaPH]_4$	2.458	89.6	90.4	597.8	B3LYP/LANL2DZ(d,p)	[39]
$[ClGaPH]_4$	2.456	89.2	90.8	646.0	B3LYP/LANL2DZ(d,p)	[39]
$[BrGaPH]_4$	2.458	88.9	91.1	694.1	B3LYP/LANL2DZ(d,p)	[39]
$[IGaPH]_4$	2.460	88.6	91.3	727.5	B3LYP/LANL2DZ(d,p)	[39]
$[HInPH]_4$	2.638	86.4	93.5	545.6	B3LYP/LANL2DZ(d,p)	[39]
$[FInPH]_4$	2.630	88.2	91.8	645.3	B3LYP/LANL2DZ(d,p)	[39]
$[ClInPH]_4$	2.628	87.9	92.0	695.3	B3LYP/LANL2DZ(d,p)	[39]
$[BrInPH]_4$	2.631	87.6	92.3	744.0	B3LYP/LANL2DZ(d,p)	[39]
$[IInPH]_4$	2.633	87.4	92.6	776.6	B3LYP/LANL2DZ(d,p)	[39]
$[HAlAsH]_4$	2.552	88.2	91.8	510.3	B3LYP/LANL2DZ(d,p)	[39]
$[HAlAsH]_4$	2.535	88.3	91.7	508.9	B3LYP/TZVP	[50]
$[FAlAsH]_4$	2.540	89.7	90.3	605.3	B3LYP/LANL2DZ(d,p)	[39]
$[ClAlAsH]_4$	2.540	89.3	90.7	651.7	B3LYP/LANL2DZ(d,p)	[39]
$[BrAlAsH]_4$	2.542	89.1	90.9	700.8	B3LYP/LANL2DZ(d,p)	[39]
$[IAlAsH]_4$	2.543	88.9	91.1	734.0	B3LYP/LANL2DZ(d,p)	[39]
$[HGaAsH]_4$	2.570	87.5	92.4	556.1	B3LYP/LANL2DZ(d,p)	[39]
$[HGaAsH]_4$	2.542	87.4	92.6	552.0	B3LYP/TZVP	[50]
$[FGaAsH]_4$	2.561	89.7	90.3	658.3	B3LYP/LANL2DZ(d,p)	[39]
$[ClGaAsH]_4$	2.559	89.2	90.8	704.7	B3LYP/LANL2DZ(d,p)	[39]

Table 8(*Continued*)

$[RMYR']_4$	r_{MY}	YMY	MYM	S°_{298}	Level of theory	Reference
$[BrGaAsH]_4$	2.562	89.0	91.0	752.6	B3LYP/LANL2DZ(d,p)	[39]
$[IGaAsH]_4$	2.563	88.6	91.4	784.8	B3LYP/LANL2DZ(d,p)	[39]
$[HInAsH]_4$	2.736	86.4	93.5	603.0	B3LYP/LANL2DZ(d,p)	[39]
$[FInAsH]_4$	2.727	88.5	91.5	709.1	B3LYP/LANL2DZ(d,p)	[39]
$[ClInAsH]_4$	2.725	88.2	91.8	756.9	B3LYP/LANL2DZ(d,p)	[39]
$[BrInAsH]_4$	2.729	87.9	92.1	805.4	B3LYP/LANL2DZ(d,p)	[39]
$[IInAsH]_4$	2.731	87.6	92.4	837.0	B3LYP/LANL2DZ(d,p)	[39]

All structures are T_d point group if not otherwise indicated. Structural parameters (bond lengths in angstroms and angles in degrees) and standard entropies S°_{298} in J (mol K)$^{-1}$.
[a] Transition state.

Table 9
Relative energy E (kJ mol^{-1}) of the planar D_{4h} isomers with respect to T_d cubic structures and difference in M—N bond distances (in angstroms): $\Delta R_{(M-N)} = R_{(M-N)}[T_d] - R_{(M-N)}[D_{4h}]$

Compound	E	$\Delta R_{(M-N)}$	Method	Reference
Planar $[HAlNH]_4$[a]	272.6	0.146	B3LYP/6-31G*	[51]
Planar $[ClAlNH]_4$[a]	271.0	0.163	B3LYP/6-31G*	[55]
Planar $[ClGaNH]_4$[b]	187.5	0.164	B3P86/6-311G(d,p)	[56]

[a] Transition state.
[b] Local minimum.

Table 10
Comparison of the theoretical and experimental structural parameters

Parameter	X = Cl		X = Br		X = I		X = Me	
	Experimental [89]	Theoretical [39]	Experimental [89]	Theoretical [39]	Experimental [89]	Theoretical [39]	Experimental [90]	Theoretical [53][a]
Mean R(In—N)	2.181	2.146	2.185	2.147	2.194	2.149	2.193	2.216
Mean R(In—X)	2.321	2.327	2.456	2.493	2.655	2.692		
Mean N—In—N	87.7	86.4	87.5	86.2	87.6	86.1	86.5	85.0
Mean In—N—In	92.3	93.5	92.5	93.7	92.4	93.8	93.4	94.8

All bond distances in angstroms and all angles in degrees. Experimental values are for $[XInN^tBu]_4$ compounds; theoretical B3LYP/LANL2DZ(d,p) values are for $[XInNH]_4$ compounds [39].
[a] B3LYP/pVDZ level of theory.

absence of OEt_2, hexameric compound $[ClAlPSi^iPr_3]_6$ was formed [110].

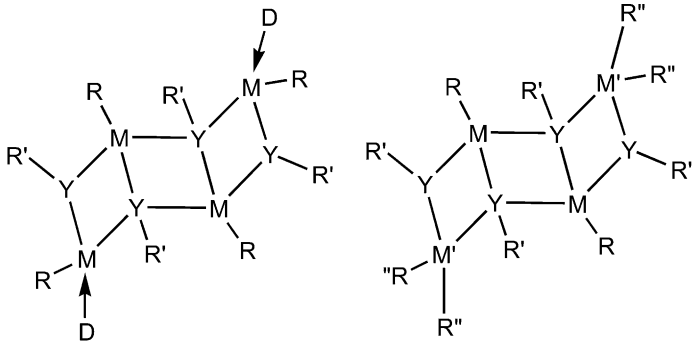

L1: M=Al, Y=P, R=Cl, R'=PSi^iPr_3, D = OEt_2 [110]
L2: M=Al, Y=P, R=Cl, R'=$PSiMe^iPr_2$, D = OEt_2 [110]
L3: M=Al, Y=As, R=Cl, R'=$PSi(CMe_2{}^iPr)Me_2$, D = OEt_2 [64]
L4: M=Ga, Y=Sb, R=Cl, R'=PSi^iPr_3, D = P^nPr_2Ph [66]
L5: M=Al, M' = Sn, Y=N, R=R"=Me, R'=^{t}Bu [86]
L6: M=Ga, M' = Sn, Y=N, R=R"=Me, R'=^{t}Bu [148]
L7: M=In, M' = Si, Y=N, R=R"=Me, R'=^{t}Bu [149]

Series of mixed group 13–14 metal ladder structures **L5**–**L7** were observed and structurally characterized. Examples include the $M_2Sn_2N_4$ core (M = Al, Ga) [86,148] and $In_2Si_2N_4$ [149]. Note that in the reaction of $[Me_2Sn{=}N^tBu]_2$ with $AlMe_3$ and $GaMe_3$, ladder structures were formed, while reaction with $InMe_3$ resulted in $[MeInN^tBu]_4$ cubane (**54**) [86]. However, the In-containing ladder **L5** was pro-

duced when Sn was substituted by Si [149]. The mixed-metal ladder structure $[(ClGa)_2(BPh)_2(N^tBu)_4]$ **L9** with a $Ga_2B_2N_4$ core was also observed [147]. The analogous indium compound containing $In_2B_2N_4$ incorporates a bissolvated lithium chloride and resulting in coordination number 5 on In center. Another type of ladder compound $[(GaH)(GaH_2)(N^iPr)(N^iPr\text{-}N{=}CMe_2)]_2$ (**L8**) was reported in [102]. The unusual $[(AlCp^*)_6P_4]$ was produced in the reaction of $AlCp^*$ with P_4 [145] and possesses a structure with some similarity to both ladder and cubane structures:

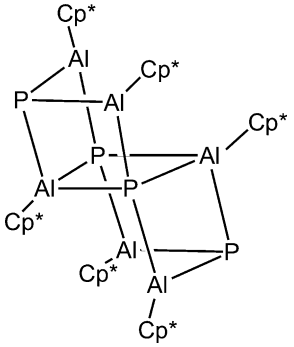

It should be noted that while P, As-containing cubanes may form ladder structures with donor molecules, indirect observations suggest that interaction of nitrogen-containing cubanes with amines may result in formation of adamantane-type cages. Thus, reactions of amido alanes $HXAlNMe_2$ (X = H, Cl, Br, I) and primary amine NH_2Me resulted in hydrogen evolution and formation of adamantane-type $[(AlX)_4(NMe_2)_4(NMe)_2]$ structures (**A1**) [162]. Note that its formal composition corresponds to $[XAlNMe]_4{*}2NMe_3$.

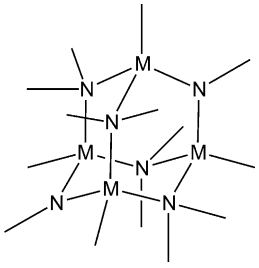

The analogous gallium compound $[(GaPh)_4(NH^iBu)_4(N^iBu)_2]$ (**A2**), which also features an adamantane-type structure, has been prepared by reaction of $[PhGa(NMe_2)_2]_2$ with $NH_2{}^iBu$ [136]. It is noteworthy that the base peak in the chemical ionization mass spectrum at ca. 310 °C was assigned to $[PhGaN^iBu]_4$, suggesting that conversion of adamantine-type to cubane-type structure occurs at elevated temperatures. The major product of pyrolysis of **A2** was $[Ph_2GaNH^iBu]_2$, and therefore it was not possible to establish whether $[PhGaN^iBu]_4$ is formed directly from **A2** with $NH_2{}^iBu$ elimination or from $[Ph_2GaNH^iBu]_2$ with benzene elimination. Formation of the Ga_4-containing species was also evidenced in the chemical ionization mass spectrum of $[^nHxGa(NMe_2)_2]_2$ at 300 °C [166].

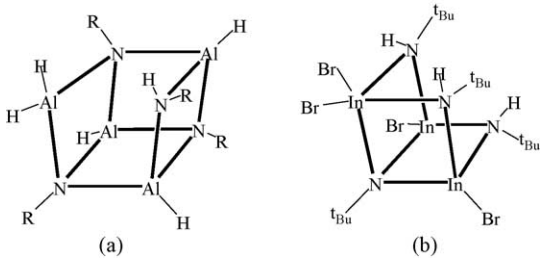

Fig. 5. Amido–imido "broken cube" compounds, a proposed intermediates in cube formation.

Recent theoretical studies of the products of the interaction of $[HGaNH]_4$ with one and two ammonia molecules suggest that formation of $[(GaH)_4(NH_2)_4(NH)_2]$ with the adamantine-type cage is energetically very favorable at low temperatures. At temperatures higher than 440 °C, liberation of extra ammonia and conversion to the cubane structure is predicted to be thermodynamically favorable [115].

The relationship between the cubane, ladder and adamantine-type structures is summarized in Scheme 5.

Formation of tetrameric cubic imido compounds from amido compounds supposedly proceed with formation of open or "broken cube" compounds as intermediates (Fig. 5). In early NMR studies of imido alanes, the existence of the amido–imido broken cube intermediates $[(AlH_2)(NHR)(AlH)_3(NR)_3]$ (Fig. 5a) was evidenced [22,41]. The optically active amido–imido compound was prepared with R = –CH(Ph)Me and its catalytic properties have been discussed [128]. The "broken cube" $[In_3Br_4(N^tBu(NH^tBu)_3]$ (Fig. 5b) has been isolated and structurally characterized as a byproduct in the synthesis of cubane **56** [89].

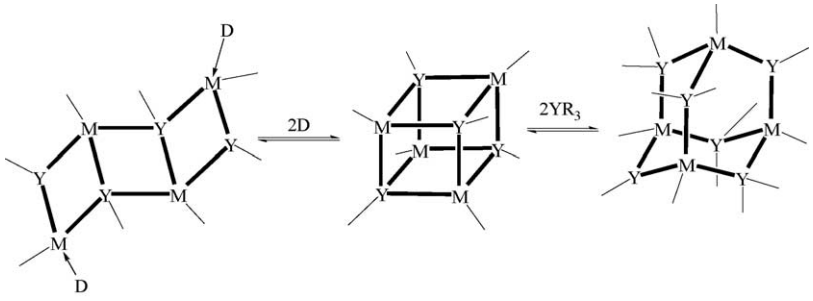

Scheme 5. Relationship between the ladder, cubane and adamantine-type structures.

3.5. Pentamers

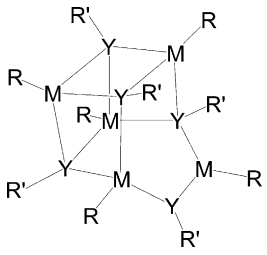

Pentameric compounds have not been isolated. Theoretical studies suggest a structure with at least one M and one Y atom with coordination number 3. C_s symmetric structures are due to the planarity of the nitrogen center, and a pyramidal environment of the P, As atoms results in asymmetric pentamers [39,51,55]. Observation of ions $[HCl_5Al_5N_5HPr_5–Me]^+$ and $[Cl_6Al_5N_5HPr_5–Me]^+$ in the mass spectra of compounds obtained from the chlorination of $[HAlN^iPr]_6$ with HCl or $HgCl_2$ indicates formation of the imido–amido pentamer compounds containing one AlHCl and one NH^iPr group [32].

3.6. Hexamers

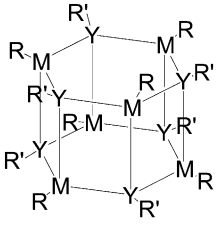

72: M=Al, Y=N, R=H, R'=^{i}Pr [103]
73: M=Al, Y=N, R=H, R'=^{n}Pr [104]
74: M=Al, Y=N, R=H, R'=^{n}Bu [41]
75: M=Al, Y=N, R=H, R'=^{i}Bu [41]
76: M=Al, Y=N, R=H, R'=^{s}Bu [41]
77: M=Al, Y=N, R=H, R'=CH_2Ph [33]
78: M=Al, Y=N, R=H, R'=CH_2(p-$CF_3C_6H_4$) [33]
79: M=Al, Y=N, R=H, R'=CH_2(p-MeC_6H_4) [33]
80: M=Al, Y=N, R=H, R'=$CH_2(C_4H_3S)$ [34]
81: M=Al, Y=N, R=$Me_{0.83}H_{0.17}$, R'=^{i}Pr [105]
82: M=Al, Y=N, R=Me, R'=Ph [99]
83: M=Al, Y=N, R=Me, R'=CH_2Ph [106]
84: M=Al, Y=N, R=Me, R'=p-Me-C_6H_4 [99]
85: M=Al, Y=N, R=Me, R'=$C_2H_4NMe_2$ [107]
86: M=Al, Y=N, R=Me, R'=4-C_6H_4F [83]
87: M=Al, Y=N, R=Et, R'=$C_2H_4NMe_2$ [107]
88: M=Al, Y=N, R=Cl, R'=^{i}Pr [105]
89: M=Al, Y=N, R=Cl, R'=$CH_2(C_4H_3S)$ [34]
90: M=Al, Y=N, R=Br, R'=$CH_2(C_4H_3S)$ [34]
91: M=Al, Y=N, R=Br, R'=Ph [33]
92: M=Al, Y=N, R=PhCC, R'=Ph [33]
93: M=Al, Y=N, R=PhCC, R'=$CH_2(C_4H_3S)$ [34]
94: M=Al, Y=N, R=Et, R'=$CH_2(C_4H_3S)$ [34]
95: M=Al, Y=N, R=PhS, R'=Ph [34]
96: M=Al, Y=N, R={$CpFeC_5H_4CC$}, R'=$CH_2(C_4H_3S)$ [37]
97: M=Ga, Y=N, R=Me, R'=^{i}Bu [24]
98: M=Ga, Y=N, R=Me, R'=CH_2Ph [106]
99: M=Ga, Y=N, R=Me, R'=4-C_6H_4F [83]
100: M=Ga, Y=N, R=Et, R'=Et [108]
101: M=Al, Y=P, R=H, R'=Si^{i}Pr$_3$ [65]
102: M=Al, Y=P, R=H, R'=Si(^{i}PrMe$_2$C)Me$_2$ [109]
103: M=Al, Y=P, R=Me, R'=Si^{i}Pr$_3$ [109]
104: M=Al, Y=P, R=Cl, R'=Si^{i}Pr$_3$ [110]
105: M=In, Y=P, R=Et, R'=Si(^{i}PrMe$_2$C)Me$_2$ [98]
106: M=Al, Y=As, R=H, R'=Si^{i}Pr$_3$ [65]
107: M=Al, Y=As, R=H, R'=Si(^{i}PrMe$_2$C)Me$_2$ [65]
108: M=Ga, Y=As, R=H, R'=Si^{i}Pr$_3$ [65]

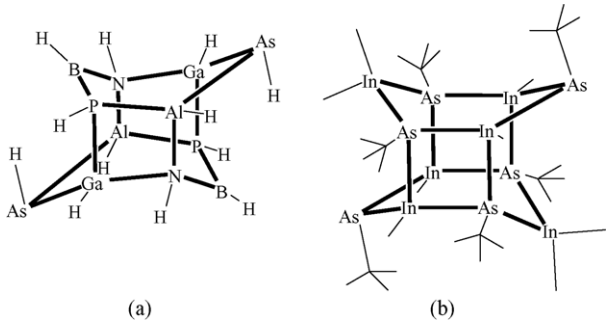

Fig. 6. (a) Theoretically predicted structure of $[BAlGaNPAs]_2H_{12}$ isomer and (b) structure of the experimentally known dianions $[(InMe_2)_2(InMe_4)(As^tBu)_6]^{2-}$ and $[(InCl_2)_2(InCl)_4(As^tBu)_6]^{2-}$.

These species are formally formed by dimerization of trimeric rings and can be produced in high yield by elimination reactions. The M_6Y_6 core of these compounds is essentially a D_{3d} symmetric drum, which allows them to withstand substitution reactions without cage degradation. Several unusual compounds (in particular, ferrocene-doped hexamers drum **96**) have been produced by substitution route [37]. For **81**, full substitution of H into Me groups was not achieved; mass spectrometry shows that single crystals have half of the molecules with only five substituted H atoms. Structural parameters of the compounds are summarized in Table 11. The M–Y bond lengths in the six-membered rings are always shorter compared to those between those rings.

Table 11
Experimentally structurally characterized hexameric $[RMYR']_6$ compounds

No.	Compound	M—Y	Y—M—Y	M—Y—M	Comments	Reference
72	$[HAlN^iPr]_6$	1.898 1.956	116.4 91.4	123.2 88.5	Not mentioned	[103]
73	$[HAlN^nPr]_6$	1.884–1.892, mean 1.890 1.953–1.972, mean 1.959	115.2 91.2	124.3 88.6	Thermolysis $LiAlH_4 + NH_2{}^nPr$	[104]
77	$[HAlNCH_2Ph]_6$	1.886–1.893 1.974	115.25 88.79–91.26	124.37 88.57	Me_3NAlH_3 + PhCN, toluene, reflux	[33]
78	$[HAlNCH_2(p\text{-}CF_3C_6H_4)]_6$	1.880–1.902 1.980, 1.959	115.3 90.8, 91.1	124.0 88.4, 88.1	Me_3NAlH_3 + p-$CF_3C_6H_4CN$, toluene, reflux	[33]
80	$[HAlNCH_2(C_4H_3S)]_6$	1.892, 1.894 1.974	115.4 90.8, 90.9	124.3 89.0, 88.9	Me_3NAlH_3 + 2-$CN(C_4H_3S)$, toluene, reflux	[34]
81	$[Me_{0.83}H_{0.17}AlN^iPr]_6[MeAlN^iPr]_6$	1.908–1.926, mean 1.917 1.964	115.7 91.1–91.6, mean 91.3	123.9 88.3–88.8, mean 88.5	Substitution from $[HAlN^iPr]_6$	[105]
82	$[MeAlNPh]_6$	1.902–1.922 1.951	113.7 90.2–90.7	126.0 88.9–89.5	Thermolysis at 180 °C of $[Me_2AlNH(Ph)]_2$	[99]
83	$[MeAlN(CH_2Ph)]_6$	1.888–1.89	114.2 91.4	125.3 88.3, 88.5	Thermolysis of $AlMe_3$ with $NH_2(CH_2Ph)$ at 135 °C for 2 h (83% yield)	[106]
86	$[MeAlN(4\text{-}C_6H_4F)]_6{\cdot}2THF$	1.905–1.913 1.952	112.8–113.7, mean 113.3 90.1–90.9	125.9–127.3, mean 126.2 88.8–89.6	Thermolysis $AlMe_3 + H_2N(4\text{-}C_6H_4F)$, crystallization at room temperature in THF	[83]
87	$[EtAlNC_2H_4NMe_2]_6$	1.892–1.910, mean 1.897 1.954–1.994, mean 1.971	113.3–114.3, mean 113.9 90.5–91.9, mean 91.3	124.6–126.1, mean 125.5 87.8–89.1, mean 88.5	Thermolysis of $Et_2AlNHC_2H_4NMe_2$ at 190 °C or $[Et_2Al(\mu\text{-}NC_2H_4NMe_2AlEt_2)]_2$ with $NH_2C_2H_4NMe_2$ at 190 °C	[107]
88	$[ClAlN^iPr]_6$	1.898–1.914, mean 1.906 1.955	117.7 91.6–92.1, mean 91.8	122.0 87.9–88.3, mean 88.1	Substitution from $[HAlN^iPr]_6$	[105]
89	$[ClAlNCH_2(C_4H_3S)]_6$	1.880, 1.884 1.972	115.7 91.5, 91.8	124.6 88.4	$[HAlNCH_2(C_4H_3S)]_6 + SiMe_3Cl$ in toluene, reflux	[34]
90	$[BrAlNCH_2(C_4H_3S)]_6$	1.873, 1.876 1.963	114.8 91.2, 91.3	124.7 88.6, 88.5	$[HAlNCH_2(C_4H_3S)]_6 + SiMe_3Br$ in toluene, reflux	[34]
91	$[BrAlNPh]_6$	1.873,1.889 1.972,1.982	116.4 91.9	123.5 –	$[HAlNPh]_6 + Me_3SiBr$ in toluene, reflux	[33]
92	$[PhC{\equiv}CAlNPh]_6$	1.876,1.884 1.972	114.3 91.66	122.12 88.3	$[HAlNPh]_6$ + PhC≡CH in toluene, reflux	[33]
94	$[EtAlNCH_2(C_4H_3S)]_6$	1.897, 1.898 1.987	114.1 91.4	125.3 88.4	$[HAlNCH_2(C_4H_3S)]_6 + ZnEt_2$ THF/toluene, r.t.	[34]
95	$[PhSAlNPh]_6$	1.890, 1.902 1.975, 1.973	115.9 90.6	125.1 88.3	$[HAlNPh]_6$ + PhSH toluene, reflux	[34]

Table 11 (*Continued*)

No.	Compound	M—Y	Y—M—Y	M—Y—M	Comments	Reference
96	$[CpFeC_5H_4C{\equiv}CAlNCH_2(C_4H_3S)]_6$	1.887, 1.882	115.4	123.9	$[HAlNCH_2(C_4H_3S)]_6$ + $CpFeC_5H_4C{\equiv}CH$, toluene, reflux	[37]
		1.981	92.0	87.6		
97	$[MeGaN^iBu]_6$	1.937–1.955	113.8	125.7	Thermolysis at 160 °C $[(Me_2GaN(^iBu)SnMe_3)]_2$, with $SnMe_4$ elimination	[24]
		2.067	90.6–91.1	88.6–89.1		
99	$[MeGaN(4\text{-}C_6H_4F)]_6{\cdot}7THF$	1.967–1.971	114.1	125.9	Thermolysis at 205 °C $[Me_2GaNH(4\text{-}C_6H_4F)]_2$	[83]
		2.033	89.3–89.4	90.3–90.4		
100	$[EtGaNEt]_6$	1.957–1.961	114.3	125.5	$[EtGa(NMe_2)_2]_2 + EtNH_2$ r.t.—glassy solid; glassy solid at 115 °C in toluene for 6 h	[108]
		2.041	90.0, 90.1	89.7		
103	$[MeAlPSi^iPr_3]_6$	2.379–2.387 2.430		122.4 84.2	Thermolysis $[Me_2AlP(H)Si^iPr_3]_2$	[109]
104	$[ClAlPSi^iPr_3]_6$	2.397, 2.407	115.0	120.2	$AlCl_3 + Li_2P(Si^iPr_3)$, heptane (in heptane/ether—ladder structures with DA bond)	[110]
		2.415	97.9	81.8		
105	$[EtInP(SiMe_2CMe_2{}^iPr)]_6$	2.566–2.633	111.0–113.5 90.6–91.8	125.3–128.1 87.6–89.0	$InEt_3 + H_2PSiMe_2CMe_2{}^iPr$	[98]
106	$[HAlAsSi^iPr_3]_6$	2.464–2.470	115.4	122.5–123.7	Thermolysis of $H_3AlNMe_3 + H_2AsSi^iPr_3$, 110 °C	[65]
		2.504–2.511	94.8–95.3	84.5–85.1		

Bond lengths in angstroms and angles in degrees. Data in the first row are for six-membered rings; in the second row, for four-membered rings.

Theoretical studies of hexamer compounds are summarized in Table 12. As expected, alternative planar (D_{6h} point group) structures with coordination number 3 on M and Y centers are much higher in energy (689 kJ mol^{-1} for $[HAlNH]_6$ [51]).

Theoretical considerations of dimerization of "true inorganic benzenes" $[BAlGaNPAs]H_6$ lead to structures $[BAlGaNPAs]_2H_{12}$, in which no B–As bonds are formed [50] (Fig. 6a). These structures are analogous to those reported by Neumüller and co-workers for the dianions in the salt $[Li(DME)_3]_2[(InMe_2)_2(InMe_4)(As^tBu)_6]{\cdot}2DME$ [146] and $[Li(THF)_4]_2[(InCl_2)_2(InCl)_4(As^tBu)_6]$ [156] (Fig. 6b). Formation of such structures can be rationalized in terms of rivalry between formation of MY bonds and pyramidalization of Y center. Since metal–arsenic bonds are the weakest in series Y = N, P, As [50], their formation does not compensate the high reorganization energy of the As center (values for planarization of YH_3 molecules are 30, 149 and 192 kJ mol^{-1} for Y = N, P and As, respectively [76]). Formation of Ga_6E_6 structures (E = O, S) analogous to those given in Fig. 6b as precursors to 13–16 hexamer drums was discussed by Barron and co-workers [167].

3.7. Heptamers

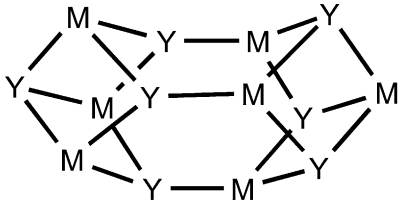

Terminal ligands R (on M) and R' (on Y) are omitted for clarity.

109: M=Al, Y=N, R=H, R'=Et [41]
110: M=Al, Y=N, R=H, R'=^{n}Bu [41]
111: M=Al, Y=N, R=Me, R'=Me [111],[112]
112: M=Al, Y=N, R=Et, R'=Me [112],[113]
113: M=Al, Y=N, R=H, R'=$CH_2$1-Ad [35]
114: M=Al, Y=N, R=$H_{4.74}F_{2.26}$, R'=$CH_2$1-Ad [35]
115: M=Al, Y=P, R=H, R'=Si(^{i}PrMe$_2$C)Me$_2$ [109]
116: M=Ga, Y=N, R=Ph, R'=Me [88]

Structurally characterized heptamers and octamers are still rare (Table 13). The cage of the heptamer can be viewed as a combination of two M_4Y_4 cubes, the first cube omitting a group 13 atom and second one omitting a group 15 atom. It is

Table 12
Summary of theoretical studies of hexameric $[RMYR']_6$ imido compounds (D_{3d} point group)

$[RMYR']_6$	r(M—Y) (six-membered)	r(M—Y) (four-membered)	∠YMY (six-membered)	∠MYM (six-membered)	∠YMY (four-membered)	∠MYM (four-membered)	S°_{298}	ΔH°_{298}	ΔS°_{298}	Level of theory	Reference
$[HAlNH]_6$	1.906	1.977	113.6	126.4	89.5	90.1	455.5	−146.8	66.2	B3LYP/LANL2DZ(d,p)	[39]
$[HAlNH]_6$	1.911	1.980	113.7	126.2	89.5	90.2	447.5			B3LYP/TZVP	[50]
$[HAlNH]_6$	1.913	1.982	114.0	125.9						B3LYP/6-31G*	[51]
$[HAlN(CH_3)]_6$	1.919	1.984	116.4	123.2	90.9	88.9	668.9			B3LYP/pVDZ	[53]
	1.920	1.985	116.6	123.5							
$[(CH_3)AlNH]_6$	1.914	1.984	113.3	126.3	89.4	90.3	730.3			B3LYP/pVDZ	[53]
	1.916		113.6	126.7							
$[FAlNH]_6$	1.894	1.964	114.6	125.2	90.1	89.8	586.8	267.8	107.5	B3LYP/LANL2DZ(d,p)	[39]
$[ClAlNH]_6$	1.895	1.965	114.5	125.4	89.8	90.0	658.2	175.1	113.9	B3LYP/LANL2DZ(d,p)	[39]
$[ClAlNH]_6$	1.901	1.972	114.5	125.4	89.6	90.2	651.8			B3LYP/DZP	[54]
$[ClAlNH]_6$	1.903	1.972								B3LYP/6-31G*	[55]
$[BrAlNH]_6$	1.897	1.967	114.3	125.6	89.7	90.0	731.6	158.3	112.5	B3LYP/LANL2DZ(d,p)	[39]
$[IAlNH]_6$	1.899	1.968	114.3	125.7	89.6	90.1	782.3	125.6	112.7	B3LYP/LANL2DZ(d,p)	[39]
$[HGaNH]_6$	1.946	2.040	113.6	126.6	88.4	91.3	523.8	−79.0	64.3	B3LYP/LANL2DZ(d,p)	[39]
$[HGaNH]_6$	1.967	2.051	113.5	126.5	88.1	91.5	524.9			B3LYP/pVDZ	[71]
$[HGaN(CH_3)]_6$	1.975	2.053	116.7	123.3	89.7	90.2	721.9			B3LYP/pVDZ	[71]
$[(CH_3)GaNH]_6$	1.970	2.056	113.2	126.8	88.1	91.5	807.3			B3LYP/pVDZ	[71]
$[(CH_3)GaNH]_6$	1.968	2.054	113.3	126.7	88.1	91.5	524.5			B3LYP/TZVP	[50]
$[FGaNH]_6$	1.931	2.028	115.7	124.3	89.0	90.9	661.6	224.6	122.4	B3LYP/LANL2DZ(d,p)	[39]
$[ClGaNH]_6$	1.932	2.028	115.3	124.8	88.8	91.1	734.8	177.1	105.2	B3LYP/LANL2DZ(d,p)	[39]
$[ClGaNH]_6$	1.954	2.044	115.4	124.7	88.6	91.2	738.4			B3LYP/pVDZ	[57]
$[BrGaNH]_6$	1.936	2.029	115.1	125.0	88.7	91.2	807.2	178.2	101.1	B3LYP/LANL2DZ(d,p)	[39]
$[IGaNH]_6$	1.939	2.030	114.9	125.1	88.5	91.2	857.0	164.2	106.9	B3LYP/LANL2DZ(d,p)	[39]
$[HInNH]_6$	2.118	2.209	112.8	127.3	86.0	93.6	594.5	−64.3	58.0	B3LYP/LANL2DZ(d,p)	[39]
$[HInN(CH_3)]_6$	2.195	2.266	116.9	123.3	87.2	92.6	800.7			B3LYP/pVDZ	[53]
	2.192	2.264	116.3	123.8	87.3						
$[(CH_3)InNH]_6$	2.185	2.262	112.3	126.9	85.5	94.1	–			B3LYP/pVDZ	[53]
	2.186		113.0	127.8							
$[FInNH]_6$	2.105	2.204	115.1	124.8	86.6	93.2	741.1	226.3	113.9	B3LYP/LANL2DZ(d,p)	[39]
$[ClInNH]_6$	2.105	2.202	111.8	125.0	86.3	93.5	815.9	204.7	118.6	B3LYP/LANL2DZ(d,p)	[39]
$[BrInNH]_6$	2.108	2.203	114.5	125.3	86.2	93.6	888.1	222.5	120.1	B3LYP/LANL2DZ(d,p)	[39]
$[IInNH]_6$	2.110	2.203	114.2	125.4	86.1	93.6	938.1	217.3	118.6	B3LYP/LANL2DZ(d,p)	[39]
$[HAlPH]_6$	2.428	2.452	111.5	128.1	90.2	89.2	607.3	−80.2	64.4	B3LYP/LANL2DZ(d,p)	[39]
$[HAlPH]_6$	2.423	2.446	111.4	127.9	90.7	88.7	615.7			B3LYP/TZVP	[50]
$[FAlPH]_6$	2.422	2.437	113.0	126.4	90.9	88.7	743.2	325.2	111.5	B3LYP/LANL2DZ(d,p)	[39]
$[ClAlPH]_6$	2.421	2.437	112.7	126.8	90.6	88.9	813.1	230.9	118.1	B3LYP/LANL2DZ(d,p)	[39]
$[BrAlPH]_6$	2.423	2.439	112.6	126.9	90.5	89.1	887.4	212.8	117.6	B3LYP/LANL2DZ(d,p)	[39]
$[IAlPH]_6$	2.423	2.441	112.5	127.1	90.4	89.1	938.9	179.3	117.9	B3LYP/LANL2DZ(d,p)	[39]
$[HGaPH]_6$	2.449	2.474	112.0	128.0	88.8	90.7	676.8	−62.4	62.1	B3LYP/LANL2DZ(d,p)	[39]
$[HGaPH]_6$	2.431	2.453	112.3	127.6	88.7	90.8	674.4			B3LYP/TZVP	[50]
$[FGaPH]_6$	2.442	2.467	115.0	124.8	90.0	89.8	823.5	223.8	105.3	B3LYP/LANL2DZ(d,p)	[39]
$[ClGaPH]_6$	2.441	2.464	114.4	125.6	89.7	90.1	893.9	177.7	110.9	B3LYP/LANL2DZ(d,p)	[39]
$[BrGaPH]_6$	2.443	2.465	114.0	125.9	89.5	90.2	967.2	178.7	111.7	B3LYP/LANL2DZ(d,p)	[39]
$[IGaPH]_6$	2.445	2.465	113.5	126.4	89.4	90.3	1017.7	165.4	112.6	B3LYP/LANL2DZ(d,p)	[39]
$[HInPH]_6$	2.622	2.652	111.0	129.2	87.3	92.0	748.6	−87.7	55.1	B3LYP/LANL2DZ(d,p)	[39]
$[FInPH]_6$	2.612	2.649	114.2	125.8	88.5	91.2	901.0	186.8	95.5	B3LYP/LANL2DZ(d,p)	[39]
$[ClInPH]_6$	2.612	2.644	113.7	126.4	88.3	91.4	973.4	164.9	102.6	B3LYP/LANL2DZ(d,p)	[39]
$[BrInPH]_6$	2.615	2.646	113.3	126.8	88.0	91.6	1046.2	182.7	104.2	B3LYP/LANL2DZ(d,p)	[39]
$[IInPH]_6$	2.618	2.647	112.8	127.3	87.9	91.7	1097.8	178.2	104.9	B3LYP/LANL2DZ(d,p)	[39]
$[HAlAsH]_6$	2.539	2.553	111.3	128.3	89.8	89.6	692.5	−93.7	61.5	B3LYP/LANL2DZ(d,p)	[39]
$[HAlAsH]_6$	2.521	2.538	111.2	128.3	90.0	89.4	696.1			B3LYP/TZVP	[50]
$[FAlAsH]_6$	2.532	2.540	112.8	126.6	90.8	88.8	831.5	311.0	109.2	B3LYP/LANL2DZ(d,p)	[39]
$[ClAlAsH]_6$	2.530	2.541	112.6	127.1	90.3	89.2	900.6	215.6	116.8	B3LYP/LANL2DZ(d,p)	[39]
$[BrAlAsH]_6$	2.533	2.542	112.6	127.0	90.3	89.2	974.6	196.7	116.2	B3LYP/LANL2DZ(d,p)	[39]
$[IAlAsH]_6$	2.534	2.544	112.3	127.3	90.1	89.4	1025.7	162.3	116.0	B3LYP/LANL2DZ(d,p)	[39]
$[HGaAsH]_6$	2.557	2.569	111.7	128.3	88.5	90.9	759.1	−81.6	58.4	B3LYP/LANL2DZ(d,p)	[39]
$[HGaAsH]_6$	2.530	2.539	119.9	128.1	88.3	91.1	756.3			B3LYP/TZVP	[50]
$[FGaAsH]_6$	2.551	2.560	114.5	125.3	90.2	89.5	909.7	202.9	104.4	B3LYP/LANL2DZ(d,p)	[39]
$[ClGaAsH]_6$	2.549	2.558	113.8	126.1	89.7	90.0	978.3	155.5	109.5	B3LYP/LANL2DZ(d,p)	[39]
$[BrGaAsH]_6$	2.552	2.560	113.4	126.4	89.5	90.1	1051.2	156.3	110.2	B3LYP/LANL2DZ(d,p)	[39]
$[IGaAsH]_6$	2.554	2.560	112.8	127.0	89.4	90.2	1101.1	142.3	110.4	B3LYP/LANL2DZ(d,p)	[39]
$[HInAsH]_6$	2.726	2.738	110.3	129.8	87.4	91.8	833.0	−113.2	52.8	B3LYP/LANL2DZ(d,p)	[39]
$[FInAsH]_6$	2.721	2.730	113.1	126.8	89.2	90.4	991.7	159.8	96.1	B3LYP/LANL2DZ(d,p)	[39]
$[ClInAsH]_6$	2.718	2.729	112.8	127.2	88.8	90.7	1061.2	136.9	102.8	B3LYP/LANL2DZ(d,p)	[39]
$[BrInAsH]_6$	2.722	2.731	112.4	127.6	88.6	90.9	1133.6	154.6	104.5	B3LYP/LANL2DZ(d,p)	[39]
$[IInAsH]_6$	2.724	2.733	112.0	128.0	88.3	91.1	1184.1	149.7	104.0	B3LYP/LANL2DZ(d,p)	[39]

Standard enthalpies ΔH°_{298} (kJ mol^{-1}) and standard entropies ΔS°_{298} (J (mol K)$^{-1}$) for the formation of the hexameric $[RMYR']_6$ imido compounds from the donor–acceptor complexes: $[MR_3(YR_3')] = \frac{1}{6}[RMYR']_6 + 2RR'$. Structural parameters (bond lengths in angstroms and angles in degrees), dipole moments, μ, in Debye and standard entropies S°_{298} in J (mol K)$^{-1}$.

Table 13
Experimentally structurally characterized heptamer and octamer compounds

No.	Compound	M—Y	Y—M—Y	M—Y—M	Comments	Reference
111	$[MeAlNMe]_7$	1.910 mean	108.7–111.1 88.4–93.0	117.7–123.5 85.9–91.7	Synthesis in reference [111] Thermolysis of $Me_3Al{-}NH_2Me$ at 215 °C in toluene	[112]
114	$[HAlNCH_2Ad]_7$	Hex 1.911 Interm 1.943–1.920 Sq 1.937–1.941	112.7–113.9 90.6–91.6 89.0	115.4–116.0 86.8–88.6 86.9	$AlH_3{-}NMe_3$ + 1-AdCN in boiling toluene	[35]
115	$[HAlPSi(CMe_2{}^iPr)Me_2]_7$	2.395			$AlH_3{-}NMe_3 + PH_2\{Si(CMe_2{}^iPr)Me_2\}$	[109]
116	$[PhGaNMe]_7$	Hex 1.932–1.956 Interm 1.968–1.999 Sq 1.982–1.995	108.7–111.99 88.07 89.92	117.31–120.48 88.41 90.98	Thermolysis of $[Ph_2GaNHPh]_2$ for 6 h at 220 °C in dodecane or 4 h in vacuum	[88]
119	$[HAlN^nPr]_8$	1.878–1.947 Mean 1.916	114.1 mean 91.2 mean	120.8 mean 88.8 mean	As reported in [141]: Al + ^{n}PrNH$_2$ at 180 °C, toluene, 16 h, $p(H_2) = 200\ kg\ cm^{-2}$	[104]

Bond lengths in angstroms and angles in degrees.

remarkable that existence of such a cube lacking a group 15 atom was experimentally evidenced: the Al_4P_3 cage is present in the anion of $Li(thf)_4{}^+[(Me_2Al)_3AlMe(PR)_3]^-$ (resulting from the reaction of $[Me_2AlP(^iPr_3Si)H]_3$ with ^{t}BuLi and Me_2AlCl in 1:2:1 ratio) [109]. Heptamer **115** was crystallized and structurally characterized from the solution, which contained mostly hexamers [109]. Attempt to produce $[FAlNR']_7$ by substitution from $[HAlNR']_7$ was unsuccessful. Full substitution was not achieved and a resulting compound **114** has lower stability [35]. The relationship between the bulkiness of the terminal groups and the degree of oligomerization of the cages was also discussed [35].

With one exception, all known heptamers are Al-containing species. Only recently, the first example of heptamer with Ga_7N_7 core **116** was synthesized by thermolysis of $[Ph_2GaNHMe]_2$ and structurally characterized [88]. Alternatively, **116** is formed from amido–imido compound $[(GaPh)_7(NHMe)_4(NMe)_5]$ at 340 °C, as indicated in the chemical ionization mass spectra [136].

Theoretical studies of heptameric compounds $[HAlNH]_7$ and $[RGaNH]_7$ (R = H, Me) were performed in [51,115], respectively. In [55], the alternative structure of $[ClAlNH]_7$ with three coordinated Al and N centers was considered.

3.8. Octamers

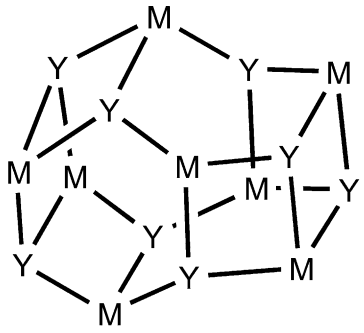

Terminal ligands R (on M) and R' (on Y) are omitted for clarity.

117: M=Al, Y=N, R=H, R'=Et [41]
118: M=Al, Y=N, R=H, R'=^{n}Bu [41]
119: M=Al, Y=N, R=H, R'=^{n}Pr [104]
120: M=Al, Y=N, R=Me, R'=Me [114]
121: M=Al, Y=N, R=Et, R'=Et [113]

All known octamers have an aluminum–nitrogen core. In [114], $[MeAlNMe]_8$ was obtained by pyrolysis of $[Me_2AlNHMe]_3$, but no structural data are available. The only structurally characterized octamer is **119**. Attempts to produce chlorinated octamers via substitution reactions were unsuccessful. Upon chlorination, octamer compound **119** was found to disproportionate into hexamer and decamer (X corresponds to H or Cl) [32]:

$$2[XAlN^nPr]_8 = [XAlN^nPr]_6 + [XAlN^nPr]_{10} \quad (15)$$

However, theoretical studies of $[HMYH]_n$ oligomers (n = 1–16, M = Al, Ga, In; Y = N, P, As) [117] indicate that the gas phase reaction (15) is endothermic by 20–40 kJ mol^{-1} (entropy change is small and ranges from 1.5 to 4.1 J (mol K)$^{-1}$) and thus process (15) is thermodynamically unfavorable for all MY pairs.

Theoretical studies have also been performed for $[HAlNH]_8$ [51], $[ClAlNH]_8$ [55] and $[RGaNH]_8$ (R = H, Me) [115].

3.9. Higher oligomers and polymers

It is well known that the size of the substituent influences the degree of oligomerization. With less bulky substituents, oligomers with high degrees of oligomerization and polymers can be obtained. Polymeric species were predominant in the first synthetic reports. Formation of polymeric compound $[ClAlNMe]_n$ from $AlEt_2Cl$ and NH_2Me was observed [4]. It was noted that in rapid pyrolysis of $[AlEt_2Cl(NH_2Me)]$ at 160 °C, the solid product had an intermediate, "amido–imido" composition $[(EtClAlNMeH)(ClAlNMe)]_x$. Prolonged heating at 210–220 °C resulted in white, non-volatile highly polymeric solid material $[ClAlNMe]_n$ insoluble in benzene, carbon tetrachloride pentane and heptane. Two- and three-dimensional network structures were suggested for $[ClAlNMe]_n$ [4].

Polymeric imides $[RAlN(CH_2)_2NAlR]_x$ (R = Me, Et) formed on the basis of bidentate donor ethylendiamine are reported in [124]. They are formed according to the reaction sequence (16):

$$R_3AlNH_2(CH_2)_2NH_2AlR_3 \xrightarrow{-2RH} R_2AlNH(CH_2)_2NHAlR_2 \xrightarrow{-2RH} \frac{1}{x}[RAlN(CH_2)_2NAlR]_x \quad (16)$$

Elimination enthalpies for R = Me were obtained from DCS curves (−142.3 and −135.3 kJ mol^{-1}, for first and second steps, respectively). Ethylene loss is observed on further heating for R = Et (17):

$$[EtAlN(CH_2)_2NAlEt]_x = [HAlN(CH_2)_2NAlEt]_x + xC_2H_4 \quad (17)$$

Pyrolysis of the obtained polymeric materials $[RAlN(CH_2)_2NAlR]_x$ in ammonia atmosphere results in formation of an off-white crystalline AlN phase at 400–650 °C, and further heating at 1000 °C results in improved crystallinity [124]. Reaction of $LiAlH_4$ with NH_4X resulted in polymeric $[HAlNH]_n$, which was converted to microcrystalline AlN at 950 °C [153].

Slightly off-white $[HGaNH]_n$ solid with mp > 270 °C was produced by the reaction of cyclotrigallazane $[H_2GaNH_2]_3$ with ammonia at 150 °C [119,120] or, alternatively, by the reaction of $[HGa(NMe_2)_2]_2$ with excess of ammonia at room temperature [116]. Analogous reaction of $[HGa(NMe_2)_2]_2$ with excess of NH_2Me resulted in $[HGaNMe]_n$ polymers [116]. It was proposed that gallazane-based adducts $[H_2GaNH_2(NH_3)]$ equilibrate via a ligand redistribution reaction and that the formation of $[HGaNH]_n$ results in NH_3 elimination from a diaminogalliumhydride $[HGa(NH_2)_2]$ (see Scheme 6) [119]. In an earlier study [121], cyclotrigallazane $[H_2GaNH_2]_3$ was found to decompose with evolution of H_2 and ammonia and formation of the polymeric product, insoluble in Et_2O (not characterized). Its pyrolysis at 300–600 °C leads to gray GaN. The authors [121] suggested elimination–condensation (18) and deamination (19) reactions. Excess ammonia used in subsequent studies [116,119,120] probably reduces the operation of deamination reactions (19).

$$\{H_2GaNH_2\} = \{–(H)GaN(H)–\} + H_2 \quad (18)$$

$$\{>GaNH_2\} + \{H_2NGa<\} = \{>GaN(H)Ga<\} + NH_3 \quad (19)$$

The authors [119] considered several possible structures of $[HGaNH]_n$ imido gallanes and concluded that the best can-

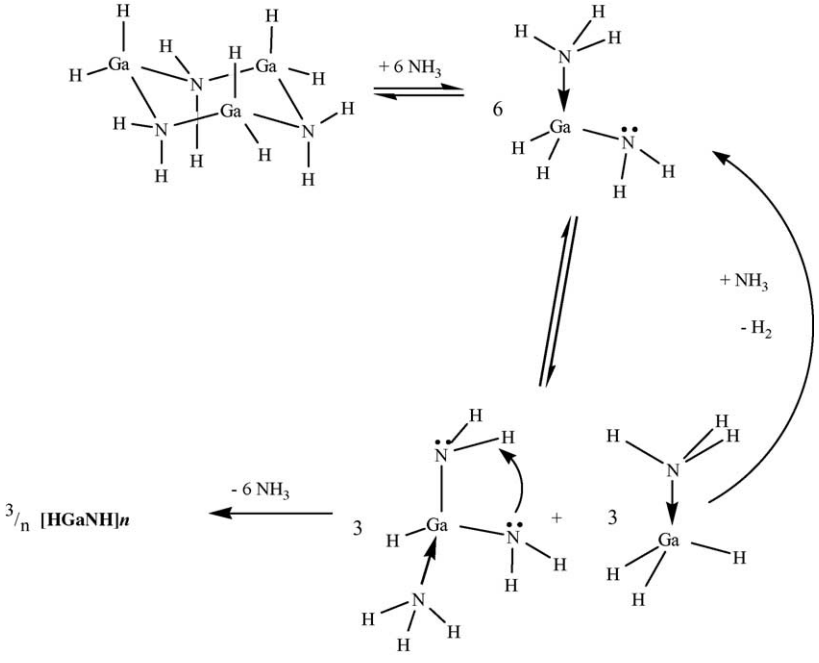

Scheme 6. Proposed pathway for conversion of cyclotrigallazane to $[HGaNH]_n$ in ammonia.

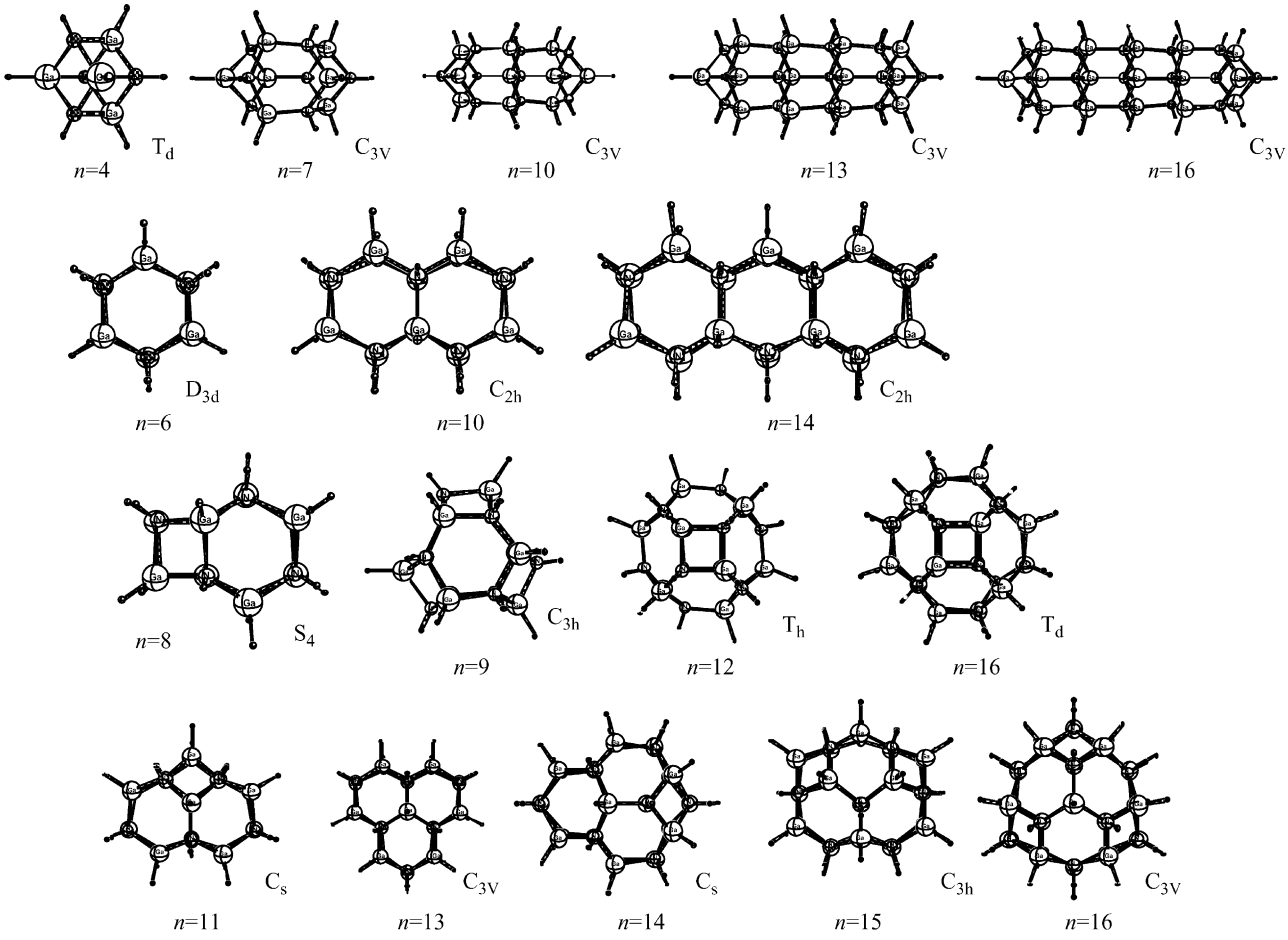

Fig. 7. Structures of theoretically studied $[HMYH]_n$ oligomers.

didate is the planar hexagonal network. Another alternative is a molecular cluster that is large enough to be insoluble, or more complex (perhaps microporous) solid-state structures [119].

Intermediate formation of zinc-blende InP cluster fragments, with external faces terminated by residual In–^{t}Bu and P–H groups was discussed in [118]. $[^tBu_2InPH_2]_3$ undergoes alkane elimination, the last step of which is catalyzed by the protic reagents MeOH, PhSH, Et_2NH, PhCOOH (20).

$$[^tBu_2InPH_2]_3 = InP + 6^tBuH \quad (20)$$

A mechanism of catalytic activity was proposed, which includes "stereochemically disfavored elimination–condensation steps". The resulting product was polycrystalline InP fibers [118]. Formation of polymeric material $[ClInPSiMe_3]_n$ was observed in the reaction of $InCl_3$ with $P(SiMe_3)_3$ at 150 °C [158]. On further heating (650 °C), polymeric material was converted to InP. Insoluble residues of $[^tBuGaYH]_n$ (Y = P, As) have been produced by reaction of Ga^tBu_3 and YH_3 [159]. No further characterization of compounds has been made.

There are some theoretical studies of imido compounds with high degrees of oligomerization. Fullerene-like cages $[HMYH]_{12}$ (M = B, Al; Y = N, P) were theoretically studied by Silaghj-Dumitrescu et al. at the AM1 level of theory [150]. In ab initio theoretical studies, $[HAlNH]_n$ (n = 1–15) [51], $[ClAlNH]_n$ (n = 1–10) [55] and $[HGaNH]_n$ series (n = 7–16) [115] were explored. Formation of gas phase $[HMYH]_n$ compounds (M = Al, Ga, In; Y = N, P, As; n = 1–16) was studied at the B3LYP/LANL2DZ(d,p) level of theory [117]. It was shown that formation of gas phase clusters from the corresponding hydrides (Eq. (21)) is thermodynamically favorable even at high temperatures.

$$MH_3 + YH_3 = \tfrac{1}{n}[HMYH]_n + 2H_2 \quad (21)$$

Structures of the theoretically studied compounds are given in Fig. 7 (taken from [115]).

Stability of the needle-shaped (Fig. 8a, c and e) versus fullerene-like (Fig. 8b, d and e) isomers of $[HGaNH]_n$ (n = 10, 13, 16) was discussed in [115]. Needle-like isomers are predicted to be more stable compared to cage structures, and their stability is increased with increase in the degree of oligomerization n [115]. This result has been recently gener-

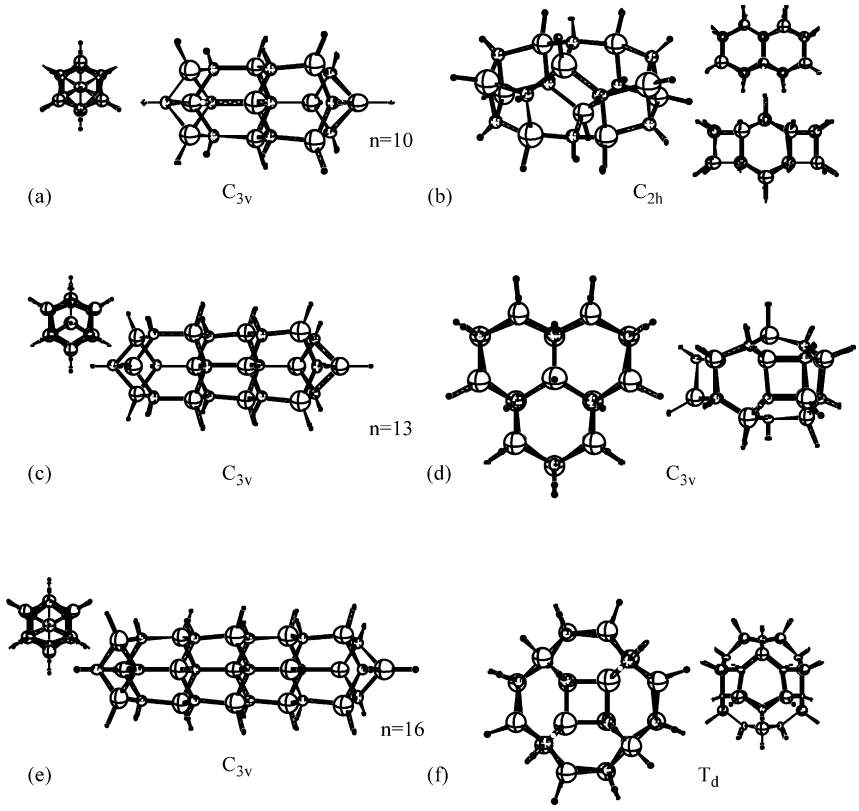

Fig. 8. Structures of needle-shaped and fullerene-like $[HMYH]_n$ isomers.

alized for all $[HMYH]_n$ compounds (M = Al, Ga, In; Y = N, P, As) [154]. The energy difference between needle-shaped and fullerene-like isomers is given in Table 14.

High stability of needle-shaped oligomers prompted the proposal of a mechanistic pathway for their formation, which involves subsequent condensation of $[H_2MYH_2]_3$ amido trimers [154]. Interestingly, needle-shaped structure terminated by OH groups was recently reported by Neumüller and co-workers for the In–As cage compound $[(InMe)_9(As^tBu)_8(OH)_2]2.5THF$ [146].

Synthesis and characterization of needle-shaped oligomeric rods $[RGaNH]_n$ (R = Me, Et, Bu, Hx) have been accomplished just recently [170].

3.10. Tendencies in structural properties

Fig. 9 presents trends in the Al–N and Al–P bond distances as a function of the degree of oligomerization *n*. Mean experimental values of the Al–N and Al–P bond distances are also shown in Fig. 9 for comparison. There is a good agreement between experimental and theoretical values. Trends for

Table 14
Relative energies E^{rel} (kJ mol^{-1}) for needle-shaped $[HMYH]_n$ isomers with respect to fullerene-like and standard enthalpies ΔH°_{298} (kJ mol^{-1}) and entropies ΔS°_{298} (J (mol K)$^{-1}$) of formation of needle-shaped oligomers from MH_3 and YH_3 (Eq. (21))

Compound	$n = 10$			$n = 13$			$n = 16$		
	E^{rel}	ΔH°_{298}	ΔS°_{298}	E^{rel}	ΔH°_{298}	ΔS°_{298}	E^{rel}	ΔH°_{298}	ΔS°_{298}
$[HBNH]_n$	13.0	−195.7	−77.5	−86.6	−201.4	−82.7	−200.0	−205.0	−85.9
$[HBPH]_n$	−3.7	−88.0	−78.3	−34.0	−96.9	−83.5	−55.1	−102.5	−86.6
$[HBAsH]_n$	0.2	−62.1	−77.9	−26.9	−70.7	−83.0	−30.1	−76.1	−86.1
$[HAlNH]_n$	0.9	−258.9	−77.1	−73.8	−263.3	−81.9	−84.7	−266.1	−84.9
$[HAlPH]_n$	−6.8	−131.9	−70.1	−38.0	−137.5	−74.6	−51.8	−140.6	−77.5
$[HAlAsH]_n$	−4.5	−134.1	−68.9	−30.1	−139.4	−73.4	−37.8	−142.5	−76.2
$[HGaNH]_n$	0.2	−170.8	−76.6	−75.6	−175.2	−81.3	−97.9	−177.9	−84.3
$[HGaPH]_n$	−8.7	−105.6	−69.4	−40.4	−111.5	−74.0	−58.9	−114.6	−76.8
$[HGaAsH]_n$	−3.0	−115.5	−68.4	−28.4	−120.7	−72.9	−35.1	−123.8	−75.7
$[HInNH]_n$	−1.7	−145.6	−74.1	−72.4	−149.6	−78.5	−88.3	−151.9	−81.4
$[HInPH]_n$	−4.6	−121.4	−66.6	−32.1	−126.0	−70.8	−34.2	−128.6	−73.5
$[HInAsH]_n$	−0.3	−139.3	−65.4	−21.7	−143.5	−69.6	−15.6	−146.1	−72.4

B3LYP/LANL2DZ(d,p) level of theory.

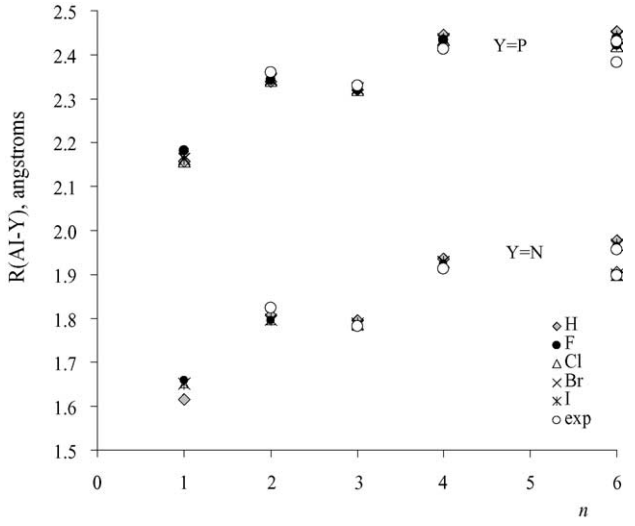

Fig. 9. Mean Al—N and Al—P distances for theoretically studied $[XAlYH]_n$ (X = H, F, Cl, Br, I) and experimentally known $[RAlYR']_n$ compounds [39].

the all other $[XMYH]_n$ species are qualitatively the same. In general, the MY bond distance increases with the increase in the degree of oligomerization *n*, but this change is not monotonic. The MY bonds in the trimers are shorter compared to those in the dimers and tetramers. This may be rationalized in terms of the strain of the four-membered ring.

It seems likely that the large charge separation and shorter M···M and Y···Y distances in the dimers are responsible for such high dimer-trimer reorganization energies (Table 16). As a result, the M–Y distances in the trimers are 0.01–0.02 Å shorter compared to those in the dimers. The M–Y distances for the four-membered rings in hexamers are also always longer compared to those in the six-membered rings. Note that if the distances in the four- and six-membered ring compounds are considered separately, the trends monomer < dimer < tetramer < hexamer and trimer < hexamer are obtained for the four- and six-membered cycles, respectively.

Further increase of the degree of oligomerization results in only slight decrease of the mean M–Y bond distance. For example, for needle-shaped $[HGaNH]_n$ clusters the predicted mean Ga–N distances are 2.001, 1.993, 1.991 and 1.990 Å for *n* = 4, 7, 10 and 13, respectively [115].

As may be seen from Fig. 9, the Al–N and Al–P distances exhibit a similar trend with the increase in the degree of oligomerization. There is a good correlation between Al–N bond distances and Ga–N (In–N) distances for cyclic and cage species, both on the basis of experimental (in compounds bearing identical terminal groups[2]) and theoretical values:

$$r(\mathrm{Ga–N})_{\mathrm{exp}} = 1.1875 \times r(\mathrm{Al–N})_{\mathrm{exp}} - 0.2928;$$
$$R^2 = 0.994 \quad (22)$$

[2] Such pairs are available for the tetramers (**34** and **48**), (**39** and **50**), and the hexamers (**86** and **99**). For dimeric cycles, values of M—N bond distances have been chosen in **5** and **11**.

Table 15
Standard enthalpies (kJ mol^{-1}) of the dissociation of hexamer compounds

Reaction	X		
	CH_3	H	Cl
$[XGaNH]_6 = [XGaNH]_2 + [XGaNH]_4$	278	320	375
$[XGaNH]_6 = 2[XGaNH]_3$	336	366	407

$$r(\mathrm{Ga–N})_{\mathrm{theor}} = 1.1313 \times r(\mathrm{Al–N})_{\mathrm{theor}} - 0.2025;$$
$$R^2 = 0.995 \quad (23)$$

$$r(\mathrm{In–N})_{\mathrm{theor}} = 1.1754 \times r(\mathrm{Al–N})_{\mathrm{theor}} - 0.1153;$$
$$R^2 = 0.996 \quad (24)$$

Correlation between the Al–Y and Ga–Y/In–Y bond distances is also observed for Y = P, As, but in this case the correlation is less perfect, reflecting the fact that the nature of M plays some role in the pyramidalization of the Y center [39].

4. Stability and thermodynamic properties of compounds

4.1. Experimental studies

The majority of experimental studies are focused on the structures of the compounds. Data on thermodynamic properties are very limited. The stability of compounds may be estimated using mass spectrometry data. The high stability of Al_4N_4 and Al_6N_6 frameworks under electron impact is shown by the almost complete absence in the mass spectra other than peaks from parent ions, from parent ions minus methyl and peaks at *m*/*z* ca. 100 from amine fragments [99]. Analysis of mass spectra for the hexamer **99** $[MeGaN(4\text{-}C_6H_4F)]_6$ reveals that under mass spectrometry conditions they do fragment. Major fragments are dimeric (100%) and tetrameric (10%) species; no trimeric species have been detected [83]. This indicates the dissociation pathway (25).

$$[MeGaN(4\text{-}C_6H_4F)]_6 = [MeGaN(4\text{-}C_6H_4F)]_2 + [MeGaN(4\text{-}C_6H_4F)]_4 \quad (25)$$

These results are in agreement with quantum-chemical computations of a model species, where dissociation into tetramer and dimer was found more favorable compared to dissociation into two trimers (Table 15) [126]. In contrast to amido compounds, where dimer–trimer equilibria are well known, equilibria between imido compounds are less explored. The tetramer–hexamer equilibrium (Eq. (26)) is discussed in [99], and the ratio depends on the temperature and substituents.

$$\tfrac{1}{4}[RAlNR']_4 = \tfrac{1}{6}[RAlNR']_6 \quad (26)$$

For $[MeAlNC_6H_4Me\text{-}p]_n$ at 200 °C, the tetramer/hexamer ratio was 1.5:1 [99]. Interconvertion reactions of higher oligomers have also been studied. It was found that Al_6P_6 hexamers were obtained from solution, and crystals of Al_7P_7

heptamer **115** were grown after several months [109]. This may be compared to slow interconversion of $[MeAlNMe]_7$ and $[MeAlNMe]_8$ in toluene solution at 200 °C, although it was possible to separate the two by vacuum sublimation at 10^{-3} Torr [125]. Since the Ga–N bond in the clusters is significantly weaker than the Al–N bond [57], the rearrangement of imido gallanes proceeds more easily compared to that of imido alanes. Thus, an effective conversion of other clusters in the family of $[EtGaNEt]_n$ to $[EtGaNEt]_6$ hexamers was observed at 115 °C in toluene solution [108]. Easy reactions of $[PhGa(NMe_2)]_2$ with excess of NH_2R produced amido–imido clusters $[(PhGa)_4(NH^iBu)_4(N^iBu)_2]$ and $[(PhGa)_7(NHMe)_4(NMe_5)]$, which exhibit ions corresponding to $[PhGaN^iBu]_4$ and $[PhGaNMe]_7$ [136] in the mass spectrum, indicating the non-rigid nature of gallium–nitrogen cages.

4.2. Theoretical studies of thermodynamic properties

Extensive theoretical studies of thermodynamic properties of imido compounds have recently been performed. Energetics of the dimerization of $[HAlYH]_2$ rings was studied by Davy and Schaefer at the CISD level of theory [70,72]. In more detail, thermodynamic properties of imido and related compounds were studied in [39,51,54,55,57,59,71,117,126,142,143]. Pioneering theoretical study of the Cl–Al–N–H system by Timoshkin et al. showed for the first time that formation of imido compounds in the gas phase may be energetically viable [54]. Subsequent studies of H–Al–N–H [51], Cl–Al–NH [55], Cl–Ga–N–H [56,57] and H–Ga–N–H, Me–Ga–N–H, H–Ga–N–Me systems [44,71,115] have been performed. It was shown that generation of imido compounds starting from X_3M and YH_3 is favorable for X = H, Me; unfavorable for X = F, Cl, Br, I (with exception of generation of $[IAlNH]_6$ from AlI_3 and NH_3) [126]. Considering $[MeGaNH]_n$ and $[HGaNMe]_n$ isomers, it was concluded that the former orientation of the substituents is preferable [44,71]. There is a correlation between the degree of oligomerization and the energy difference between $[MeGaNH]_n$ and $[HGaNMe]_n$ isomers: E^{rel} $([HGaNMe]_n) = 77.716n - 26.9\,kJ\,mol^{-1}$ [126]. Values of the thermodynamic characteristics for the formation of hexamer imido compounds from donor–acceptor complexes $[MR_3(YR'_3)]$ are given in Table 12. As can be seen, the process of generation with H_2 elimination is exothermic, and with HX (H = F–I) elimination is endothermic. Both processes are favorable by entropy; therefore, they are expected to proceed at elevated temperatures. Subsequent oligomerization enthalpies are provided in Table 16. The energetics of formation of higher oligomers [n = 7–16] was presented in

Table 16
Calculated standard enthalpies (kJ mol^{-1}) of subsequent oligomerization reactions given per mole of monomer: $\frac{1}{(n-1)}[XMYH]_{n-1} = \frac{1}{n}[XMYH]_n$

XMYH	Y=N				Y=P				Y=As			
	n = 2	n = 3	n = 4	n = 6[a]	n = 2	n = 3	n = 4	n = 6[a]	n = 2	n = 3	n = 4	n = 6[a]
HAlYH	−282	−58	−57	−24	−166 −165[b]	−33	−28	−21	−152	−29	−15	−20
FAlYH	−320	−65	−63	−29	−207	−35	−25	−23	−210	−30	−8	−22
ClAlYH	−312 −301[c]	−64 −63[c]	−61 −57[c]	−27 −26[c]	−173	−34	−26	−22	−178	−30	−9	−21
BrAlYH	−305	−62	−59	−26	−168	−33	−24	−22	−169	−29	−8	−21
IAlYH	−299	−62	−58	−25	−163	−33	−24	−22	−155	−29	−9	−21
HGaYH	−228 −207[d]	−60 −59[d]	−38 −41[d]	−21 −20[d]	−166	−35	−10	−19	−168	−32	0.4	−20
MeGaYH	−201[d]	−55[d]	−42[d]	−19[d]								
FGaYH	−247	−72	−38	−29	−155	−39	2	−21	−132	−34	15	−22
ClGaYH	−246 −221[e]	−69 −68[e]	−37 −42[e]	−27 −26[e]	−137	−37	−0.2	−20	−129	−32	13	−21
BrGaYH	−241	−68	−36	−26	−134	−36	−0.2	−20	−127	−32	12	−21
IGaYH	−237	−66	−36	−24	−135	−35	−1	−20	−124	−31	11	−20
HInYH	−213	−53	−57	−18	−150	−35	−21	−16	−155	−32	−8	−17
FInYH	−218	−64	−58	−26	−157	−38	−10	−20	−162	−33	7	−20
ClInYH	−220	−63	−56	−24	−133	−37	−10	−19	−140	−32	6	−19
BrInYH	−217	−62	−55	−23	−131	−36	−9	−19	−132	−31	6	−19
IInYH	−215	−60	−54	−22	−127	−36	−10	−18	−125	−31	5	−19

All data are at B3LYP/LANL2DZ(d,p) level of theory [39], if not otherwise indicated.
[a] Values are given for the reaction $\frac{1}{4}[XMYH]_4 = \frac{1}{6}[XMYH]_6$.
[b] DZP/CCSD level of theory, calculated using thermochemical cycle from data in refs. [48,72].
[c] B3LYP/DZP level of theory (ref. [54]).
[d] B3LYP/pVDZ level of theory (ref. [71]).
[e] B3LYP/pVDZ level of theory (ref. [57]).

[117] and a detailed report on $[HGaNH]_{7–16}$ oligomers has appeared recently [115].

5. Reactivity and catalytical properties of imido compounds

Catalytic activity of oligomeric imido alanes has been investigated in [127]. The order of catalytic activity for hydrogenation of 4-vinylcyclohexene is hexamer ≥ octamer > tetramer. However, catalytic activity of oligomers was less compared to that of AlH_3 adducts. No activity of $[HAlN(CHMePh)]_4$, $[HAlN(CHMePh)]_6$ in reduction of sulfoxides was evidenced in [128]. At the same time, the open cube amido–imido $[HAlN(CHMePh)]_3AlH_2NH(CHMePh)$ compound was found to be active in this reaction.

Reaction of cubane $[MeAlNMes]_4$ with $Li[PH(C_6H_{11})]$ was described in [129] and it leads to an imido anion based on a Al_4P_6 cage. The same cubane was used as a transamination reagent in reaction with η^5-$(C_5H_4Me)_2TiF_2$ to produce $[\eta^5$-$(C_5H_4Me)TiF(NMes)]_2$ in low yield [130]. Reactions of trimer **26** with titanocene fluorides have also been reported [155]. Thus, organoimidoalanes are potentially active transfer reagents for the imido function to organotitanium fluorides, due to the high fluorine affinity towards aluminum.

Dimeric $[(\eta^5$-Cp)AlNTrip$]_2$ was reported to react cleanly with 1,3-di-*p*-tolylcarbodiimide to supposedly form the 2 + 2 cycloaddition product [17].

6. Imido compounds as precursors to 13–15 binary materials and composites

Use of imido alanes as precursors to aluminum nitride was demonstrated numerous times by Sugahara and coworkers [131–133]. In 1992, they reported [131] use of the poly(isopropyliminoalane) $[HAlN^iPr]_n$ produced by hydrogen elimination from $^iPrNH_2$ and $LiAlH_4$. It mainly consisted of the cage-type hexamer $[HAlN^iPr]_6$, although the presence of some other structures (believed to be tetramers, as mentioned in subsequent report [132]) was detected by ^1H NMR spectroscopy. The precursor was converted in argon atmosphere into black solid aluminum nitride (reaction (27)) with very high (20.6 mass%) carbon contamination. Pyrolysis of the same precursor in ammonia/H_2 atmosphere [134] resulted in formation of white solid aluminum nitride with significantly reduced carbon content (0.5%). However, the ceramic yield of the final product was relatively low (40%).

$$LiAlH_4 + {}^iPrNH_2 \xrightarrow[-LiH]{-2H_2} \tfrac{1}{6}[HAlN^iPr]_6 \rightarrow \tfrac{1}{n}[AlN]_n + {}^iPrH \quad (27)$$

Analogous decomposition of ethylimido alane was reported in [133]. In this case, the polymeric compound formed by reaction of $LiAlH_4$ with $EtNH_2{\cdot}HCl$ was mostly octamer $[HAlNEt]_8$, with presence of other structures, as was shown by ^1H NMR spectroscopy. The compound was pyrolyzed to yield AlN with carbon content 17.1% (in argon) and 0.1% (ammonia/H_2 atmosphere) and higher ceramic yields (50 and 57%), respectively. In all cases, the final product contained 3.7–7.5 mass% of oxygen, the presence of which is believed to be due to high sensitivity of products to moisture and oxygen impurities in the carrier gases. The authors [133] speculated that the surfaces of the obtained products are partially hydrolyzed to form Al–OH groups.

Detailed investigation of the pyrolysis of $[HAlN^iPr]_n$ at different temperatures appeared in [132]. ^1H NMR analysis of the low temperature (160 °C) pyrolysis products showed the signals of $[HAlN^iPr]_6$, most of the other oligomers disappeared. The hexameric compound was observed to partially sublime at 240–320 °C, and the remaining non-volatile products are supposed to have polymeric cross-linked structure. Above 340 °C, decomposition with evolution of different organic molecules was observed.

Significant lowering of the carbon content in ammonia/H_2 atmosphere was attributed to reaction of $[HAlNR]_6$ with ammonia to produce Al–NH_2 groups to form $[H_2NAlN^iPr]_n$ [133]. It was suggested by analogy with known reaction $[HAlN^iPr]_6$ with $^iPrNH_2$, which resulted in H_2 evolution and formation of cubane structure with amido substituents $[^iPrHNAlN^iPr]_4$ [40].

$$2[HAlN^iPr]_6 + 12\,{}^iPrNH_2 = 3[{}^iPrHNAlN^iPr]_4 + 12H_2 \quad (28)$$

It was also observed that in the presence of excess $^iPrNH_2$, the cube compound was converted to dimer $[Al(N^iPrH)_3]_2$ [40]. Since excess of ammonia is usually employed as carrier gas, then similar reactions may occur with all imido compounds.

Imido–iodide polymeric materials were used as a GaN source [122]. Polymeric gallium imide $[Ga(NH)_{3/2}]_n$ was used as starting material to form GaN in the presence of

Table 17
Standard enthalpies (kJ mol^{-1}) for elimination reactions $X_3MNCR = \frac{1}{n}[X_2MNC]_n + RX$

Leaving molecule	M	R	X	$n=1$	$n=2$	$n=3$	$n=4$
H_2	Al	H	H	11	−77	−132	−142
H_2	Ga	H	H	32	−53	−101	−111
H_2	In	H	H	39	−64	−100	−105
CH_4	Al	H	CH_3	−49	−126	−178	−187
CH_4	Ga	H	CH_3	−42	−114	−158	−165
CH_4	Al	CH_3	H	11	−76	−132	−142
CH_4	Ga	CH_3	H	20	−65	−113	−122
C_2H_6	Al	CH_3	CH_3	17	−61	−113	−122
C_2H_6	Ga	CH_3	CH_3	19	−53	−97	−104
HCl	Al	H	Cl	184	93	33	24
HCl	Ga	H	Cl	172	89	36	27
HCl	In	H	Cl	192	82	41	35
CH_3Cl	Al	CH_3	Cl	273	181	122	112
CH_3Cl	Ga	CH_3	Cl	258	175	121	113

B3LYP/pVDZ level of theory [53].

mineralizer (NH_4X) [123]. Note that as was shown in [135], pyrolysis of $[Ga(NEt_2)_3]_2$ in ammonia atmosphere leads to polymeric products according to (29).

$$[Ga(NEt_2)_3]_2 + NH_3 = Ga(NH_2)_3 = Ga(NH_2)(NH) = Ga(NH)_{3/2} \quad (29)$$

The resulting ammonolysis product was converted to mixture of cubic/hexagonal GaN with 77% ceramic yield (in Ar as carrier gas at $T = 600\,^{\circ}C$). Thus, it appears that polymerization of the imido alanes in ammonia atmosphere has a complicated pattern and may proceed via intermediate formation of amido compounds $M(NH_2)_3$. Another possibility, of course, is the formation of adamantane-type cages that were structurally characterized [136,146,162] and theoretically studied [115]. Insolubility of the oligomeric products in Et_2O [121] and aromatic hydrocarbons [112] suggests high dipole moments for the oligomers.

Some experimental evidence suggests that formation of cluster species occurs in the gas phase in the course of the CVD process. Thus, estimated molecular weight of the intermediates responsible for AlN nanoparticle growth from $AlCl_3$ and NH_3 was ~460 amu [168], which agrees well with molecular weight of the hexameric cluster $[ClAlNH]_6$. In recent work by Demchuk and co-workers [151], laser irradiation has been used to initiate AlN and GaN CVD processes from $AlMe_3$, $GaMe_3$ and ammonia. Unexpectedly, extensive clustering in the gas phase is evidenced. Major species correspond to amido–imido $[Me_2MNH_2{\cdot}MeMNH]_3$ compounds. Formation of the related amido–imido compound, $[Me_2AlNHMe]_3[MeAlNMe]_4$, was suggested in [114]. Theoretical studies [115] show that formation of such amido–imido structures is viable. Competitiveness of clustering between NH_3 and oxygen-containing donors (H_2O, MeOH, MeOMe) was experimentally studied in a recent report [151d]. In recent laser irradiation experiments, gas phase nanoparticles were observed in situ for AlN, GaN, InN MOCVD from MMe_3 and NH_3 [152]. The authors concluded that the AlN "parasitic" chemistry is different in nature from the corresponding GaN and InN chemistry [152]. These results are in accord with theoretical findings of stronger bonding and higher favorability of formation of $[HAlNH]_n$ clusters [117,126].

Phosphorus-containing cubanes have been successfully used for the synthesis of aluminum and indium phosphides. Thus, $[^{i}BuAlPSiPh_3]_4$ was converted to AlP at 500 °C [91]. Polycrystalline films of indium phosphide have been grown on Si(1 0 0) wafers from $[^{i}PrInPSiPh_3]_4$ in a horizontal hot-wall reactor at 500 °C [96].

Detailed study of thermal decomposition of the amido compound $[Cl_2GaN(H)SiMe_3]_2$ was performed by Carmalt et al. [137]. $[ClGaNH]_n$ intermediates were observed at temperatures below 500 °C. In the temperature interval 500–650 °C, their incomplete decomposition to GaN was observed, and at temperatures above 650 °C GaN was produced, but it contained significant amount of impurities (Si, Cl, C, H). These experiments indicate resistance of the polymeric imido compounds towards Cl elimination. Results obtained for $[Br_2GaN(H)SiMe_3]_2$ were similar to that of the Cl-substituted analog.

One possible explanation for the high carbon content observed in case of organometallic precursors may be carbon inclusion into cluster core due to competitiveness of the energies of M–C and M–N bonds. Theoretical studies of M–C–N bonded cages $[HMCH_2NH]_n$ ($n = 2$–4, 6), which are isomers of $[(CH_3)MNH]_n$ imido compounds [53], show that formation of clusters with [M–C–N] core is feasible. Thus, the initial step of the process of carbon incorporation may be presented as (30).

$$[(CH_3)MNH]_n \rightarrow [HMCH_2NH]_n \quad (30)$$

It should be noted that M–C–N bonded cages $[Mes^{*}AlCH_2N^{t}Bu]_2$ [16b], $[HAlCH_2\text{-}N^{t}Bu]_4$ and $[FAlCH_2N^{t}Bu]_4$ [35] have been obtained experimentally and structurally characterized. Preferable elimination of hydrocarbons over HCl and RCl elimination was experimentally evidenced in [4]. Thus, thermal decomposition of $Et_2ClAlNH_2Me$ adduct resulted in the stepwise evolution of ethane (31).

$$Et_2ClAlNH_2Me = \tfrac{1}{m}[EtClAlNHMe]_m + C_2H_6 = \tfrac{1}{n}[ClAlNMe]_n + 2C_2H_6 \quad (31)$$

Thermodynamics of elimination reactions from the X_3MNCR donor–acceptor complexes with formation of $[X_2MNC]_n$ oligomers was considered in [53]. Among several leaving groups explored, elimination of HCl and CH_3Cl was found endothermic, and H_2, CH_4 and C_2H_6—exothermic (Table 17). Formation of $[XGaNH]_6$ clusters from the donor–acceptor complexes X_3GaNH_3 follows the same trend [126]:

$$H_3GaNH_3 = \tfrac{1}{6}[HGaNH]_6 + 2H_2, \quad \Delta H^{\circ}_{298} = -36.9\,kJ\,mol^{-1} \quad (32)$$

$$Me_3GaNH_3 = \tfrac{1}{6}[MeGaNH]_6 + 2CH_4, \quad \Delta H^{\circ}_{298} = -134.9\,kJ\,mol^{-1} \quad (33)$$

$$Cl_3GaNH_3 = \tfrac{1}{6}[ClGaNH]_6 + 2HCl, \quad \Delta H^{\circ}_{298} = 194.1\,kJ\,mol^{-1} \quad (34)$$

It should be mentioned that 13–15 oligomers serve as precursors not only for binary materials, but also for composites. Thus, production of Al–Si–C–N [138,139] and Ti–Al–N–C [140] nanocomposites was achieved on the basis of "hybrid" ceramic precursors, containing $[HAlN^{i}Pr]_6$. They were constructed as mixtures of $[HAlN^{i}Pr]_6$ and methylcyclosilazane $[MeSi(H)NH]_n$ to yield Al–Si–C–N ceramics [138,139],

Table 18
Summary of experimentally studied $[RMYR']_n$ compounds

M—Y	No.	Compound	Melting point (°C)	Structural data	Reference
Al—N core					
	3	$\{HC(MeCDippN)_2\}AlN$-(2,6-$Trip_2C_6H_3$)	342	No	[28]
	5	$Cp^*\{(Me_3Si)_2N\}AlN(\mu$-$AlCp^*)(\mu$-$Al\{N(SiMe_3)_2\}NAlCp_2^*$	194	Yes	[26]
	6a	$[Mes^*AlNPh]_2$	>300	Yes	[16a]
	6b	$[Mes^*AlNSiPh_3]_2$	>300	Yes	[16b]
	6c	$[Mes^*AlNSiMe_3]_2$	–	No	[16c]
	7	$[\eta^5$-CpAlNDipp$]_2$	272.5 (turns brown 220.5)	Yes	[17]
	8	$[\eta^5$-$Cp^*AlNSi^iPr_3]_2$	173	No	[62]
	9	$[\eta^1$-$Cp^*AlNSiPh_3]_2$	151	No	[62]
	10	$[\eta^1$-$Cp^*AlNSi^tBu_3]_2$	246	Yes	[62]
	23	$[HAlNDipp]_2\cdot 2NMe_3$	>270	No	[60]
	24	$[HAlNDipp]_2\cdot 2NEtMe_2$	110 (decomposition)	No	[60]
	26	$[MeAlNDipp]_3$	272	Yes	[73,18]
	30	$[HAlN^iPr]_4$	63	Yes	[80,81]
	31a	$[HAlN^tBu]_4$	–	Yes	[36]
	31b	$[DAlN^tBu]_4$	–	No	[164]
	32	$[Me_{0.22}H_{0.78}AlN^tBu]_4$	–	Yes	[36]
	33	$[MeAlN^iPr]_4$	–	Yes	[80]
	34	$[MeAlN^tBu]_4$	–	Yes	[36]
	35	$[MeAlNMes]_4\cdot 3C_7H_8$		Yes	[18]
	36	$[MeAlNSiMe_3]_4$	242 (sublimed at 145 °C/10^{-2} Torr)	No	[20]
	37	$[MeAlNSiEt_3]_4$	229–232	No	[20]
	38	$[MeAlNSiPh_3]_4$	Does not melt below 400	No	[20]
	39	$[MeAlN(C_6F_5)]_4$	175	Yes	[84]
	40	$[MeAlN(4$-$C_6H_4F)]_4$	179	Yes	[83]
	41	$[MeAlNC_6H_4Me$-o$]_4$	–	No	[99]
	42	$[MeAlNC_6H_4Me$-p$]_4$	–	No	[99]
	43	$[PhAlNPh]_4$	–	Yes	[82]
	44	$[^iBuAlNSiPh_3]_4\cdot 0.5$hexane	360 (decomposition)	Yes	[20]
	45	$[^iBuAlNSi^tBu_2H]_4$	309–310	No	[20]
	46a	$[ClAlNSiPh_3]_4$	Does not melt below 400	No	[20]
	46b	$[ClAlN^tBu]_4$	–	No	[164]
	47	$[Me_{0.5}H_{0.5}AlN^tBu]_4$	–	No	[36]
	L5	$[(AlMe)_2(SnMe_2)_2(N^tBu)_4]$		Yes	[86]
	72	$[HAlN^iPr]_6$	–	Yes	[103]
	73	$[HAlN^nPr]_6$	–	Yes	[104]
	74	$[HAlN^nBu]_6$	–	No	[41]
	75	$[HAlN^iBu]_6$	–	No	[41]
	76	$[HAlN^sBu]_6$	–	No	[41]
	77	$[HAlNCH_2Ph]_6$	245 (decomposition)	Yes	[33]
	78	$[HAlNCH_2(p$-$CF_3C_6H_4)]_6$	240 (decomposition)	Yes	[33]
	79	$[HAlNCH_2(p$-$MeC_6H_4)]_6$	233 (decomposition)	No	[33]
	80	$[HAlNCH_2(C_4H_3S)]_6$	238–240	Yes	[34]
	81	$[Me_{0.83}H_{0.17}AlN^iPr]_6[MeAlN^iPr]_6$ (MS analysis shows that single crystals have half molecules with only 5 substituted H atoms)	–	Yes	[105]
	82	$[MeAlNPh]_6$	>320	Yes	[99]
	83	$[MeAlN(CH_2Ph)]_6$	328 (decomposition)	Yes	[106]
	84	$[MeAlNC_6H_4Me$-p$]_6$	–	No	[99]
	85	$[MeAlNC_2H_4NMe_2]_6$	167	No	[107]
	86	$[MeAlN(4$-$C_6H_4F)]_6\cdot 2THF$	179	Yes	[83]
	87	$[EtAlNC_2H_4NMe_2]_6$	179	Yes	[107]
	88	$[ClAlN^iPr]_6$	–	Yes	[105]
	89	$[ClAlNCH_2(C_4H_3S)]_6$	218–223	Yes	[34]
	90	$[BrAlNCH_2(C_4H_3S)]_6$	284–287	Yes	[34]
	91	$[BrAlNCH_2Ph]_6$	296 (decomposition)	Yes	[33]
	92	$[PhC{\equiv}CAlNCH_2Ph]_6$	293 (decomposition)	Yes	[33]
	93	$[PhC{\equiv}CAlNCH_2(C_4H_3S)]_6$	270 (decomposition)	No	[34]
	94	$[EtAlNCH_2(C_4H_3S)]_6$	262	Yes	[34]
	95	$[PhSAlNCH_2Ph]_6$	–	Yes	[34]
	96	$[CpFeC_5H_4C{\equiv}CAlNCH_2(C_4H_3S)]_6$	297 (decomposition)	Yes	[37]
	109	$[HAlNEt]_7$	–	No	[41]

Table 18 (*Continued*)

M—Y	No.	Compound	Melting point (°C)	Structural data	Reference
	110	$[HAlN^nBu]_7$	–	No	[41]
	111	$[MeAlNMe]_7$	–	Yes	[111,112]
	112	$[EtAlNMe]_7$	–	No	[112,113]
	113	$[HAlNCH_2(1\text{-Ad})]_7$	–	Yes	[35]
	114	$[F_{0.32}H_{0.68}AlNCH_2(1\text{-Ad})]_7$	–	Yes	[35]
	117	$[HAlNEt]_8$	–	No	[41]
	118	$[HAlN^nBu]_8$	–	No	[41]
	119	$[HAlN^nPr]_8$	–	Yes	[104]
	120	$[MeAlNMe]_8$	Sublimates in vacuum at 180	No	[114]
	121	$[EtAlNEt]_8$	–	No	[113]
Ga—N core					
	1	$\{C_6H_3\text{-}2,6\text{-}Dipp_2\}GaN\{C_6H_3\text{-}2,6(Xyl\text{-}4\text{-}^tBu_2)\}$	215–216	Yes	[29]
	4	$\{HC(MeCDippN)_2\}GaN\text{-}(2,6\text{-}Trip_2C_6H_3)$	229–230	Yes	[28]
	11	$[\eta^1\text{-}Cp^*GaNXyl]_2$	210–220 (slow decomposition)	Yes	[27]
	48	$[MeGaN^tBu]_4$	328 (sublimed at 140 °C/10^{-3} hPa)	Yes	[85]
	49	$[MeGaNSiMe_3]_4$	278	Yes	[86]
	50	$[MeGaN(C_6F_5)]_4$	202	Yes	[87]
	51	$[PhGaNPh]_4$	230 (decomposition without melting)	Yes	[88]
	52	$(C_6F_5)HNGa(MesGa)_3(\mu_3\text{-}NC_6F_5)_4$	287–290	Yes	[84]
	53	$[MeGaN^iPr]_4$	304 (sublimated at 120 °C/10^{-3} hPa)	No	[85]
	L6	$[(GaMe)_2(SnMe_2)_2(N^tBu)_4]$		Yes	[148]
	L8	$[(GaH)(GaH_2)(N^iPr)(N^iPr\text{-}N{=}CMe_2)]_2$		Yes	[102]
	L9	$[(ClGa)_2(BPh)_2(N^tBu)_4]$		Yes	[147]
	98	$[MeGaN(CH_2Ph)]_6$	290 (decomposition)	No	[106]
	99	$[MeGaN(4\text{-}C_6H_4F)]_6$ 7THF	320	Yes	[83]
	100	$[EtGaNEt]_6$	230 (decomposition without melting)	Yes	[108]
	116	$[PhGaNMe]_7$	288–290, remelted 260–270	Yes	[88]
In—N core					
	2	$\{C_6H_3\text{-}2,6\text{-}Dipp_2\}InN\{C_6H_3\text{-}2,6(Xyl\text{-}4\text{-}^tBu_2)\}$	184–185	Yes	[29]
	54	$[(MeInN^tBu]_4$	–	Yes	[90]
	55	$[ClInN^tBu]_4$	–	Yes	[89]
	56	$[BrInN^tBu]_4$	–	Yes	[89]
	57	$[IInN^tBu]_4$	–	Yes	[89]
	58	$[MeInN(C_6F_5)]_4$	225 (decomposition)	Yes	[87]
	59	$[MeIn(THF)N(4\text{-}C_6H_4F)]_4$	232	Yes	[83]
	60	$[MeInNSiMe_3]_4$	310 (decomposition, brown color)	No	[86]
	L7	$[(InMe)_2(SiMe_2)_2(N^tBu)_4]$		Yes	[149]
Al—P core					
	14	$[ClAlPSi^iPr_3]_2{\cdot}2Py$	–	Yes	[64]
	27	$[Mes^*AlPPh]_3$	Softens 193, melts 241–242	Yes	[16]
	61	$[^iBuAlPSiPh_3]_4$	Decomposes below 150	Yes	[91]
	L1	$[(AlCl)_4(PSi^iPr_3)_4(OEt_2)_2]$		Yes	[110]
	L2	$[(AlCl)_4(PSiMe^iPr_2)_4(OEt_2)_2]$		Yes	[110]
	101	$[HAlPSi^iPr_3]_6$	105 (decomposition)	No	[65]
	102	$[HAlPSi(^iPrMe_2C)Me_2]_6$	–	No	[109]
	103	$[MeAlPSi^iPr_3]_6$	–	Yes	[109]
	104	$[ClAlP(Si^iPr_3)]_6$	–	Yes	[110]
	115	$[HAlPSi(^iPrMe_2C)Me_2]_7$	–	Yes	[109]
Ga—P core					
	12	$[^tBuGaPMes^*]_2$	125–128	Yes	[58]
	15	$[(2,6\text{-}CH_2NMe_2)C_6H_3GaPSiPh_3]_2$; intramolecular DA stabilized ($NMe_2 \rightarrow Ga$)	234–237	Yes	[31]
	16	$[(P^tBu_2Me)ClGaP(SiMe_3)]_2$; DA stabilized ($P^tBu_2Me \rightarrow Ga$)	145–155 (decomposition, orange color)	Yes	[23]
	25	$[^tBu_3SiP(H)\text{-}GaPSi^tBu_3]_2$	–	Yes	[67]
	29	$[2,4,6\text{-}Ph_3C_6H_2GaP(cyclo\text{-}C_6H_{11})]_3$	>200 (decomposition)	Yes	[30]
	62a	$[EtGaPSiMe_2(CMe_2{}^iPr)]_4$	–	Yes	[144]
	62b	$(MesGa)_3[GaP(H)Mes](PMes)_4$ toluene	>230 (decomposition)	Yes	[92]
	63	$[^iPrGaP^tBu]_4$	–	Yes	[93]
	64	$[MesGaP^tBu]_4$	–	No	[93]
	65	$(MesGa)_3[GaP(H)^tBu](P^tBu)_4$	>230 (decomposition)	Yes	[93]
	66	$[\{CpFe(CO)_2\}GaP(SiMe_3)]_4$	–	Yes	[94]

Table 18 (*Continued*)

M—Y	No.	Compound	Melting point (°C)	Structural data	Reference
In—P core					
	67	$[MesInPMes]_4 \cdot 4.5THF$	174 (decomposition)	Yes	[95]
	68	$[^iPrInPSiPh_3]_4$	310 (decomposition)	Yes	[96]
	69	$[\{CpMo(CO)_3\}InPSiMe_3]_4$	–	Yes	[97]
	70	$[EtInPSi^iPr_3]_4$	–	Yes	[98]
	105	$[EtInP(SiMe_2CMe_2{}^iPr)]_6$	–	Yes	[98]
Al—As core					
	17	$[HAlAsSi(^iPr)_3]_2 \cdot 2NMe_3$; DA stabilized ($NMe_3 \rightarrow Al$)	135 (decomposition)	Yes	[65]
	18	$[ClAlAsSi(CMe_2{}^iPr)Me_2]_2 \cdot 2NEt_3$	–	Yes	[64]
	22	$[HAlAsSi(CMe_2{}^iPr)Me_2]_2 \cdot 2NMe_3$; DA stabilized ($NMe_3 \rightarrow Al$)	109 (decomposition)	No	[65]
	28	$[Mes^*AlAsPh]_3$	Turns orange 208, melts to red at 212–216	Yes	[16]
	L3	$[(AlCl)_4(AsSi\{CMe_2{}^iPr\}Me_2)_4(OEt_2)_2]$	–	Yes	[64]
	106	$[HAlAsSi^iPr_3]_6$	198 (decomposition)	Yes	[65]
	107	$[HAlAsSi(^iPrMe_2C)Me_2]_6$	109 (decomposition)	No	[65]
Ga—As core					
	13	$[\{Li(THF)_3AsSi^iPr_3\}GaAsSi^iPr_3]_2$	–	Yes	[63]
	19	$[ClGaAs(SiMe_3)]_2 \cdot 2P^tBu_2Me$; DA stabilized ($P^tBu_2Me \rightarrow Ga$)	135 (decomposition, brown color)	Yes	[23]
	20	$[^tBuGaAsC_6H_3(CH_2NMe_2)_2]_2$; intramolecular stabilized dimer	247–249	Yes	[61]
	108	$[HGaAsSi^iPr_3]_6$	98 (decomposition)	No	[65]
In—As core					
	71	$[EtInAsSi^iPr_3]_4$	–	No	[98]
Ga—Sb core					
	21	$[ClGaSbSi^iPr_3]_2 \cdot 2PPh^nPr_2$	–	Yes	[66]
	L4	$[(GaCl)_4(SbSi^iPr_3)_4(P^nPr_2Ph)_2]$	–	Yes	[66]

or $[HAlN^iPr]_6$ was combined with pyrolysis products of $Ti(NMe_2)_4$ and $MeHNCH_2CH_2NHMe$ (Ti:Al ratio 2:1) to yield Ti–Al–N–C composites [140]. Conversion of unspecified $[HAlNH]_n$ and $[HGaNH]_n$ imides to AlN (including AlN/BN composites) and GaN has been discussed by Jegier and Gladfelter [169].

7. Conclusions

During recent years, a rapid progress in synthetic 13–15 chemistry resulted in preparation and characterization of many imido compounds and their P, As analogs. Summary of the experimentally studied compounds is given in Table 18. Experimental studies were complemented by extensive theoretical studies of the structural and thermodynamic properties of these compounds. Use of these compounds as precursors to novel 13–15 composites and their potential for the stoichiometry controlled CVD processes promises a bright future for their chemistry. Now that the structural properties of $[RMYR']_n$ are relatively well explored, experimental studies of their reactivity and thermal stability are highly desirable.

Acknowledgements

Financial support of the Educational Ministry of the Russian Federation and St. Petersburg Administration (Grants T02-09.4-902 and PD 03-1.3-117), Alexander-von-Humboldt Foundation (return fellowship) is gratefully acknowledged. The hospitality of the Center for Computational Chemistry, University of Georgia (Professor Henry F. Schaefer, III), is especially esteemed.

References

[1] (a) A.C. Jones, P. O'Brien, CVD of Compound Semiconductors. Precursor Synthesis, Development and Applications, VCH, Weinheim, 1997;
(b) S.P. DenBaars, Proc. IEEE 85 (1997) 1740;
(c) W.M. Chen, E. O'Reilly, A. Forchel, C.W. Tu (Eds.), N-Containig III–V Semiconductors: Fundamentals and Applications. European Materials Research Society Symposia Proceedings, vol. 136, Elsevier, Amsterdam, 2003, Solid State Electron. 47 (2003) 385.
[2] J. Emsley, Chem. World 1 (3) (2004) 30.
[3] G. Bähr, Fiat Review of German Science, 1939–1946, vol. 24, Inorg. Chem. 155 (as cited in work [4]).
[4] A.W. Laubengayer, J.D. Smith, G.G. Ehrlich, J. Am. Chem. Soc. 83 (1961) 542.
[5] M. Veith, Chem. Rev. 90 (1990) 3.
[6] F.C. Sauls, L.V. Interrante, Coord. Chem. Rev. 128 (1993) 193.
[7] C.J. Carmalt, Coord. Chem. Rev. 223 (2001) 217.
[8] W. Uhl, Structure and Bonding, vol. 105, Springer-Verlag, 2003, p. 42.
[9] M. Cesari, S. Cucinella, The Chemistry of Inorganic Homo- and Heterocycles, vol. 1, Academic Press, London, 1987, p. 167.

[10] G.H. Robinson (Ed.), Coordination Chemistry of Aluminum, VCH, New York, 1993.
[11] A.J. Downs (Ed.), Chemistry of Aluminum, Gallium, Indium and Thallium, Chapman & Hall, New York, 1993.
[12] C.E. Housecroft (Ed.), Comprehensive Organometallic Chemistry, vol. 1, Pergamon, London, 1995.
[13] I. Haiduc, F.T. Edelmann (Eds.), Supramolecular Organometallic Chemistry, VCH, New York, 1999.
[14] I. Haiduc, The Chemistry of Inorganic Ring Systems, Wiley/Interscience, London, 1970.
[15] G. Dozzi, S. Cucinella, A. Mazzei, T. Salvatory, Inorg. Chim. Acta 15 (1975) 179.
[16] (a) R.J. Wehmschulte, P.P. Power, J. Am. Chem. Soc. 118 (1996) 791;
(b) R.J. Wehmschulte, P.P. Power, Inorg. Chem. 37 (1998) 6906;
(c) R.J. Wehmschulte, P.P. Power, Inorg. Chem. 37 (1998) 2106.
[17] J.D. Fischer, P.J. Shapiro, G.P.A. Yap, A.L. Rheingold, Inorg. Chem. 35 (1996) 271.
[18] K.M. Waggoner, P.P. Power, J. Am. Chem. Soc. 113 (1991) 3385.
[19] (a) P.P. Power, J. Organomet. Chem. 400 (1990) 49;
(b) P.B. Hitchcock, H.A. Jasim, M.F. Lappert, H.D. Williams, Polyhedron 9 (1990) 245.
[20] D.M. Choquette, M.J. Timm, J.L. Hobbs, T.M. Nicholson, M.M. Olmstead, R.P. Planalp, Inorg. Chem. 32 (1993) 2600.
[21] S. Cucinella, G. Dozzi, A. Mazzei, T. Salvatori, J. Organomet. Chem. 90 (1975) 257.
[22] (a) C. Busetto, S. Cucinella, T. Salvatori, Inorg. Chim. Acta 26 (1978) 51;
(b) C. Busetto, M. Cesari, S. Cucinella, T. Salvatori, J. Organomet. Chem. 132 (1977) 339.
[23] C. von Hänisch, Z. Anorg. Allg. Chem. 627 (2001) 68.
[24] K. Schmid, M. Niemeyer, J. Weidlein, Z. Anorg. Allg. Chem. 625 (1999) 186.
[25] O.T. Beachley, G.E. Coates, J. Chem. Soc. (1965) 3241.
[26] S. Schulz, L. Häming, R. Herbst-Irmer, H.W. Roesky, G.M. Sheldrick, Angew. Chem. 106 (1994) 1052;
S. Schulz, L. Häming, R. Herbst-Irmer, H.W. Roesky, G.M. Sheldrick, Angew. Chem. Int. Ed. 33 (1994) 969.
[27] P. Jutzi, B. Neumann, G. Reumann, H.-G. Stammler, Organometallics 18 (1999) 2037.
[28] N.J. Hardman, C. Cui, H.W. Roesky, W.H. Fink, P.P. Power, Angew. Chem. Int. Ed. 40 (2001) 2172.
[29] R.J. Wright, A.D. Phillips, T.L. Allen, W.H. Fink, P.P. Power, J. Am. Chem. Soc. 125 (2003) 1694.
[30] H. Hope, D.C. Pestana, P.P. Power, Angew. Chem. 103 (1991) 726;
H. Hope, D.C. Pestana, P.P. Power, Angew. Chem. Int. Ed. 30 (1991) 691.
[31] A.H. Cowley, R.A. Jones, M.A. Mardones, J. Ruiz, J.L. Atwood, S.G. Bott, Angew. Chem. 102 (1990) 1169.
[32] S. Cucinella, T. Salvatori, C. Busetto, A. Mazzei, J. Organomet. Chem. 108 (1976) 13.
[33] N.D. Reddy, H.W. Roesky, M. Noltemeyer, H.-G. Schmidt, Inorg. Chem. 41 (2002) 2374.
[34] N.D. Reddy, S.S. Kumar, H.W. Roesky, D. Vidovic, J. Magull, M. Noltemeyer, H.-G. Schmidt, Eur. J. Inorg. Chem. (2003) 442.
[35] Y. Peng, J. Rong, D. Vidovic, H.W. Roesky, T. Labahn, J. Magull, M. Noltemeyer, H.-G. Schmidt, J. Fluor. Chem. 125 (2004) 951.
[36] C.J. Harlan, S.G. Bott, A.R. Barron, J. Chem. Soc. Dalton Trans. (1997) 637.
[37] S.S. Kumar, N.D. Reddy, H.W. Roesky, D. Vidovic, J. Magull, R.F. Winter, Organometallics 22 (2003) 3348.
[38] S. Cucinella, T. Salvatori, C. Busetto, M. Cesari, J. Organomet. Chem. 121 (1976) 137.
[39] A.Y. Timoshkin, H.F. Schaefer, Inorg. Chem. 43 (2004) 3080.
[40] S. Cucinella, G. Dozzi, C. Busetto, A. Mazzei, J. Organomet. Chem. 113 (1976) 233.
[41] S. Cucinella, T. Salvatori, C. Busetto, G. Perego, A. Mazzei, J. Organomet. Chem. 78 (1974) 185.
[42] H. Zhu, J. Chai, V. Chandrasekhar, H.W. Roesky, J. Magull, D. Vidovic, H.-G. Schmidt, M. Noltemeyer, P.P. Power, W.A. Merrill, J. Am. Chem. Soc. 126 (2004) 9472.
[43] P. Praetzold, Prog. Inorg. Chem. 31 (1987) 123.
[44] A.Y. Timoshkin, H.F. Bettinger, H.F. Schaefer, J. Phys. Chem. A 105 (2001) 3240.
[45] H.-J. Himmel, A.J. Downs, J.C. Green, T.M. Greene, J. Chem. Soc. Dalton Trans. (2001) 535.
[46] H.-J. Himmel, A.J. Downs, T.M. Greene, J. Am. Chem. Soc. 122 (2000) 9793.
[47] H.-J. Himmel, A.J. Downs, T.M. Greene, Inorg. Chem. 40 (2001) 396.
[48] R.D. Davy, H.F. Schaefer, J. Phys. Chem. A 101 (1997) 3135.
[49] R.D. Davy, K.L. Jaffrey, J. Phys. Chem. 98 (1994) 8930.
[50] A.Y. Timoshkin, G. Frenking, Inorg. Chem. 42 (2003) 60.
[51] H. Wu, C. Zhang, X. Xu, F. Zhang, Q. Zhang, Chin. Sci. Bull. 46 (2001) 1507.
[52] X. Chen, C. Li, T. Wu, T. Yao, G. Ju, Theor. Chem. Acc. 99 (1998) 272.
[53] A.Y. Timoshkin, H.F. Schaefer, J. Am. Chem. Soc. 125 (2003) 9998.
[54] A.Y. Timoshkin, H.F. Bettinger, H.F. Schaefer, J. Am. Chem. Soc. 119 (1997) 5668.
[55] X.-H. Xu, H.-S. Wu, F.-Q. Zhang, C.-J. Zhang, Z.-H. Jin, J. Mol. Struct. 542 (2001) 239.
[56] A. Kovacs, Inorg. Chem. 41 (2002) 3067.
[57] A.Y. Timoshkin, H.F. Bettinger, H.F. Schaefer, Inorg. Chem. 41 (2002) 738.
[58] D.A. Atwood, A.H. Cowley, R.A. Jones, M.A. Mardones, J. Am. Chem. Soc. 113 (1991) 7050.
[59] A.Y. Timoshkin, Phosph. Sulf. Silic. Relat. Elem. 168 (2001) 275.
[60] T. Bauer, S. Schulz, H. Hupfer, M. Nieger, Organometallics 21 (2002) 2931.
[61] D.A. Atwood, A.H. Cowley, R.A. Jones, M.A. Mardones, J. Organomet. Chem. 439 (1992) 33.
[62] S. Schulz, A. Voigt, H.W. Roesky, L. Häming, R. Herbst-Irmer, Organometallics 15 (1996) 5252.
[63] C. von Hänisch, O. Hampe, Angew. Chem. Int. Ed. 41 (2002) 2095.
[64] C. von Hänisch, Z. Anorg. Allg. Chem. 629 (2003) 1496.
[65] M. Driess, S. Kuntz, K. Merz, H. Pritzkow, Chem. Eur. J. 4 (1998) 1628.
[66] C. von Hänisch, P. Scheer, B. Rolli, Eur. J. Inorg. Chem (2002) 3268.
[67] S. Weinrich, H. Piotrovski, M. Vogt, A. Schulz, M. Westerhausen, Inorg. Chem. 43 (2004) 3756.
[68] C. Üffing, C. von Hänisch, H. Schnöckel, Z. Anorg. Allg. Chem. 626 (2000) 1557.
[69] M.A. Petrie, P.P. Power, Organometallics 12 (1993) 1592.
[70] R.D. Davy, H.F. Schaefer, Inorg. Chem. 37 (1998) 2291.
[71] A.Y. Timoshkin, H.F. Bettinger, H.F. Schaefer, J. Phys. Chem. A 105 (2001) 3249.
[72] R.D. Davy, H.F. Schaefer, J. Phys. Chem. A 101 (1997) 5707.
[73] K.M. Waggoner, H. Hope, P.P. Power, Angew. Chem. 100 (1988) 1765;
K.M. Waggoner, H. Hope, P.P. Power, Angew. Chem. Int. Ed. 27 (1988) 1699.
[74] W.H. Fink, J.C. Richards, J. Am. Chem. Soc. 113 (1991) 3393.
[75] N. Matsunaga, M.S. Gordon, J. Am. Chem. Soc. 116 (1994) 11407.
[76] E.D. Jemmis, B. Kiran, Inorg. Chem. 37 (1998) 2110.
[77] P.v.R. Schleyer, H. Jiao, N.J.R.v.E. Hommes, V.G. Malkin, O.L. Malkina, J. Am. Chem. Soc. 119 (1997) 12669.
[78] (a) J. Pinkas, H. Wessel, Y. Yang, M.L. Montero, M. Noltemeyer, M. Fröba, H.W. Roesky, Inorg. Chem. 37 (1998) 2450;
(b) J. Pinkas, J. Löbl, D. Dastyc, M. Necas, H.W. Roesky, Inorg. Chem. 41 (2002) 6914;

(c) J. Pinkas, J. Löbl, H.W. Roesky, Phosph. Sulf. Silic. Relat. Elem. 179 (2004) 759.
[79] M. Driess, K. Merz, H. Pritzkow, R. Janoschek, Angew. Chem. Int. Ed. 35 (1996) 2507.
[80] G. Del Piero, M. Cesari, G. Dozzi, A. Mazzei, J. Organomet. Chem. 129 (1977) 281.
[81] W. Uhl, J. Molter, B. Neumüller, Chem. Eur. J. 7 (2001) 1510.
[82] (a) T.R.R. McDonald, W.S. McDonald, Acta Crystallogr. B28 (1972) 1619;
(b) T.R.R. McDonald, W.S. McDonald, Proc. Chem. Soc. (1963) 382.
[83] C. Schnitter, S.D. Waezsada, H.W. Roesky, M. Teichert, I. Usón, E. Parsisini, Organometallics 16 (1997) 1197.
[84] T. Belgardt, S.D. Waezsada, H.W. Roesky, H. Gornitzka, L. Häming, D. Stalke, Inorg. Chem. 33 (1994) 6247.
[85] F. Cordeddu, H.-D. Hausen, J. Weidlein, Z. Anorg. Allg. Chem. 622 (1996) 573.
[86] S. Kühner, R. Kuhnle, H.-D. Hausen, J. Weidlein, Z. Anorg. Allg. Chem. 623 (1997) 25.
[87] T. Belgardt, H.W. Roesky, M. Noltemeyer, H.-G. Schmidt, Angew. Chem. 105 (1993) 1101;
T. Belgardt, H.W. Roesky, M. Noltemeyer, H.-G. Schmidt, Angew. Chem. Int. Ed. 32 (1993) 1056.
[88] B. Luo, W.L. Gladfelter, Inorg. Chem. 41 (2002) 590.
[89] T. Grabowy, K. Merzweiler, Z. Anorg. Allg. Chem. 626 (2000) 736.
[90] K. Schmid, S. Kühner, H.-D. Hausen, J. Weidlein, Z. Anorg. Allg. Chem. 623 (1997) 1499.
[91] A.H. Cowley, R.A. Jones, M.A. Mardones, J.L. Atwood, S.G. Bott, Angew. Chem. 102 (1990) 1504.
[92] K. Niediek, B. Neumüller, Z. Anorg. Allg. Chem. 621 (1995) 889.
[93] K. Niediek, B. Neumüller, Chem. Ber. 127 (1994) 67.
[94] E. Leiner, M. Scheer, Organometallics 21 (2002) 4448.
[95] B. Werner, B. Neumüller, Organometallics 15 (1996) 4258.
[96] D.A. Atwood, A.H. Cowley, R.A. Jones, M.A. Mardones, J. Organomet. Chem. 449 (1993) 1.
[97] U. App, K. Merzweiler, Z. Anorg. Allg. Chem. 621 (1995) 1731.
[98] C. von Hänisch, B. Rolli, Z. Anorg. Allg. Chem. 628 (2002) 2255.
[99] A.-A. Al-Wassil, P.B. Hitchcock, S. Sarisaban, J.D. Smith, C.L. Wilson, J. Chem. Soc. Dalton Trans. (1985) 1929.
[100] A.Y. Timoshkin, Solid State Electron. 47 (2003) 543.
[101] M. Schiefer, N.D. Reddy, H.W. Roesky, D. Vidovic, Organometallics 22 (2003) 3637.
[102] W. Uhl, J. Molter, B. Neumüller, J. Organomet. Chem. 634 (2001) 193.
[103] M. Cesari, G. Perego, G. Del Piero, S. Cucinella, E. Cernia, J. Organomet. Chem. 78 (1974) 203.
[104] G. Del Piero, M.C. Cesari, G. Perego, S. Cucinella, E. Cernia, J. Organomet. Chem. 129 (1977) 289.
[105] G. Del Piero, G. Perego, S. Cucinella, M.C. Cesari, A. Mazzei, J. Organomet. Chem. 136 (1977) 13.
[106] E.K. Styron, C.H. Lake, D.H. Powell, L.K. Krannich, C.L. Watkins, J. Organomet. Chem. 649 (2002) 78.
[107] J.E. Park, B.-J. Bae, Y. Kim, J.T. Park, I.-H. Suh, Organometallics 18 (1999) 1059.
[108] B. Luo, W.L. Gladfelter, J. Clust. Sci. 13 (2002) 461.
[109] M. Driess, S. Kuntz, C. Monsé, K. Merz, Chem. Eur. J. 6 (2000) 4343.
[110] C. von Hänisch, F. Weigend, Z. Anorg. Allg. Chem. 628 (2002) 389.
[111] P.B. Hitchcock, J.M. McLaughlin, J.D. Smith, K.M. Thomas, Chem. Commun. (1973) 934.
[112] P.B. Hitchcock, J.D. Smith, K.M. Thomas, J. Chem. Soc. Dalton Trans. (1976) 1433.
[113] K. Gosling, J.D. Smith, D.H.W. Wharmby, J. Chem. Soc. (A) (1969) 1738.
[114] K.J. Alford, K. Gosling, J.D. Smith, J. Chem. Soc. Dalton Trans. (1972) 2203.
[115] A.Y. Timoshkin, H.F. Schaefer, J. Am. Chem. Soc. 126 (2004) 12141.
[116] B. Luo, W.L. Gladfelter, J. Organomet. Chem. 689 (2004) 666.
[117] (a) A.Y. Timoshkin, Inorg. Chem. Commun. 6 (2003) 274;
(a) A.Y. Timoshkin, Phosph. Sulf. Silic. Relat. Elem. 179 (2004) 707.
[118] T.J. Trentler, S.C. Goel, K.M. Hickman, A.M. Viano, M.Y. Chiang, A.M. Beatty, P.C. Gibbons, W.E. Buhro, J. Am. Chem. Soc. 119 (1997) 2172.
[119] J.A. Jegier, S. McKernan, W.L. Gladfelter, Inorg. Chem. 38 (1999) 2726.
[120] J.A. Jegier, S. McKernan, W.L. Gladfelter, Chem. Mater. 10 (1998) 2041.
[121] J.F. Janik, R.L. Wells, Inorg. Chem. 36 (1997) 4135.
[122] J.A. Jegier, S. McKernan, A.P. Purdy, W.L. Gladfelter, Chem. Mater. 12 (2000) 1003.
[123] R.J. Jouet, A.P. Purdy, R.L. Wells, J.F. Janik, J. Clust. Sci. 13 (2002) 469.
[124] Z. Jiang, L.V. Interrante, Chem. Mater. 2 (1990) 439.
[125] S. Amirkhalili, P.B. Hitchcock, J.D. Smith, J. Chem. Soc. Dalton Trans. (1979) 1206.
[126] A.Y. Timoshkin, H.F. Schaefer, Chem. Record. 2 (2002) 319.
[127] G. Dozzi, S. Cucinella, A. Mazzei, J. Organomet. Chem. 164 (1979) 1.
[128] R. Annunziata, G. Borgogno, F. Montanari, S. Quici, S. Cucinella, J. Chem. Soc. Perkin Trans. (1981) 113.
[129] R.E. Allan, M.A. Beswick, P.R. Raithby, A. Steiner, D.S. Wright, J. Chem. Soc. Dalton Trans. (1996) 4153.
[130] F.-Q. Liu, A. Herzog, H.W. Roesky, I. Usón, Inorg. Chem. 35 (1996) 741.
[131] Y. Sugahara, T. Onuma, O. Tanegashima, K. Kuroda, C. Kato, J. Ceram. Soc. Jpn. 100 (1992) 101.
[132] Y. Saito, Y. Sugahara, K. Kuroda, J. Am. Ceram. Soc. 83 (2000) 2436.
[133] S. Koyama, H. Takeda, Y. Saito, Y. Sugahara, K. Kuroda, J. Mater. Chem. 6 (1996) 1055.
[134] Y. Saito, S. Koyama, Y. Sugahara, K. Kuroda, J. Ceram. Soc. Jpn. 104 (1996) 143.
[135] S. Koyama, Y. Sugahara, K. Kuroda, Mater. Res. Soc. Proc. 468 (1997) 93.
[136] B. Luo, W.L. Gladfelter, Inorg. Chem. 41 (2002) 6249.
[137] C.J. Carmalt, J.D. Mileham, A.J.P. White, D.J. Williams, J. Chem. Soc. Dalton Trans. (2003) 4255.
[138] S. Koyama, H. Nakashima, Y. Sugahara, K. Kuroda, Chem. Lett. (1998) 191.
[139] H. Nakashima, S. Koyama, K. Kuroda, Y. Sugahara, J. Am. Ceram. Soc. 85 (2002) 59.
[140] F. Cheng, Y. Sugahara, K. Kuroda, Appl. Organomet. Chem. 15 (2001) 710.
[141] S. Cucinella, A. Mazzei, G. Dozzi, J. Organomet. Chem. 84 (1974) 19.
[142] A.Y. Timoshkin, Electrochem. Soc. Proc. 13 (2001) 25.
[143] A.Y. Timoshkin, H.F. Bettinger, H.F. Schaefer, J. Cryst. Growth 222 (2001) 170.
[144] C. von Hänisch, B. Rolli, Phosph. Sulf. Silic. Relat. Elem. 179 (2004) 749–757.
[145] C. Dohmeier, H. Schnöckel, C. Robl, U. Schneider, R. Ahlrichs, Angew. Chem. Int. Ed. 33 (1994) 199.
[146] E. Iravani, A. Dashti-Mommertz, B. Neumüller, Z. Anorg. Allg. Chem. 629 (2003) 1136.
[147] T. Chivers, C. Fedorchuk, G. Schatte, M. Parvez, Inorg. Chem. 42 (2003) 2084.

[148] H.-D. Hausen, R. Kuhnle, J. Weidlein, Z. Naturforsch. Teil B 50 (1995) 1419.
[149] M. Veith, H. Lange, O. Recktenwald, W. Frank, J. Organomet. Chem. 294 (1985) 273.
[150] I. Silaghi-Dumetrescu, F. Lara-Ochoa, I. Haiduc, J. Mol. Struct. (Theochem.) 370 (1996) 17.
[151] (a) A. Demchuk, J. Porter, B. Koplitz, Electrochem. Soc. Proc. 23 (1998) 129;
(b) A. Demchuk, J. Cahill, B. Koplitz, Chem. Mater. 12 (2000) 3192;
(c) A. Demchuk, S. Simpson, B. Koplitz, Electrochem. Soc. Proc. 13 (2001) 389;
(d) M. Lynch, A. Demchuk, S. Simpson, B. Koplitz, Chem. Phys. Lett. 388 (2004) 12.
[152] J.R. Creighton, G.T. Wang, W.G. Breiland, M.E. Coltrin, J. Cryst. Growth 261 (2004) 204.
[153] J.F. Janik, R.T. Paine, J. Organomet. Chem. 449 (1993) 39.
[154] A.Y. Timoshkin, H.F. Schaefer, Inorg. Chem. 44 (2005) 843.
[155] H. Wessel, H.-S. Park, P. Müller, H.W. Roesky, I. Usón, Angew. Chem. Int. Ed. 38 (1999) 813.
[156] A. Dashti-Mommeretz, B. Neumüller, Z. Anorg. Allg. Chem. 625 (1999) 954.
[157] A. Downard, T. Chivers, Eur. J. Inorg. Chem. (2001) 2193.
[158] M.D. Healy, P.E. Laibinis, P.D. Stupik, A.R. Barron, Chem. Commun. (1989) 359.
[159] A.H. Cowley, P.R. Harris, R.A. Jones, C.M. Nutt, Organometallics 10 (1991) 652.
[160] C.W. Bock, M. Trachtman, J. Phys. Chem. 97 (1993) 3183.
[161] S.J. Schauer, C.H. Lake, C.L. Watkins, L.K. Krannich, Organometallics 15 (1996) 5641.
[162] H. Nöth, P. Wolfgardt, Z. Naturforsch. 31b (1976) 1447.
[163] H. Nöth, P. Wolfgardt, Z. Naturforsch. 31b (1976) 697.
[164] H. Nöth, P. Wolfgardt, Z. Naturforsch. 31b (1976) 1201.
[165] O.T. Beachley Jr., D.B. Rosenblum, M.R. Churchill, D.G. Churchill, L.M. Krajkovski, Organometallics 18 (1999) 2543.
[166] J.A. Jegier, B. Luo, C.E. Buss, W.L. Gladfelter, Inorg. Chem. 40 (2001) 6017.
[167] (a) A.S. Borovik, S.G. Bott, A.R. Barron, Organometallics 18 (1999) 2668;
(b) T.J. Barbarich, S.G. Bott, A.R. Barron, J. Chem. Soc. Dalton Trans. (2000) 1679.
[168] (a) Y. Egashira, H.J. Kim, H. Komiyama, J. Am. Ceram. Soc. 77 (1994) 2009;
(b) H.J. Kim, Y. Egashira, H. Komiyama, Appl. Phys. Lett. 59 (1991) 2521.
[169] J.A. Jegier, W.L. Gladfelter, Coord. Chem. Rev. 206–207 (2000) 631.
[170] B.L. Kormos, J.A. Jegier, P.C. Ewbank, U. Pernisz, V.G. Young Jr., C.J. Cramer, W.L. Gladfelter, J. Am. Chem. Soc. 127 (2005) 1493.